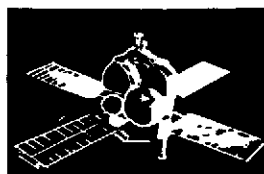
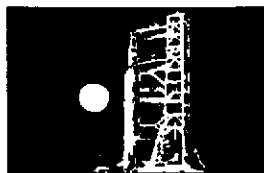
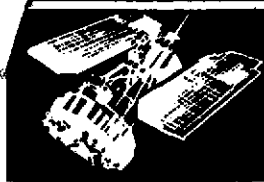


**SPACE
DIVISION**



NASA CR-

140376

GE Report No. 74SD4248
September 1974

AUTOMATED BIOWASTE SAMPLING SYSTEM

IMPROVED FECES

COLLECTION, MASS MEASUREMENT AND SAMPLING

(NASA-CR-140376) AUTOMATED BIOWASTE
SAMPLING SYSTEM IMPROVED FECES COLLECTION,
MASS MEASUREMENT AND SAMPLING Final
Report (General Electric Co.) 150 p HC
\$5.75

N75-13504

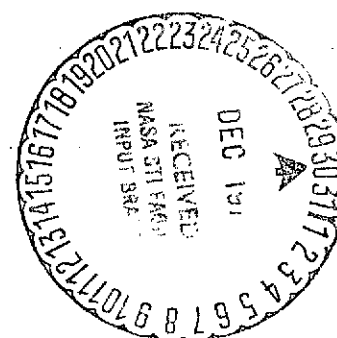
Unclas

CSCS 061 G3/51 03683

FINAL REPORT

Contract NAS1-11443, Mod. 5S

National Aeronautics and Space Administration
Lyndon B. Johnson Space Center
Houston, Texas 77058



GENERAL  ELECTRIC

GE Report No. 74SD4248
September 1974

AUTOMATED BIOWASTE SAMPLING SYSTEM
IMPROVED FECES
COLLECTION, MASS MEASUREMENT AND SAMPLING

FINAL REPORT

Contract NAS1-11443, Mod. 5S

National Aeronautics and Space Administration
Lyndon B. Johnson Space Center
Houston, Texas 77058

Prepared By: G. L. Fogal
J. Mangialardi
R. Young

General Electric Company
Valley Forge Space Center
P. O. Box 8555
Philadelphia, Pennsylvania 19101

TABLE OF CONTENTS

	<u>Page</u>
Foreward	ii
1.0 SUMMARY	1
2.0 TECHNICAL	1
2.1 Inertial Collector	1
2.2 Mass Measurement	5
2.3 Sampling	7
2.4 ABSS Integration	8
3.0 RECOMMENDATIONS	12
3.1 Design Optimization	12
3.2 Testing	13
4.0 APPENDIX	13
4.1 Performance Specification	13
4.2 List of Drawings	15
4.3 Misc. Analyses/Reports	17

FOREWORD

This report covers the evaluation of Feces Inertial Collector, Mass Measurement and sampling concepts via the design and test of breadboard hardware.

NASA technical direction was provided by Mr. R. Sauer, Contract Technical Monitor, and Mr. B. Westover.

ABSS IMPROVED FECES COLLECTION, MASS
MEASUREMENT AND SAMPLING

1.0 SUMMARY

The main objective of the improved feces collection, mass measurement and sampling activity was to improve and extend the capability of the basic ABSS hardware. This objective was accomplished through the design, fabrication and test of breadboard hardware. A preliminary system design effort established the feasibility of integrating the breadboard concepts into the ABSS.

2.0 TECHNICAL

As an extension of the effort initiated under Contract NAS1-11443, an automated Biowaste Sampling System for Medical Research, the Statement of Work specifies the evaluation of feces inertial collector, mass measurement and sampling concepts via the design and test of breadboard hardware. General design requirements are listed in Table 2-1. Subsequent to the evaluation effort, preparation of a preliminary engineering prototype system design integrated with the ABSS is also specified.

2.1 Inertial Collector

Inertial collection refers to the use of inertial forces to cause bolus disengagement after defecation is completed. The detached bolus is then conveyed by transport air into the feces storage container. PIR 1R60-74-101, Appendix 4.3, describes and analyzes the general inertial collection concept and concludes that an automated compressed spring approach can provide the desired

Table 2-1. General Design Requirements

The design or operational requirements shall include the following:

1. Accommodate defecations of all possible consistencies.
2. Provide concurrent feces mass measurement and sampling.
3. Provide minimum cross contamination between defecations. The design goal shall be a maximum of 0.5 grams of fecal material carryover between defecations.
4. Provide for maximum automation. The goal shall be to minimize crew manipulation and time required to perform defecation, mass measurement, sampling and deactivation.
5. Compatible and integrable with the Automated Biowaste Sampling System (ABSS).
6. Provide measurement accuracy of ± 1 gram or $\pm 2\%$ whichever is greater.
7. Provide gravity independent operation.

inertial forces. Figure 2-1 shows the resulting breadboard hardware. Both quantitative and qualitative tests were performed using the breadboard model. These tests indicate that the inertial collector concept can provide positive user/feces disengagement during zero g defecation. Results are reported in detail in PIR 1R60-74-119, Appendix 4.3.

Several operational and system advantages occur from using the inertial collection concept. Thus,

- (a) Transport airflow requirements can be significantly reduced. Zero gravity tests using both male and female subjects indicate about 30 CFM is required if transport air flow only is used to provide disengagement; see GE Report No. 74SD4221. By adding inertial collection, the 30 CFM could be reduced to 10 CFM (or less), with a consequent saving in power. A lower airflow will also help reduce particle carryover through the feces phase separator to the filter, particularly for feces of diarrhetic composition.
- (b) A good seal at the seat/user interface is not required when using inertial collection. A good seal is difficult to achieve and maintain, yet an important consideration for an effective capability using transport airflow alone to provide bolus disengagement force. As a result, the seat and user body restraint hardware can be simplified.
- (c) The positive disengagement capability when using inertial collection increases user confidence (and consequently user acceptance).

In summary, the inertial collection concept appears to be a practical and useful approach to providing positive bolus disengagement during zero g defecations. Seat/user interface problems and transport airflow can be minimized by adding inertial collection.

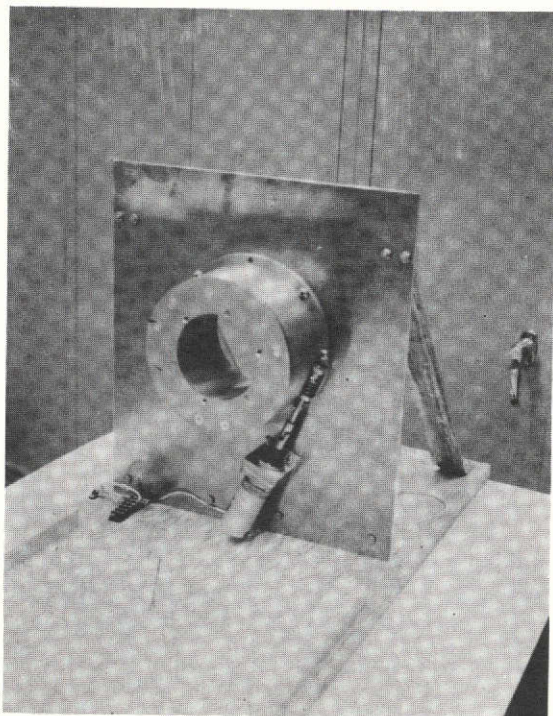


Figure 2-1(a). Inertial Collector Breadboard Mounted on Test Support Plate (Seat Attachment Side)

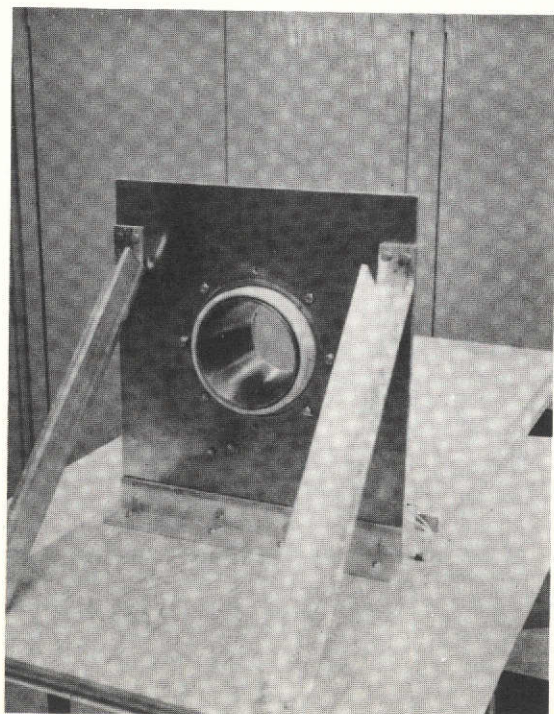


Figure 2-1(b). Inertial Collector Breadboard Mounted on Test Support Plate (Storage Container Side)

2.2 Mass Measurement

The feces mass measurement breadboard design was based on previous General Electric funded effort. Specifically the mass measurement concept uses the ABSS Dry-John "slinger assembly" as the mass sensing element. To determine mass, the incremental change in power input (or equivalent) to the constant speed slinger motor is monitored. This power change is due to the impact of the feces with the rotating slinger and is proportional to the incremental feces mass. Total mass is then obtained by integration of the delta power input signal with time multiplied by a proportionality factor.

The breadboard model, Figure 2-2, was designed to meet the requirements specified in PIR 1R60-74-102, Appendix 4.3. Design and operation of the breadboard electronics (including motor) is discussed in PIR 1JL3-1019, Appendix 4.3. Briefly, a tach feedback speed control loop is used to hold the 28 VDC slinger motor at a preset constant speed. Mass is determined by monitoring motor current. The motor current is converted to digital form by a conventional A-D converter. A IMP-16 microprocessor continually monitors the A-D converter output. When the value exceeds a preset threshold, a measurement cycle begins. Corrections for threshold bias and offset are made by arithmetic operations. The current waveform integral is approximated by equal-interval repetitive additions until the instantaneous current value falls below threshold. The waveform integral is added to the previous integral and the sum is converted to BCD for display. The microprocessor via software changes provide the capability to try different measurement algorithms or variations without modification or redesign of the electronics.

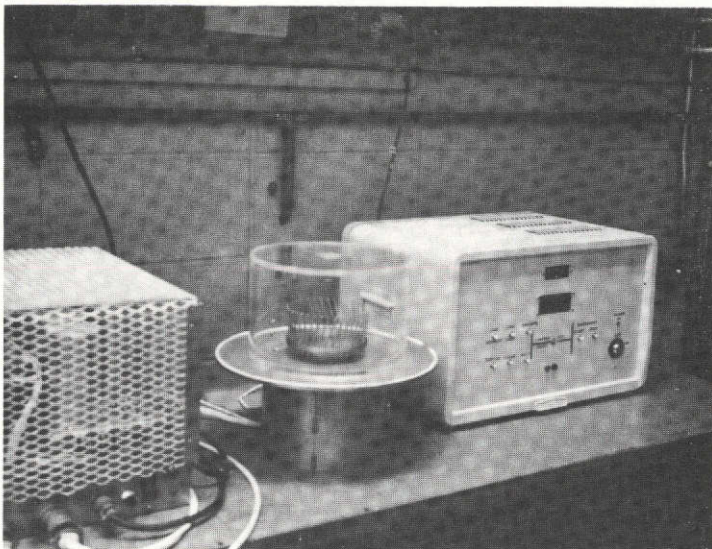


Figure 2-2. Mass Measurement Breadboard Hardware

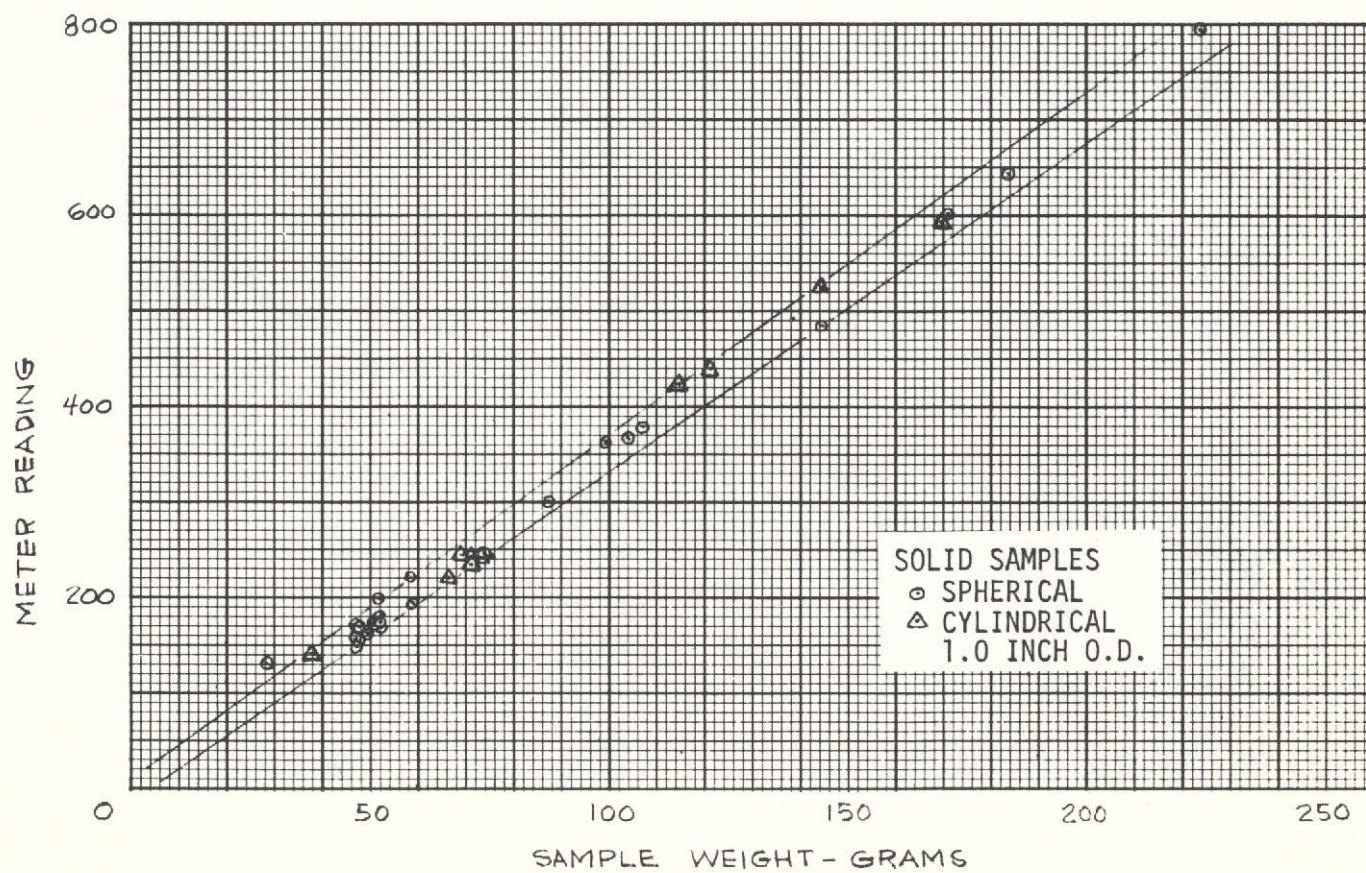


Figure 2-3. Mass Measurement Data, Type 1 Slinger at 1500 rpm

Detail test results are reported in PIR 1R60-74-129, Appendix 4.3. Figure 2-3 shows the results for one slinger configuration. The data envelope represents an error of about $\pm 3.5\%$ at 250 grams up to about $\pm 8\%$ at 50 grams sample weight. In general, the test results indicate that measurement accuracy is largely dependent on slinger rotational speed and blade configuration. Additional combinations of these two factors need to be investigated in order to refine the concept down to a maximum $\pm 2\%$ error capability in the mass measurement.

In summary, the mass measurement concept was demonstrated in breadboard form. Additional design refinement effort will be required to achieve the $\pm 2\%$ maximum error goal.

2.3 Sampling

The Feces sampling concept for the ABSS is described in detail in GE Report No. 74SD4208, Part II. In this concept, the sampling function is located downstream of the slinger element. Sampling is automatic and accomplished by deploying from the sampling container a collection strip in a manner to partially or completely surround the slinger. All (or part) of the fecal material which passes through the slinger is intercepted by the collection strip (depending on the length deployed). The collection strip is then automatically returned to the sample container. With this technique, sampling does not interfere with real time automatic feces mass measurement.

Effort under the feces sampling task was largely directed towards improving the collection and operating performance and reducing the size of the sample container. Results of these efforts are detailed in PIR's 1R60-74-130 and 1R60-74-132, Appendix 4.3. Retaining the basic ABSS sampling concept, two design alternates were investigated. One alternate was directed towards collecting the total defecation; the other towards collecting only a portion

of the total defecation. Figure 2-4 illustrates the sample container elements of the two designs in breadboard form.

In summary, the approach collecting the total defecation, Figure 2-4(b), exhibited the best performance and considerable improvement over the existing ABSS Solids S/S hardware. Tests show excellent collection capabilities for both normal and diarrhetic type fecal material. Although the alternate concept, Figure 2-4(a), performed satisfactorily mechanically, the size of the collected sample will exhibit wide variations from the nominal. This is due to the relatively poor distribution of the feces by the slinger. Although a sample will always be collected, the quantity may not always be sufficient for post flight analysis; in other cases, the quantity may be too large and thus exceed the sample container storage capability. Refinement of the slinger design for improved feces distribution is necessary, with a reduction in refrigerated storage volume requirements as the end result payoff.

2.4 ABSS Integration

Figure 2-5 shows the inertial collector, feces sampling and mass measurement (less electronics) capabilities integrated into the ABSS Solids S/S design. Other than requiring an increase in overall height (deck to seat), no deviation from the basic ABSS solids S/S performance requirements was necessary. A raised foot restraint can cancel the effect of the height increase. Changes to the Solids S/S performance specification to incorporate the feces mass measurement, sampling and inertial collection features are listed in Appendix 4.1.

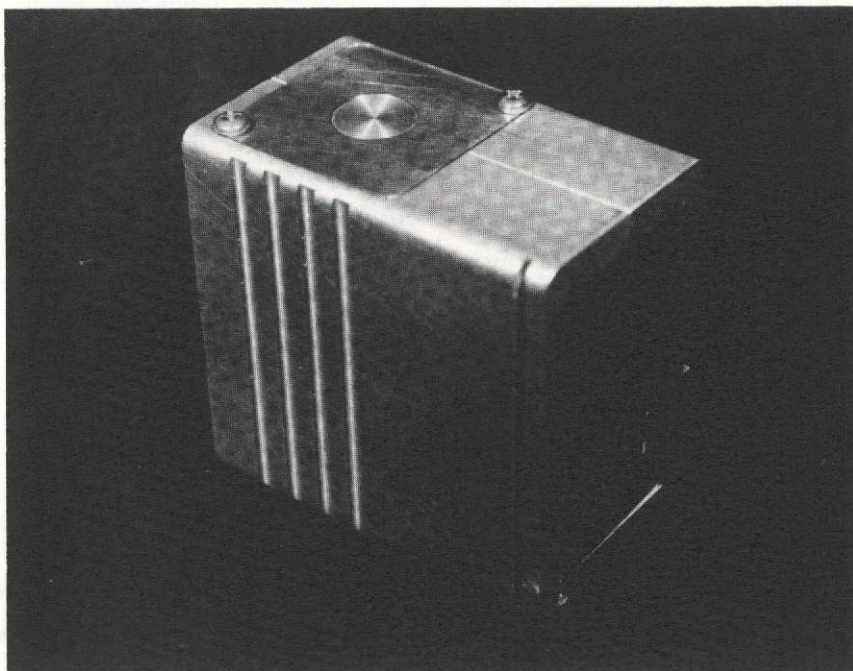
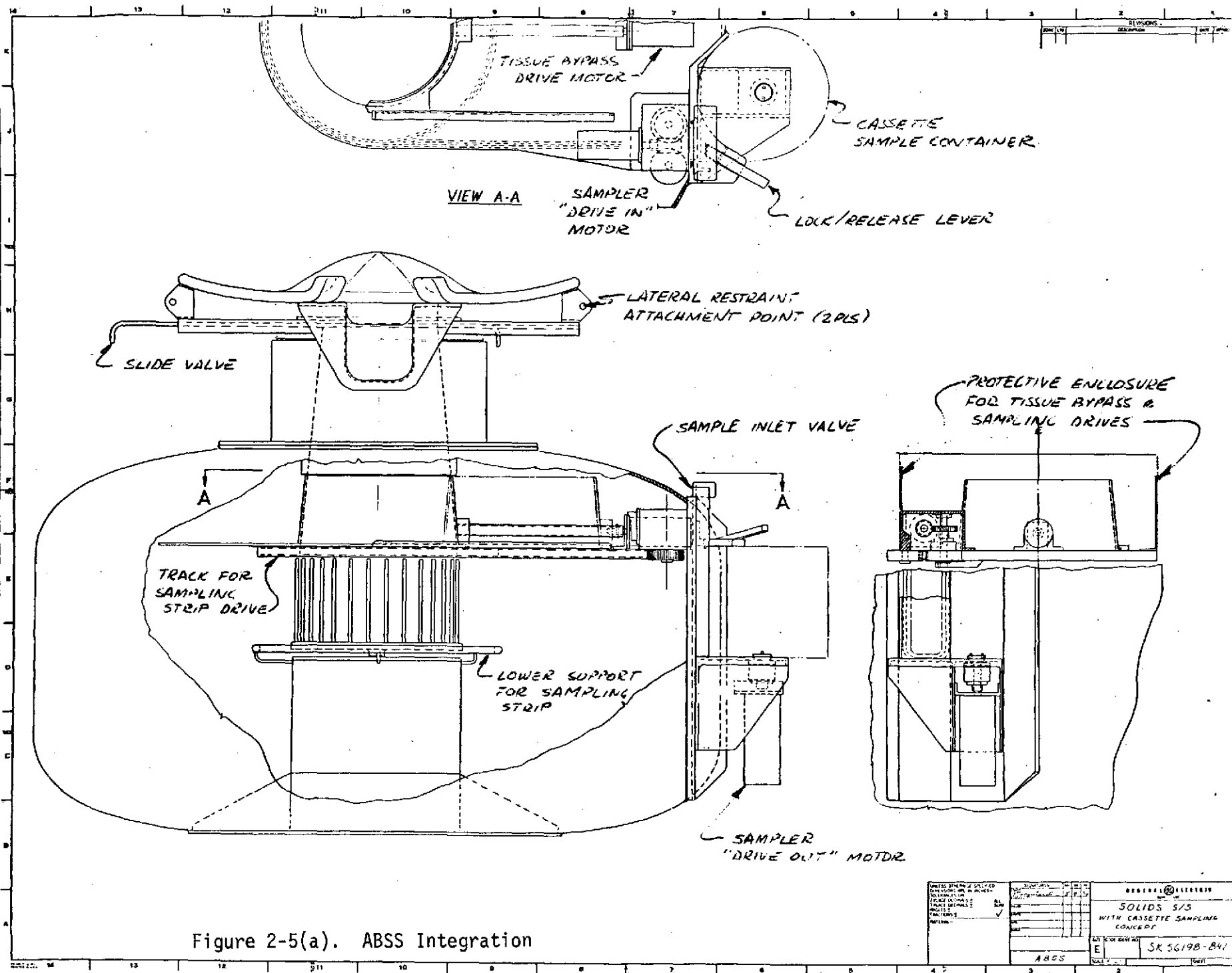


Figure 2-4(a). Breadboard Sample Container for Collecting a Nominal 20% of the Total Fecal Mass per Defecation



Figure 2-4(b). Breadboard Sample Container for Collecting the Total Fecal Mass Per Defecation



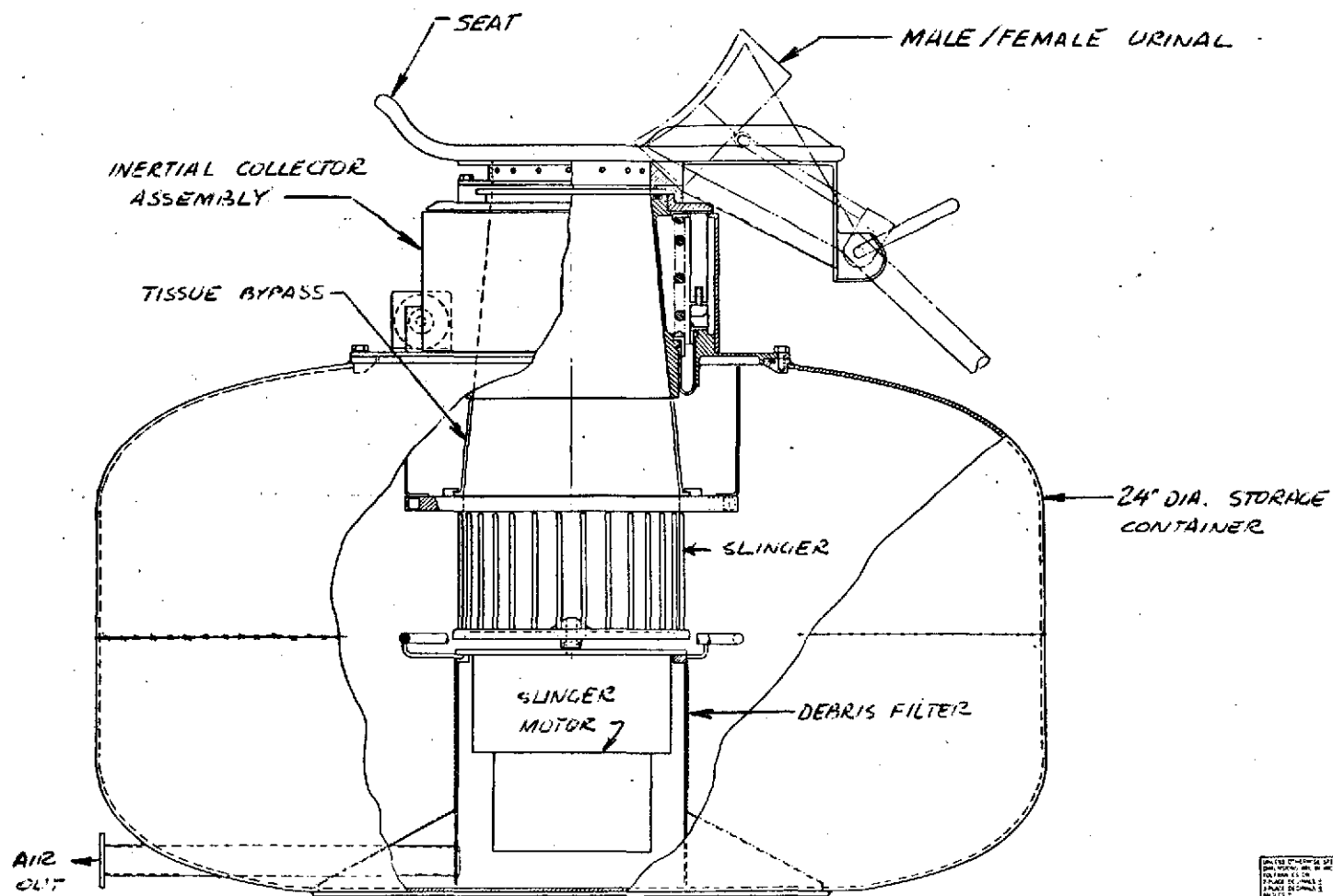


Figure 2-5(b). ABSS Integration

DESIGNED BY: [] DRAWN BY: [] CHECKED BY: [] APPROVED BY: [] DATE: []		SOLIDS S/S WITH INERTIAL COLLECTOR	
SK 56178-B40		ABSS	

3.0 RECOMMENDATIONS

Recommendations for possible follow-on activity are in two general areas: design optimization and zero gravity testing.

3.1 Design Optimization

3.1.1 Mass Measurement

The mass measurement breadboard demonstrated the feasibility of the concept and established the criticality of slinger blade configuration and rotational velocity on measurement error. Further laboratory investigation directed toward improvement in measurement accuracy is recommended. Briefly, a systematic variation of blade configuration and rotational velocity coupled with the use of a high speed stop action camera (to visually observe the interaction between feces and slinger blades) is suggested. The mass measurement breadboard electronics can be used without modification to accomplish the recommended program.

3.1.2 Microprocessor

The mass measurement breadboard incorporates a microprocessor as a key element. In this role, the microprocessor is underutilized and thus could be used to perform other ABSS functions. An investigation to assess the merits of this approach is recommended. A program scope is suggested as follows:

- (1) Conduct study investigation to determine feasibility of utilizing a microprocessor as the electronics module for providing system electronic functions. Electronic functions will include those for:
 - (a) Cycle sequence control,
 - (b) Data manipulation for feces mass measurement, urine volume measurement, urine analysis, and
 - (c) User/sample identification.

- (2) Compare microprocessor approach (weight, volume, reliability, growth capability, etc.) with the standard electronic approach used for ABSS.

3.1.3 Sampling

Collection of only a partial sample was unsuccessful due to the relatively erratic nature of feces distribution by the slinger. Refinement of the slinger blade configuration is suggested as a means of improving this distribution. A combination of this effort and the mass measurement activity suggested above appears practical and desirable.

3.2 Testing

The feces inertial collector, mass measurement and sampling concepts investigated represent a significant advance in automated equipment. Breadboard laboratory testing was largely confined to concept feasibility demonstration. Since the concepts are applicable to the Shuttle application, further testing under simulated flight conditions is recommended. A program scope involving (1) the presently available breadboard hardware either as is or redesigned as appropriate using simulated samples and/or integrated with the existing ABSS hardware, (2) laboratory baseline checkout testing followed by a limited series of zero g aircraft flight tests, and (3) analysis of the data obtained, is suggested.

4.0 APPENDIX

4.1 Performance Specification

The following shall be added to appropriate sections of the basic ABSS Solids Subsystem operating model requirements specification (see Appendix 7.1, GE Report No. 74SD4208, Part II).

4.1.1 Inertial Collection

The function of the inertial collector element is to provide inertial forces for positive bolus disengagement after completion of defecation. Specific requirements are as follows:

- (a) Provide cycle of slow acceleration followed by rapid deceleration (to accomplish disengagement).
- (b) Accelerate user to minimum velocity of 58 cm/second at impact with deceleration stop; limit acceleration to 0.5 g maximum. Assume deceleration travel of 0.5 cm maximum, 0.25 cm minimum (travel provided by user body compliance and coupling to hardware).
- (c) Accommodate user mass range of 75 ± 10 Kg.
- (d) Start/stop of inertial cycle initiated by operator; all other functions automatic.
- (e) Automatically provide two acceleration/deceleration cycles.
- (f) Design to operate on 28 VDC.

4.1.2 Mass Measurement

The function of the mass measurement element is to provide automatic real time measurement of the fecal mass discharged at each defecation. This shall be accomplished by monitoring delta input power to the slinger motor. Specific requirements are as follows:

- (a) Provide real time feces mass measurement with measurement error of less than $\pm 2\%$ of the actual value or ± 1 gram, whichever is greater.

- (b) Accommodate individual defecations ranging in mass up to a maximum of 500 grams (110 grams average) of normal composition or a maximum of 500 grams for feces of diarrhetic composition and one or more increments per defecation.
- (c) Operate slinger at a constant rotational velocity (or correct mass measurement to this condition), nominally 2000 rpm.
- (d) Design system to operate on 28 VDC.
- (e) System start/stop shall be initiated by the operator; all other functions shall be automatic.

4.1.3 Sampling

No additions required to basic specification.

4.2 List of Drawings

4.2.1 Inertial Collection

<u>Drawing Title</u>	<u>GE Drawing Number</u>
Breadboard Assembly	SK56198-870
Spring	SK56198-871
Worm Gear	SK56198-872
Transport Tube	SK56198-873
Spring Seat	SK56198-874
Cam Seat	SK56198-875
Mounting Flange	SK56198-876
Transport Tube Seal	SK56198-877
Housing	SK56198-878
Worm Bracket	SK56198-879

<u>Drawing Title</u>	(cont'd)	<u>GE Drawing Number</u>
Cam		SK56198-880
Cam Follower		SK56198-881
Roller		SK56198-882
Impact Pad		SK56198-883
Adapter Plate		SK56198-884
Motor Support		SK56198-885

4.2.2 Mass Measurement

<u>Drawing Title</u>	<u>GE Drawing Number</u>
Slinger, Type 1	SK56198-890
Slinger, Type 2	SK56198-889
Slinger, Type 3	SK56198-888
Electronics	ER47E223520

4.2.3 Sampling

4.2.3.1 Partial Sample

<u>Drawing Title</u>	<u>GE Drawing Number</u>
Feces Sampling Assembly	SK56198-830
Reel Knob	SK56198-831
Guard	SK56198-832
Guide Rail	SK56198-833
Base Plate	SK56198-834
Guide Plant	SK56198-835
Slide Assembly	SK56198-836
Stop Lever	SK56198-837
Sample Container Assembly	SK56198-891
Reel	SK56198-892
Plate	SK56198-893

<u>Drawing Title</u>	(cont'd)	<u>GE Drawing Number</u>
Housing - Left Half		SK56198-894
Housing - Right Half		SK56198-895
Collection Strip		SK56198-896
Scraper		SK56198-897
Bushing		SK56198-898
Test Collection Strip		SK56198-899

4.2.3.2 Total Sample

<u>Drawing Title</u>	<u>GE Drawing Number</u>
Demonstration Model Assembly	SK56198-842
Container	SK56198-843
Shaft	SK56198-844
Support Angle	SK56198-845
Container Support	SK56198-846
Guide Plate	SK56198-847
Slide Valve, etc.	SK56198-848
Sample Container Assembly	SK56198-849

4.2.4 ABSS Integration

<u>Drawing Title</u>	<u>GE Drawing Number</u>
Solids S/S with Inertial Collector	SK56198-840
Solids S/C with Cassette Sampler	SK56198-841

4.3 Misc. Analyses/Reports

The following internal GE memoranda are included as supplemental information.

4.3.1 Inertial Collector

- (a) GE PIR 1R60-74-101, "Inertial Collector"
- (b) GE PIR 1R60-74-119, "Inertial Collector Breadboard Model Test Results"

4.3.2 Mass Measurement

- (a) GE PIR 1R60-74-102, "Mass Measurement"
- (b) GE PIR 1J13-1019, "ABSS Feces Mass Measurement Microprocessor System"
- (c) GE PIR 1R60-74-129, "Mass Measurement Breadboard Test Results"

4.3.3 Sampling

- (a) GE PIR 1R60-74-130, "Feces Sampling Breadboard Test Results"
- (b) GE PIR 1R60-74-132, "Improved ABSS Feces Sampling"

GENERAL ELECTRIC

SPACE DIVISION
PHILADELPHIA

PROGRAM INFORMATION REQUEST / RELEASE

CLASS. LTR.	OPERATION	PROGRAM	SEQUENCE NO.	REV. LTR.
U	1R60	74	101	
PIR NO.				
*USE "C" FOR CLASSIFIED AND "U" FOR UNCLASSIFIED				

FROM G. L. Fogal, Program Manager-Environmental Engineering, Room #M-2101, VFSC	TO Distribution		
DATE SENT 1-14-74	DATE INFO. REQUIRED	PROJECT AND REQ. NO. ABSS Improved Feces Measurement and Sampling	REFERENCE DIR. NO.
SUBJECT INERTIAL COLLECTOR			

INFORMATION REQUESTED/RELEASED

1.0 SUMMARY

Inertial collection design requirements are determined, alternate hardware concepts examined and a hardware concept for application to the ABSS breadboard selected.

2.0 BACKGROUND

Inertial collection refers to the use of inertial forces to cause disengagement of the bolus after defecation is completed. The detached bolus is then conveyed by the transport air into the feces storage container. For the ABSS application, inertial collection will be based on previous work accomplished under contract NAS 9-11268, Inertial Waste Separation System. In this system concept, the user is located on a seat which is suspended on four shafts (with coaxial springs). The seat (and user) are thus free to move axially "up and down". In operation, the user manually induces the desired axially movement, the springs acting to keep the seat in the up position and in contact with the user. Travel is limited by mechanical stops. With some practice, significant accelerational forces are induced in attached fecal material thereby causing separation (and subsequent collection). As applied to the ABSS, this inertial collection design will be refined to improve performance and appearance and to increase user acceptance.

3.0 APPROACH

3.1 Operating Mode

Figure 3-1 illustrates bolus disengagement in simplified form, i.e. a small mass (the bolus) attached to a large mass (the man) by the equivalent of a frangible attachment link. The function of the inertial collection hardware is to rupture the frangible link by the application of inertial forces.

Rupture of the frangible link is accomplished by accelerating the man in a direction to cause tensile forces in the frangible link (the bolus attachment point). This can be accomplished by two modes of operation; the man can be accelerated from a zero velocity condition or the man can be decelerated from a finite velocity condition. Figure 3-2 illustrates these two modes. A major influence on the hardware design for the two modes is the direction of the axial motion, up for Mode 1 and down for Mode 2. Reviewing the relative merits of the two modes, Mode 2 is favored over Mode 1 for the following reasons:

cc: R. W. Murray
G. L. Fogal (4)
J. K. Mangialardi
S. R. Hunt, Ph.D.

PAGE NO.

1 OF 13

RETENTION REQUIREMENTS

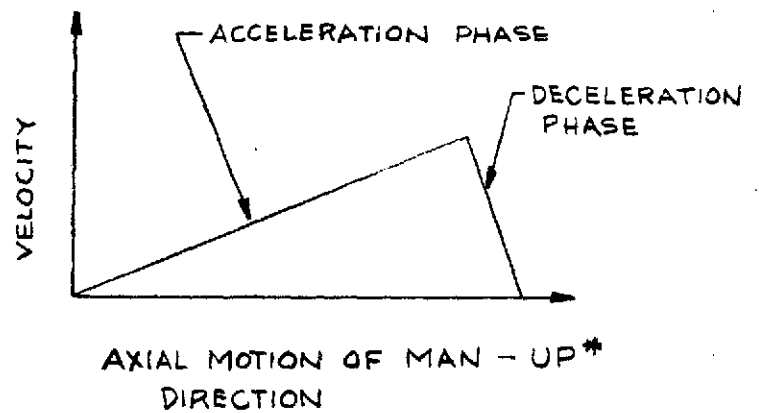
COPIES FOR

☐ 1 MO.
☐ 3 MOS.
☐ 6 MOS.
☐ 12 MOS.
☐ MOS.
☐

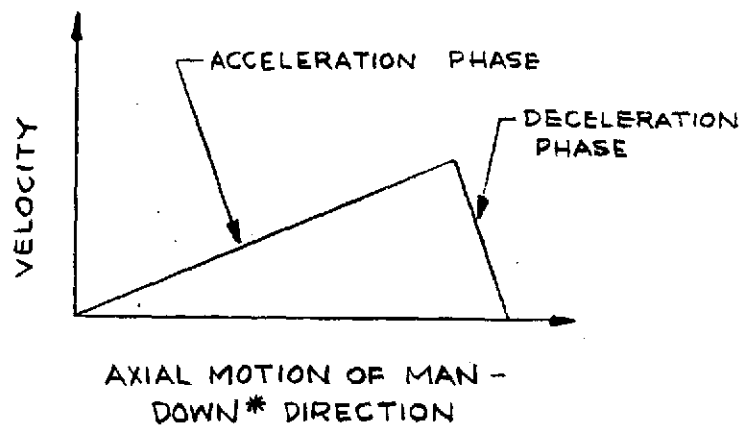
MASTERS FOR

☐ 3 MOS.
☐ 6 MOS.
☐ 12 MOS.
☐ MOS.
☐ DO NOT DESTROY

MODE 1:
DISENGAGEMENT OCCURS
DURING ACCELERATION PHASE.



MODE 2:
DISENGAGEMENT OCCURS
DURING DECELERATION PHASE.



* AS IN A NORMAL GRAVITY ENVIRONMENT.

FIGURE 3-2 OPERATING MODES

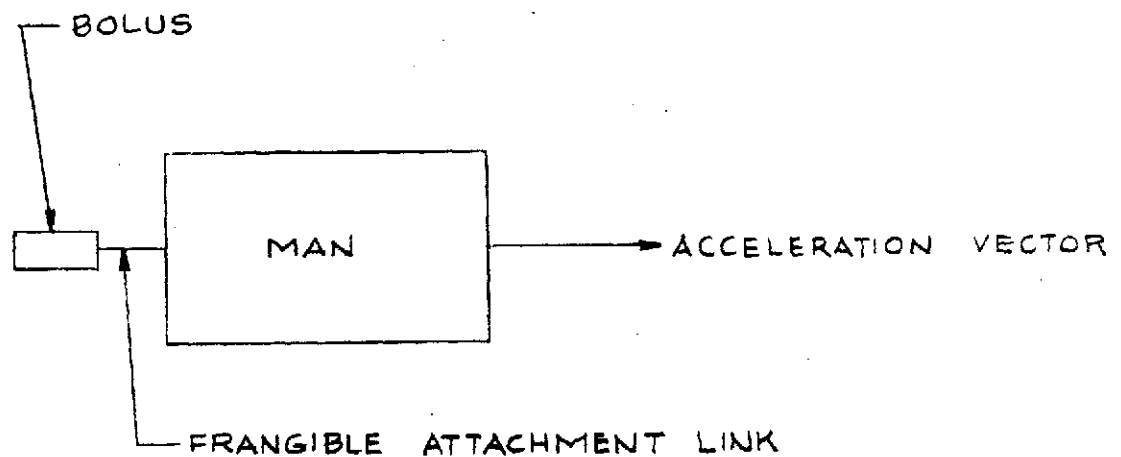


Figure 3-1. Man-Bolus Equivalent System

- (a) For Mode 1, the bolus, after separation, retains an upward velocity component which opposes the transport air flow. In Mode 2, the bolus residual velocity at separation is down thus augmenting the transport air flow.
- (b) In Mode 1, the acceleration must be in excess of one g for worse case conditions (see below). Force requirements are thus relatively large. In Mode 2, the acceleration during the acceleration phase is not critical and may be limited to 0.5 g (or less at the expense of additional axial movement).

For both modes, deceleration is accomplished by use of a cushioned mechanical stop. Imperfect mechanical coupling to the man and body tissue resilience will serve to limit g values seen by the man during the deceleration phase.

3.2 Disengagement Requirement

The apparent force required to reapture the frangible connection of Figure 3-1 is a function of sphincter effectiveness, bolus ejection velocity and composition and interference by one or both of the gluteal prominences. Engineering data are largely non-existent for the above parameters. However, a worse case condition can be postulated as follows:

- (a) Bolus composition derived from a normal diet and of average water content.
- (b) Bolus ejection velocity zero.
- (c) Sphincter effectiveness completely nullified by gluteal prominence interference.

If diarrhetic type feces, little force will be required to rupture the frangible link. If compartmented feces (low water content), the yield strength (of the bolus) will probably be higher than for a bolus of average water content but sphincter effectiveness will not be nullified by gluteal prominence interference.

Fortunately actual stress-strain data for feces of average composition is available and is shown on Figure 3-3. From the upper curve ($X = .32$ cm), the work required to rupture is $43.5 \times .125 = 5.45$ gm - cm/cm². Note that this is for a slowly applied force. A suddenly applied force will, by analogy to other materials, reduce energy requirements significantly.

For worse case conditions as noted above, sphincter action will be nullified by the gluteal prominences. Thus, disengagement energy requirements will be proportional to bolus cross-sectional area. Thus the energy to disengage a bolus 2 cm in diameter = 17.1 gm - cm.

3.3 Acceleration/Deceleration Requirement

Assuming the Mode 2 operating concept, the energy for disengagement of the bolus is provided by accelerating the man-bolus system to a velocity sufficient to provide the necessary energy. Thus for a 2 cm diameter, 10 gram bolus,

$$KE = \frac{Wv^2}{2g} = 17.1 \text{ gm - cm}$$

where W = bolus weight in grams

$$g = 980.7 \text{ cm/sec}^2$$

v = minimum velocity, cm/sec, to provide disengagement energy

$$v^2 = \frac{2g(17.1)}{W} = \frac{2(980.7)(17.1)}{10}$$

$$v = 58 \text{ cm/sec}$$

Different assumptions on worse case bolus diameter and weight will, of course, result in a different value of v .

Having determined the desired minimum velocity, velocity and average acceleration levels as a function of axial motion (of the man) can be calculated with results as shown in Figure 3-4. Figure 3-4(a) is for a 85 kg man; Figure 3-4(b) for a 65 kg man. In both cases, the deceleration travel is assumed to be 0.5 cm (to account for body tissue resilience and imperfect mechanical coupling). Also, the same accelerating force used for the 85 kg man (worse case condition) was used in calculations for the 65 kg man. As would be expected, the g levels are slightly higher for the lighter weight man. However, in neither case can the g levels be considered a danger to the user. Figure 3-5, an excerpt from the NASA Bioastronautic Data Book, shows allowable g limits. For the 65 kg man (worse case), both acceleration (0.497 g @ 0.136 sec, Figure 3-5(b) and deceleration (4.48 g @ 0.015 sec, Figure 3-5(a) values are well within acceptable limits.

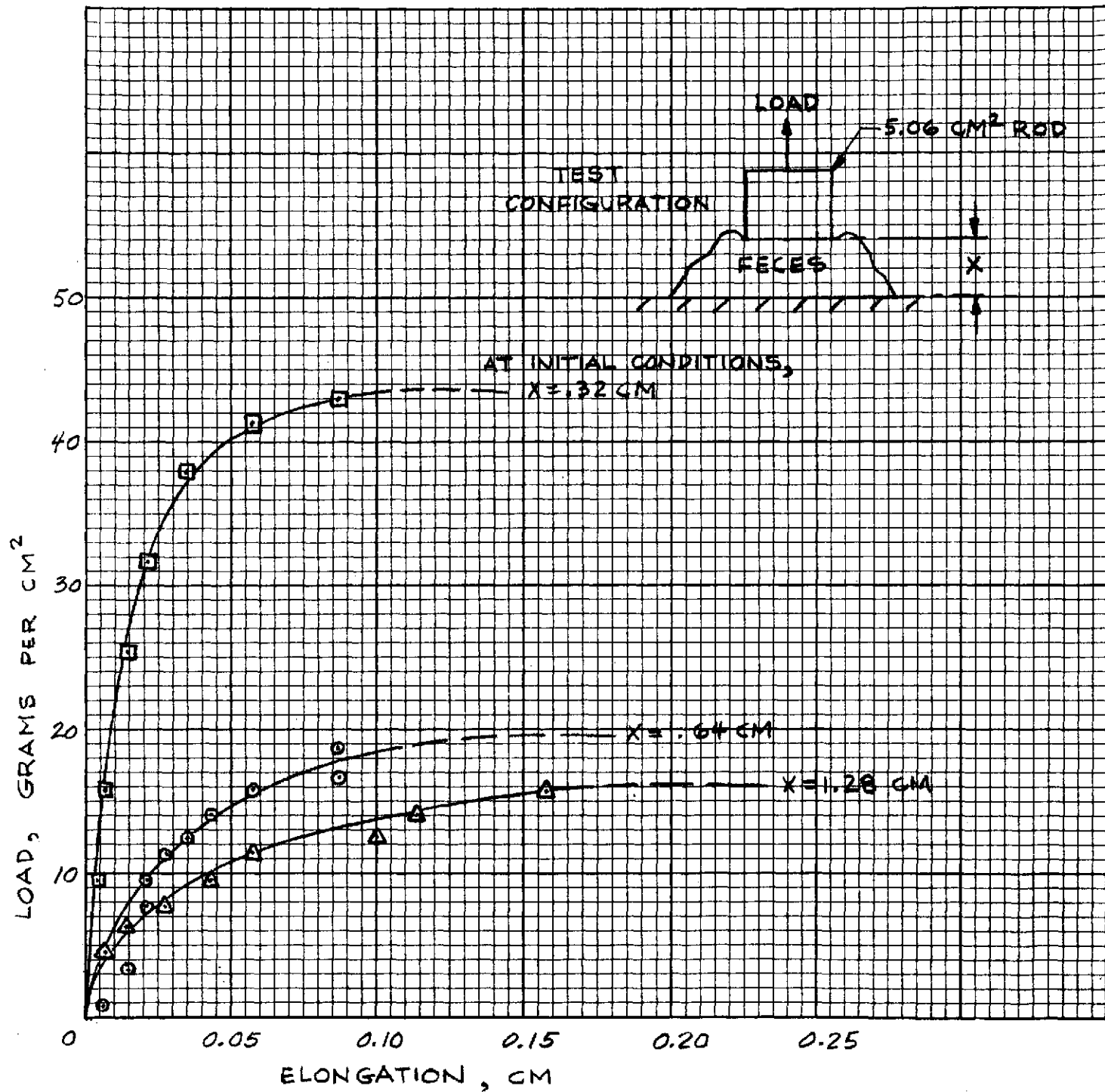
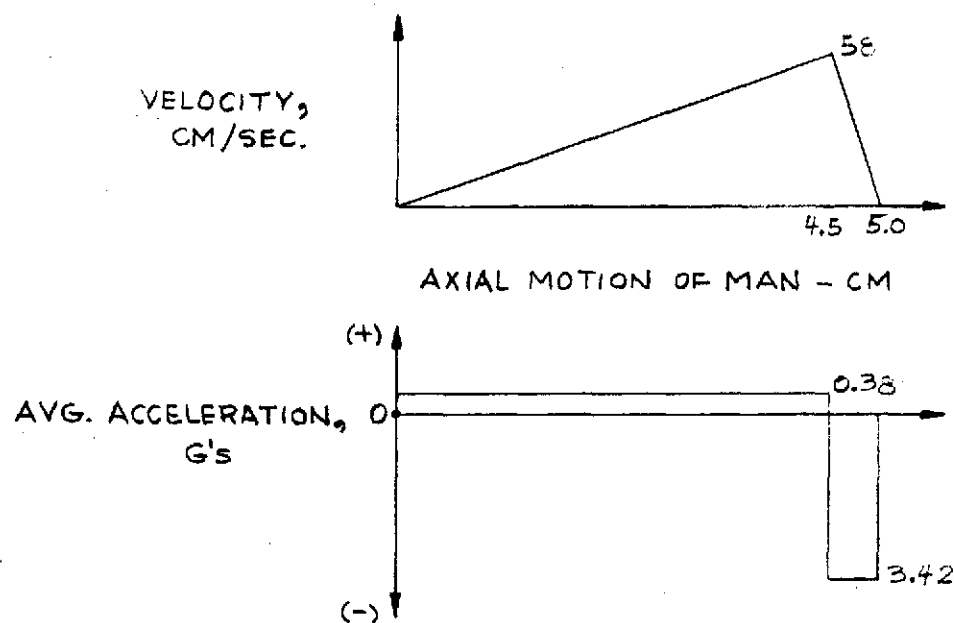


FIGURE 3-3 LOAD/ELONGATION TEST DATA FOR FECES
OF APPROXIMATE AVERAGE COMPOSITION
(REPRODUCED FROM GE PIR 1RG2-73-105)

(a) FOR 85 KG MAN



(b) FOR 65 KG MAN

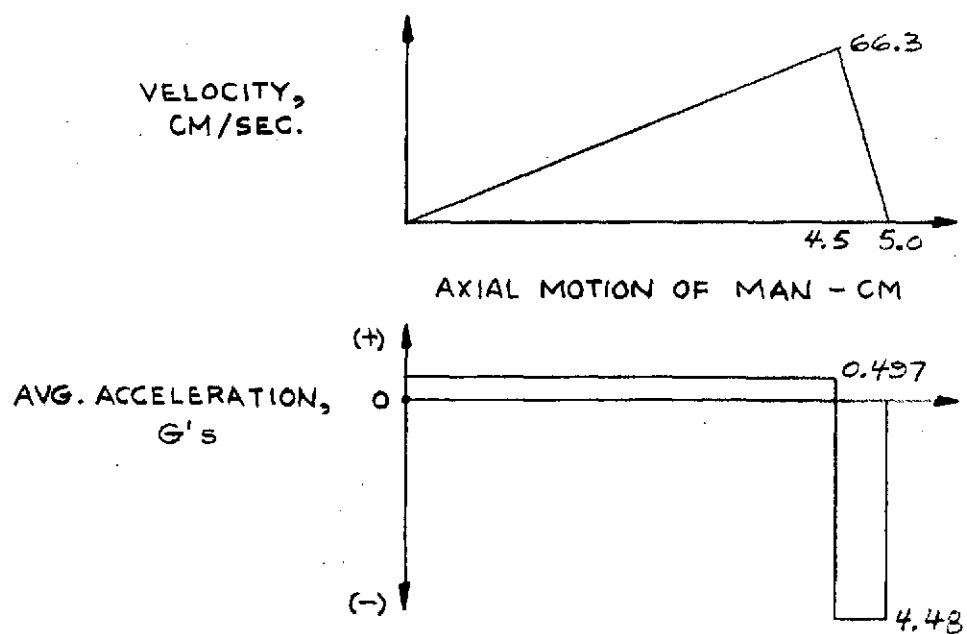
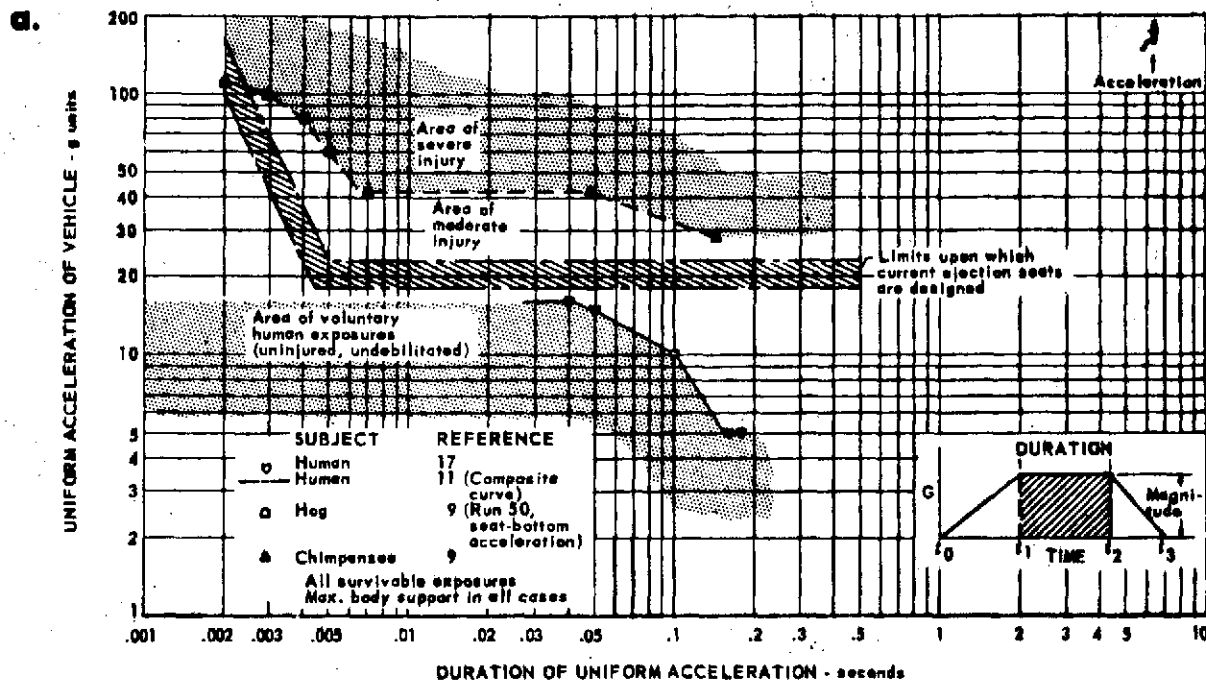


FIGURE 3-4 VELOCITY / ACCELERATION PROFILES



These two graphs show the durations and magnitudes of abrupt deceleration in the G_z (longitudinal) directions which have been endured by various animals and man, showing areas of voluntary endurance without injury, moderate injury, and severe injury marked by shading. Graph a shows data of $+G_z$ acceleration (headward), and b shows data for $-G_z$ acceleration (tailward). Reference numbers on the graphs are those in the original reports.

Source: Eiband [5].

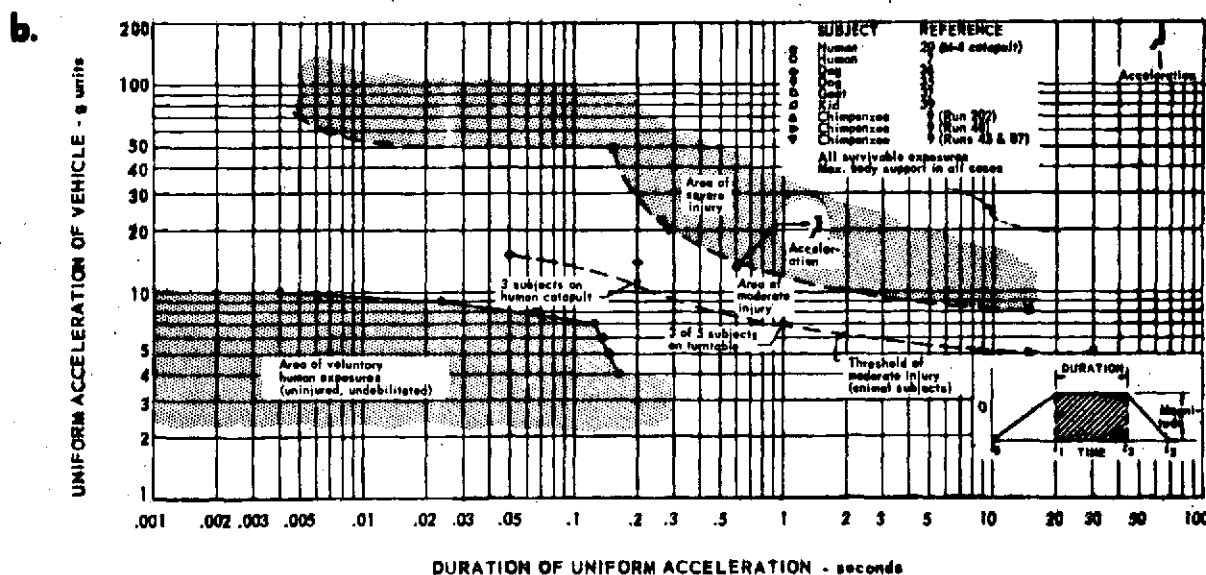


FIGURE 3-5 ABRUPT LONGITUDINAL ACCELERATION
(EXCERPT FROM NASA BIOASTRONAUTICS DATA BOOK)

As previously noted, disengagement energy requirements are a function of cross-sectional area. Thus for a given velocity, the minimum fecal mass which can be disengaged is shown in Figure 3-6. Note that this is for the 85 kg man condition; the bolus mass will be about 30% smaller for the 65 kg man condition.

3.4 General Design Requirements

Table 3-1 lists the general design requirements for the inertial collection hardware. These requirements are based on the above discussion plus consideration of integration operationally and physically with the ABSS. Design of the breadboard hardware will be based on the Table 3-1 requirements.

3.5 Hardware Design Approach

A number of design configurations were considered as noted below.

3.5.1 Manual

Analagous to the configuration designed and tested under contract NAS 9-11268, the necessary axial motion can be accomplished manually by the user. Using mechanical advantage features to assist, the user could push down (against his body restraint) to "elevate" the seat to the "up" position. The user would then pull up to accelerate the seat "downward" to achieve the minimum axial velocity required at the start of the deceleration phase. Although disengagement can be accomplished with a relatively simple mechanical system, several operational problems are apparent.

- (a) The user cannot sense that the required g levels have been obtained. Thus the user will lack confidence that disengagement has been achieved.
- (b) Depending on the effectiveness of the user's body constraint, the physical action/movement required can "uncenter" the user and thereby create a contamination problem.
- (c) The user must be physically capable of applying the required forces. An arm injury or a debilitating illness could prevent effective operation.

Operational problems (a) and (b) above may be negated by design innovation. However, problem (c) reaffirms the need for an automated approach.

3.5.2 Compressed Spring

Figure 3-7 shows conceptually an approach using compressed springs to provide the required accelerating force. The total spring force ($85 \times 0.38 = 32.3 \text{ kg} = 71 \text{ lbs.}$) and deflection ($4.5 \text{ cm} = 1.77 \text{ in.}$) appears reasonable. As shown in Figure 3-7, the accelerating springs are compressed by a motor driven cam rotating coaxially with the transport tube. Compressing the springs moves the seat (and user constrained thereto) to the "up" position. Continued rotation of the cam suddenly releases the seat, the compressed springs accelerating the seat (and user) to the desired velocity at impact. Continued rotation of the cam can produce as many acceleration/deceleration cycles (Mode 2 operation, see Section 3.1) as desired.

Power requirements are minimal; a 10 second cycle time will require a drive motor output of 38 watts. Minimizing sliding and rotary friction will be an important design consideration.

TABLE 3-1. INERTIAL COLLECTION REQUIREMENTS

Objective

Provide inertial forces to accomplish bolus disengagement after defecation.

Approach

Using ABSS type collector configuration, add necessary mechanisms to provide inertial forces coincident with the vertical axis of the storage container.

Design Parameters

1. Provide cycle of slow acceleration followed by rapid deceleration (to accomplish disengagement).
2. Accelerate user to minimum velocity of 58 cm/second at impact with deceleration stop; limit acceleration to 0.5 g maximum. Assume deceleration travel of 0.5 cm maximum, 0.25 cm minimum (travel provided by user body compliance and coupling to hardware).
3. Accomodate user mass range of 75 ± 10 Kg.
4. Start/stop of inertial cycle initiated by operator; all other functions automatic.
5. Automatically provide two acceleration/deceleration cycles.
6. Design to operate on 28 VDC.
7. Integrate mechanically and electrically with sampling and feces mass sensor capabilities.
8. Assume feces deactivation by air drying.

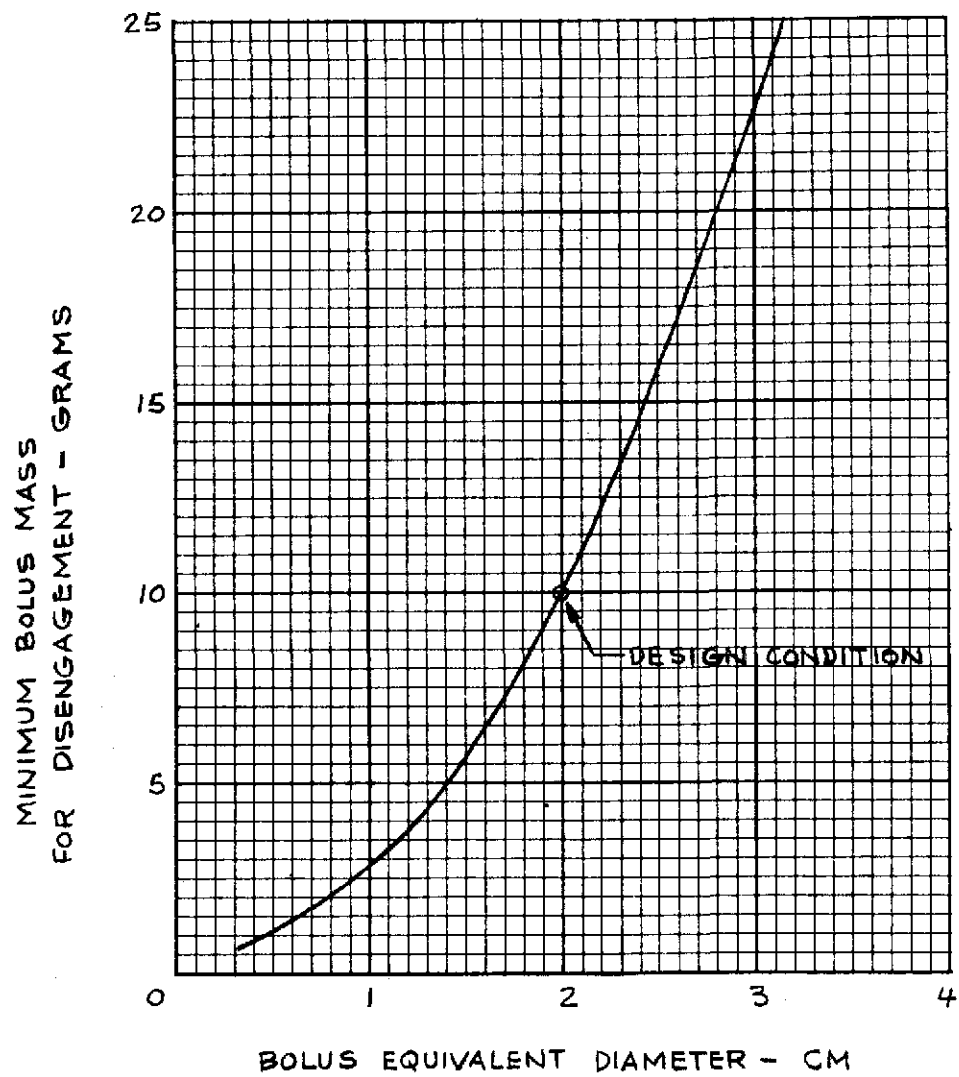


FIGURE 3-6 MINIMUM BOLUS SIZE

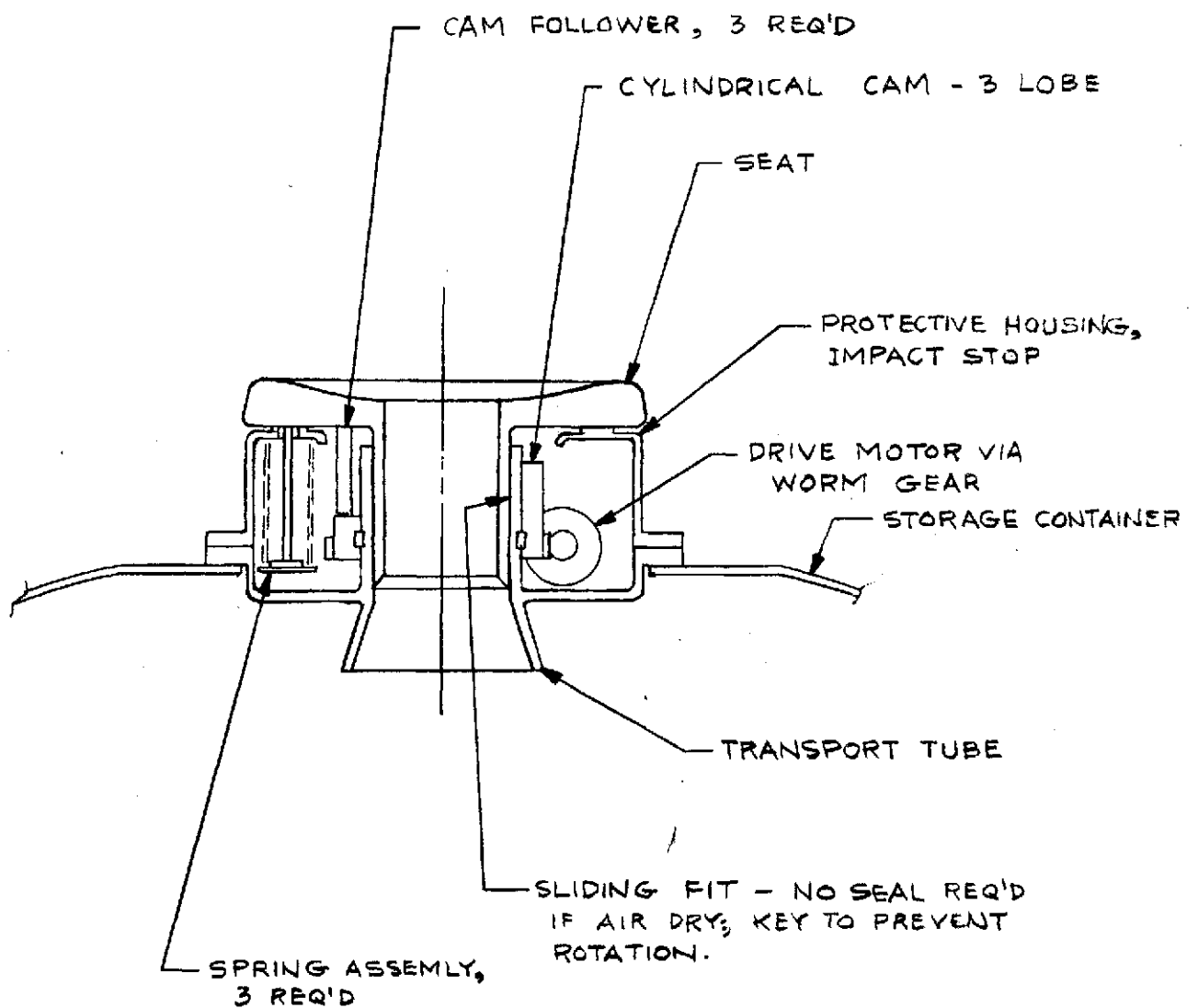


FIGURE 3-7 COMPRESSED SPRING CONCEPT

3.5.3 Pneumatic Actuator

Figure 3-8 illustrates a pneumatically powered concept. Gas from the spacecraft high pressure supply is reduced to two pressure levels. About 5 psig gas pressure could be used to elevate the seat to the up position. Assuming an effective actuator piston area of 3.0 in², gas at about 25 psig admitted to the DOWN manifold via solenoid valve S2 (S1 open to vent) will provide the necessary force to accelerate the seat (and attached user) to the desired impact velocity.

As with the compressed spring concept, a balance of forces coaxial with the transport tube is important for successful operation. Also the DN manifold and/or the pressure regulator must be capable of maintaining the necessary gas pressure within the actuators throughout the total piston stroke. An operational disadvantage is the required interface with the spacecraft high pressure gas supply.

3.5.4 Electro-Mechanical

The preceding two concepts store the energy necessary for powering the acceleration phase of the cycle. Alternately, a direct electro-mechanical drive can be used to translate the seat (and user) during the acceleration phase. Although mechanical complexity can be reduced significantly, peak power demand is considered impractical for spacecraft application. For the 85 kg man, an output of 2.5 KW is required (for about 0.015 second).

3.5.6 Selected Approach

A compressed spring concept (See Example, Section 3.5.2) appears to be the preferred hardware design approach and thus will be the design basis for the breadboard hardware.

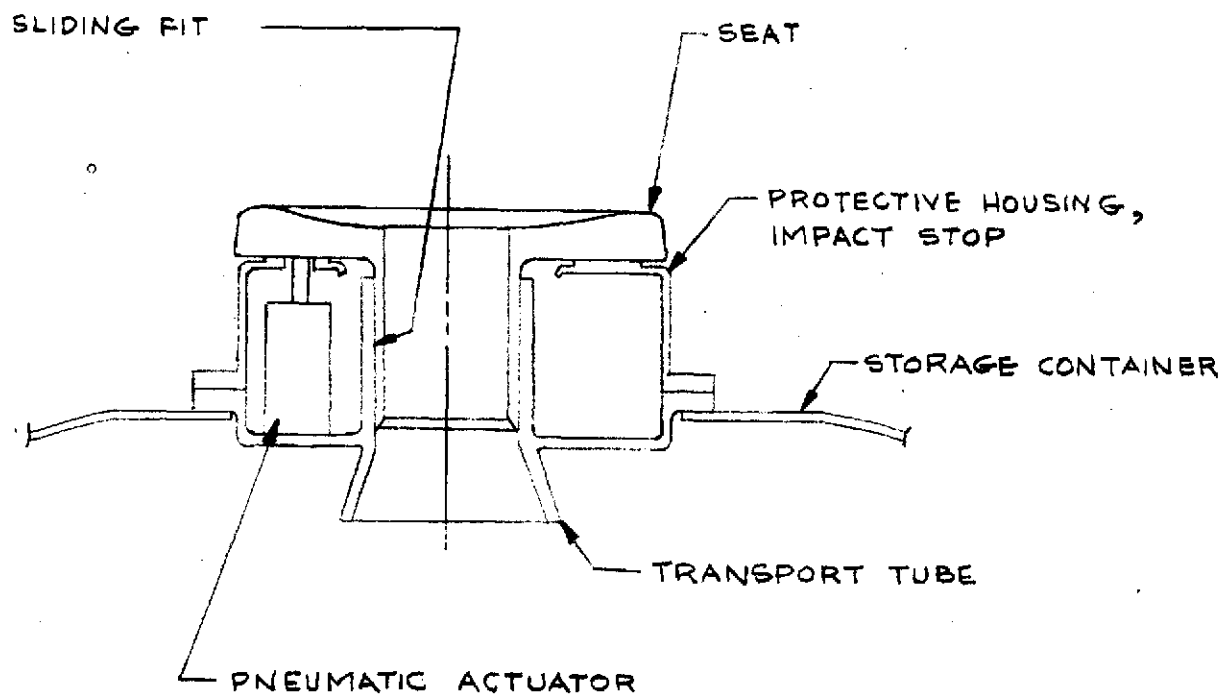
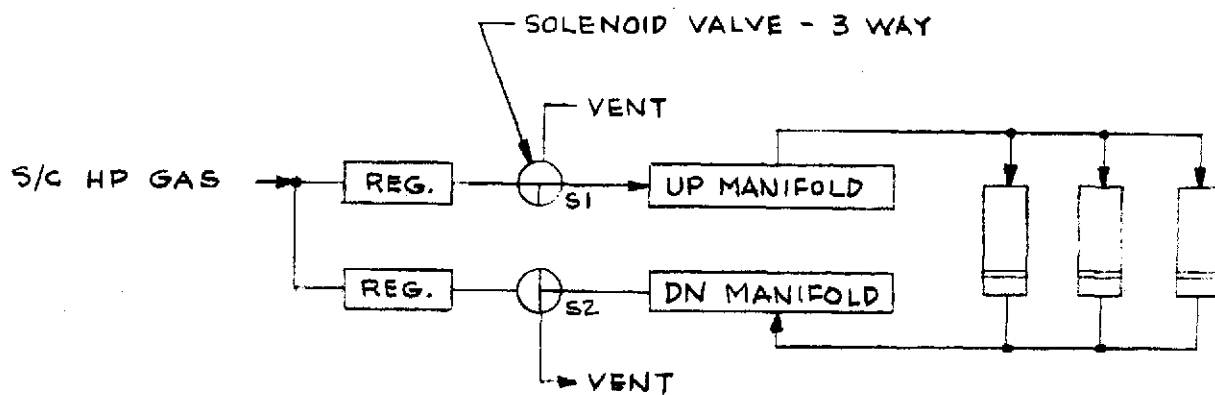


FIGURE 3-8 PNEUMATIC ACTUATOR CONCEPT

GENERAL ELECTRIC

SPACE DIVISION
PHILADELPHIA

PROGRAM INFORMATION REQUEST / RELEASE

*CLASS. LTR.		OPERATION	PROGRAM	SEQUENCE NO.	REV. LTR.
U		1R60	74	119	
PIR NO.					
*USE "C" FOR CLASSIFIED AND "U" FOR UNCLASSIFIED					
FROM G. L. Fogal, Bioengineering Programs Mgr. Room #M-2101, VFSC Extension - 5636			TO File		
DATE SENT	DATE INFO. REQUIRED	PROJECT AND REQ. NO.		REFERENCE DIR. NO.	
6/6-27-74		ABSS Improved Feces Measurement and Sampling			
SUBJECT					

INERTIAL COLLECTOR BREADBOARD MODEL TEST RESULTS

INFORMATION REQUESTED/RELEASED

1.0 SUMMARY

Both quantitative and qualitative tests were performed using the Inertial Collector Breadboard Model. The test results indicate that the Inertial Collector concept, as depicted by the breadboard model and subject to the limitations of simulated zero "g" testing in the laboratory, can provide satisfactory user/feces disengagement during zero "g" defecation.

2.0 TEST SET-UP

The Inertial Collector concept is described in PIR 1R60-74-101; the breadboard model assembly is shown in Figure 2-1, GE SK 56198-870. Figure 2-2 shows the Breadboard Model Assembly (less motor drive). In order to simulate zero "g" operating conditions, the breadboard model was constrained to move horizontally. This eliminates gravity effects but not the inertial loading effect of the user's body. As shown in Figure 2-3, the user (or equivalent weight) is supported on a wheeled cart which is attached to the constrained breadboard model Inertial Collector. As shown in Figure 2-3, the test assembly is raised at one end (1.5° angle with horizontal) to compensate for the cart rolling friction.

3.0 TEST RESULTS

3.1 Qualitative

Live subjects were subjected to several cycles of the breadboard model. Accelerations and decelerations induced by the breadboard model did not cause subject discomfort.

3.2 Quantitative

3.2.1 Power Input

Drive motor power input was found to be independent of user weight (over the tested range of 110 to 190 lbs., i.e. weight of user or equivalent plus weight of cart). For 27 VDC to the motor, 5.4 watts were required during free rotation of the cam; after contact of the cam with the cam followers, power input increased to 18.9 ± 1.4 watts until cam follower release. Average cycle time under these conditions was found to be 9 seconds. It should be noted that the worm gear drive was lubricated. Also since the spring (SK 56198-871) was slightly oversize and rubbed on the inner surface of one or

cc: R. W. Murray
S. R. Hunt, Ph.D.

PAGE NO.

1 OF 7

RETENTION REQUIREMENTS

COPIES FOR

☐ 1 MO.

☐ 3 MOS.

☐ 6 MOS.

☐ 12 MOS.

☐ MOS.

☐

MASTERS FOR

☐ 3 MOS.

☐ 6 MOS.

☐ 12 MOS.

☐ MOS.

☐ DO NOT DESTROY

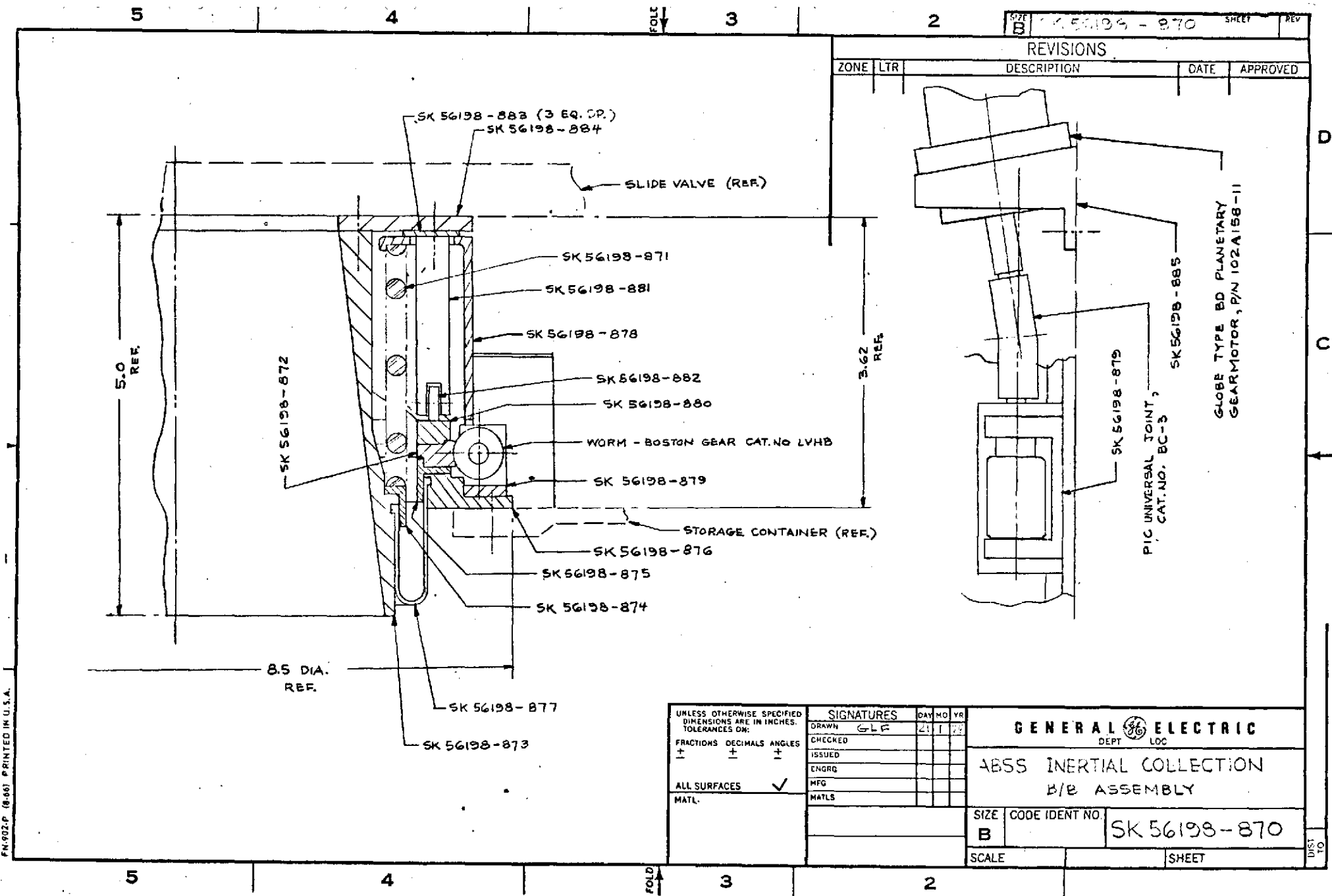


Figure 2-1 Inertial Collector Breadboard Model Assembly

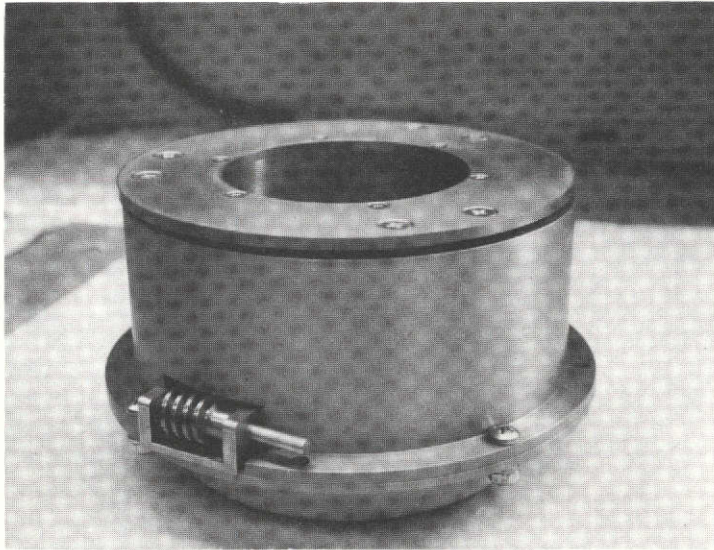


Figure 2-2(a) Inertial Collector Breadboard Model Assembly
(Less Drive Motor)

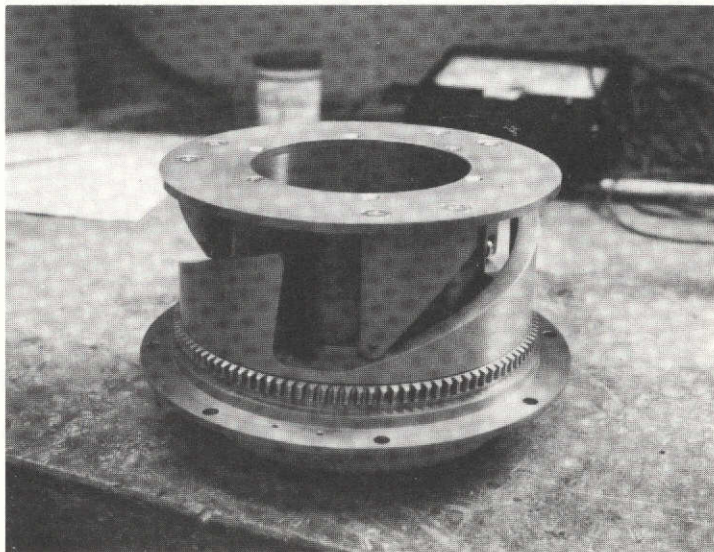


Figure 2-2(b) Inertial Collector Breadboard Model
(Partially Assembled)

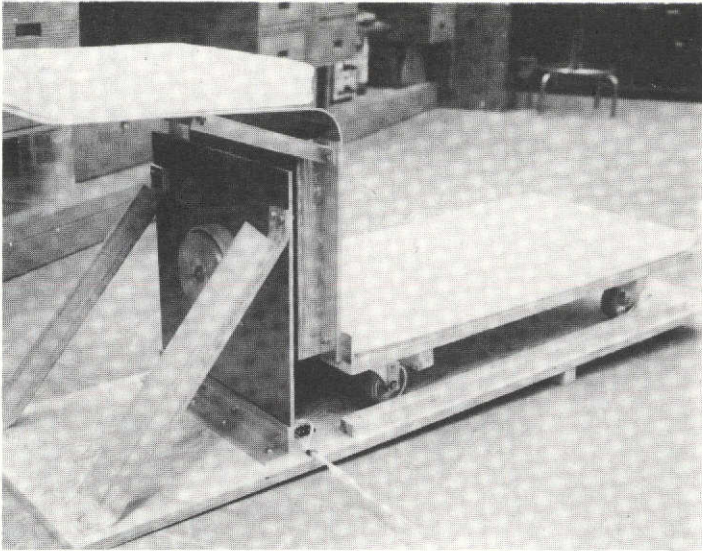


Figure 2-3(a) Test Assembly

Figure 2-3(b) Test Assembly (with
4-40 lb iron weights)

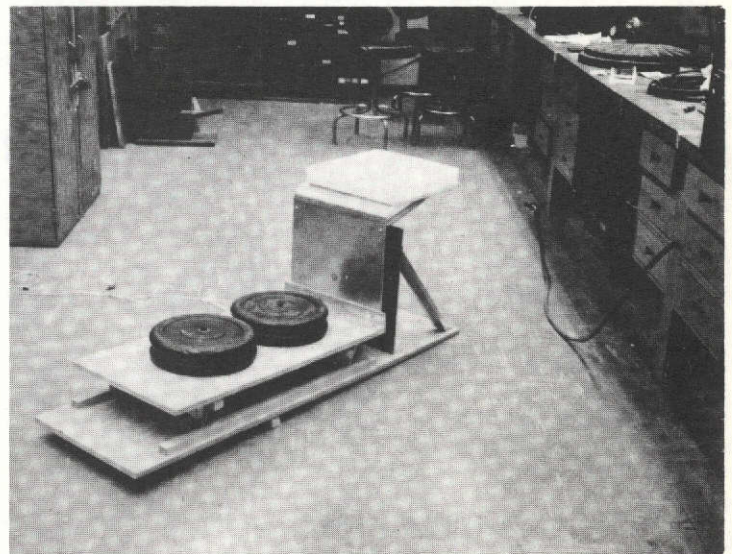


Figure 2-3(c) Test Assembly (with
test subject)

two of the cam followers (SK 56198-881), this interface was also lubricated.

3.2.2 Deceleration/Time Data

Figure 3-1 shows a typical deceleration/time trace for the Inertial Collector breadboard model. Both the test subject and breadboard model were instrumented with crystal type accelerometer sensors oriented to pick-up axial motion (horizontal) accelerations. For the subject, the accelerometer was cemented to a hardhat (less liner) and held firmly in contact with the top of the subject's head. The subject also was positioned (and held himself) snugly against the end of the cart attached to the breadboard model. ENDEVCO model 2213C crystal accelerometer sensors were used. These were conditioned by CRL model 9006 Charge Amplifiers and a 500 Hz filter (no filter used for subject) followed by a DC amplifier and CEC galvanometer recorder model 7-326.

Table 3-1 summarizes the deceleration/time data for a number of test conditions. For a given test condition, the deceleration/time trace was found to be highly consistent. It should be remembered that the disengagement forces seen by an attached bolus are those induced into the subject's body and not the acceleration experienced by the breadboard model per se. Further, in addition to the difficulty of instrumenting the subject's body, contact of the subject's torso and the test cart are not realistic of zero "g" use conditions. Thus the attenuation (as compared to the breadboard model per se) of the subject deceleration/time data can only be considered as representative of the possible attenuation which will be experienced in actual zero "g" operational use.

4.0 CONCLUSIONS

The Inertial Collector concept as exemplified by the breadboard model can alleviate or eliminate disengagement problems experienced in zero gravity operations of past spacecraft missions. Added power and volume requirements for the Inertial Collector are minimal. Mechanical failures were not encountered during breadboard model checkout or subsequent testing. Although projected deceleration levels experienced by the user were less than planned (3.4g, see PIR-1R60-74-101), this could be due to the difficulty of simulating zero "g" conditions in the laboratory as well as the assumptions used in arriving at the projected value.

TABLE 3-1 DECELERATION/TIME DATA SUMMARY

CONDITION	PEAK DECELERATION	RISE TIME (1)	DURATION(2)
1. 185 lb load (subject plus cart)			
Subject	2.2g ⁽³⁾	.02 sec.	.05 sec.
Breadboard Model	12.7	.002	.0067
2. 110 lb load ⁽⁴⁾	19.6	.002	.006
3. 160 lb load ⁽⁴⁾	14.6	.002	.006
4. 190 lb load ⁽⁴⁾	14.6	.002	.006

(1) Time to peak deceleration.

(2) 1/2 cycle time, i.e. from start to decay to zero after peak deceleration reached.

(3) Top of head.

(4) Weights plus cart.

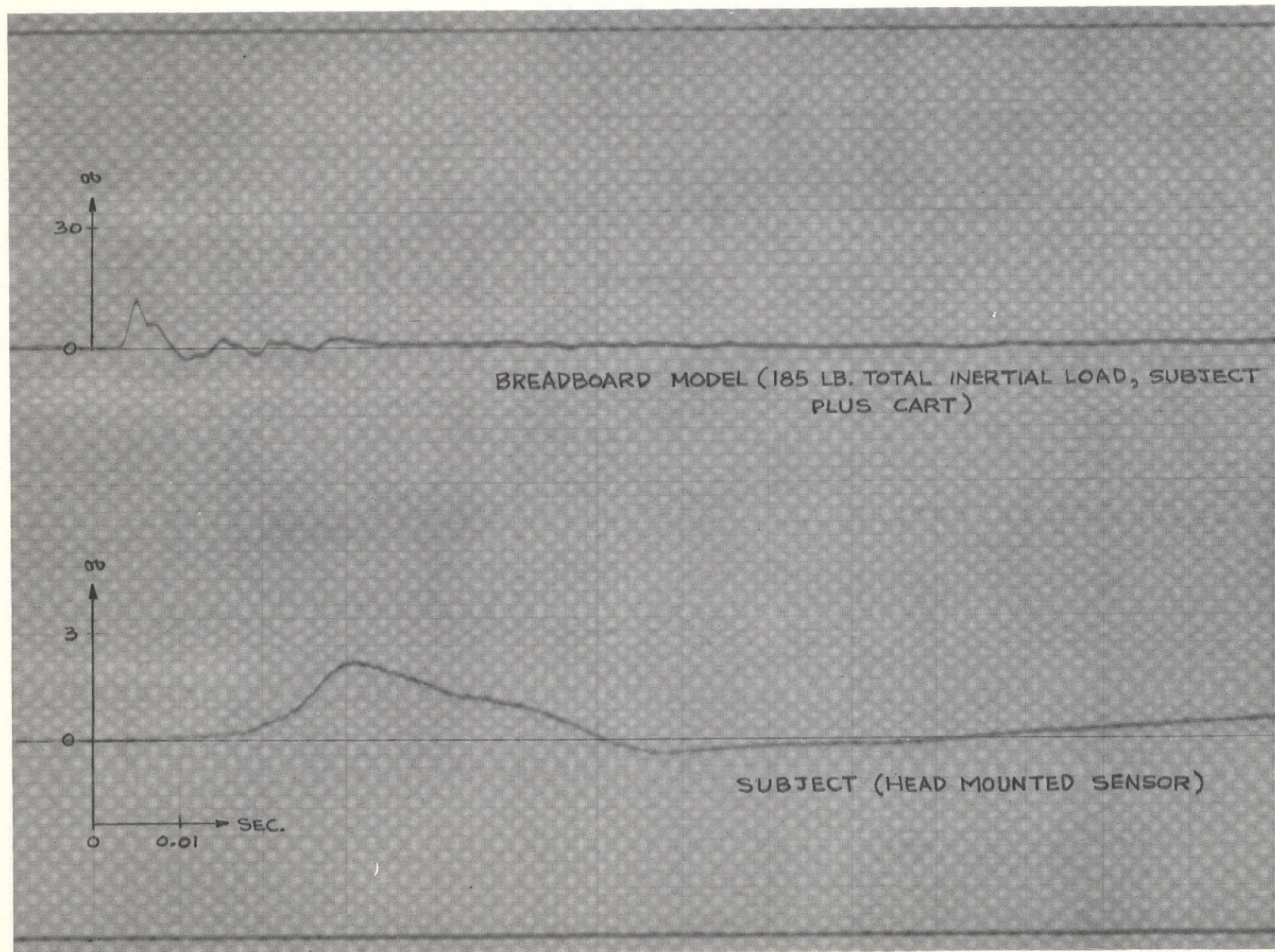


Figure 3-1 Deceleration/Time Trace

GENERAL ELECTRIC

SPACE DIVISION
PHILADELPHIA

PROGRAM INFORMATION REQUEST / RELEASE

PIR NO.	*CLASS. LTR. U	OPERATION 1R60	PROGRAM 74	SEQUENCE NO. 102	REV. LTR.
*USE "C" FOR CLASSIFIED AND "U" FOR UNCLASSIFIED					

FROM G. L. Fogal, Program Manager-Environmental Engineering, Room #M-2101, VFSC	TO Distribution
--	--------------------

DATE SENT 1-15-74	DATE INFO. REQUIRED	PROJECT AND REQ. NO. ABSS Improved Feces Measurement and Sampling	REFERENCE DIR. NO.
----------------------	---------------------	--	--------------------

SUBJECT MASS MEASUREMENT

INFORMATION REQUESTED/RELEASED

1.0 SUMMARY

First cut design requirements for real time measurement of feces mass are determined.

2.0 BACKGROUND

The feces mass measurement design will be based on previous General Electric funded effort as described in GE PIR's 1R62-73-114/119. Specifically, the feces mass measurement design will use the ABSS DRY-JOHN "slinger assembly" as the sensing element. As described in PIR 1R62-73-119, the incremental change in power input (or equivalent, e.g. change in torque requirements) to the constant speed slinger motor is monitored. This power change (or equivalent) is due to the impact of the feces with the slinger assembly and is proportional to the incremental feces mass. Total mass is then obtained by integration of the delta power input (or equivalent) signal times a proportionality factor, this latter being a function of slinger assembly geometry and rpm. Figure 2-1 illustrates the relationship of the basic system components needed for feces mass measurement.

3.0 DESIGN REQUIREMENTS

Table 3-1 lists projected design requirements for the feces mass sensor. These were derived from assumed operational considerations and experience gained from the previous GE funded effort noted above. Figure 3-1 shows a derived relationship between weight of feces and energy transfer (from the slinger to the feces sample). The data below 100 grams represents actual data points as reported in PIR 1R62-73-119. The values noted in Table 3-1 assumes the projection for samples over 100 grams is valid.

cc: R. W. Murray
G. L. Fogal (4)
S. Lowenberg

PAGE NO.

1 OF 4

RETENTION REQUIREMENTS

COPIES FOR

MASTERS FOR

<input type="checkbox"/> 1 MO.	<input type="checkbox"/> 3 MOS.
<input type="checkbox"/> 3 MOS.	<input type="checkbox"/> 6 MOS.
<input type="checkbox"/> 6 MOS.	<input type="checkbox"/> 12 MOS.
<input type="checkbox"/> MOS.	<input type="checkbox"/> MOS.
<input type="checkbox"/>	<input type="checkbox"/> DO NOT DESTROY

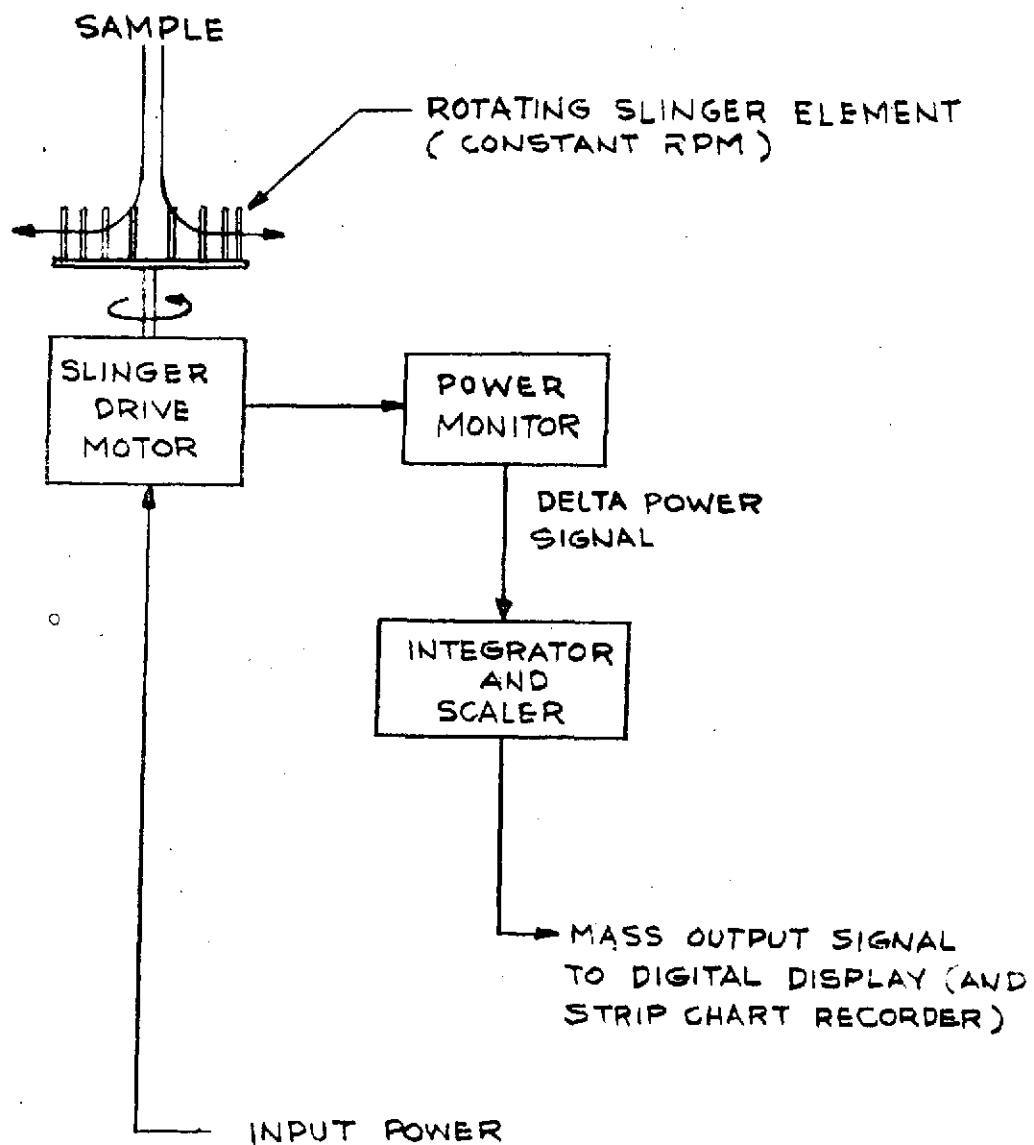


FIGURE 2-1 FECS MASS MEASUREMENT

TABLE 3-1. FECES MASS SENSOR

Objective

Provide real time measurement of total feces mass per defecation.

Approach

Using ABSS type collector configuration, relate slinger delta input power to the total feces mass.

Design Parameters

1. Provide real time feces mass measurement with measurement error of less than $\pm 2\%$ of the actual value or ± 1 gram, whichever is greater.
2. Accomodate individual defecations ranging in mass up to a maximum of 400 grams (110 grams average) of normal composition or a maximum of 500 grams for feces of diarrhetic composition and one or more increments per defecation.
3. Operate slinger at a constant rotational velocity (or correct mass measurement to this condition), nominally 2000 rpm.
4. Total delta power input range projected to be 1.5 to 375 watt-seconds, however, provide a normal range of 1.5 to 35 watt-seconds (for 30 to 150 grams mass range) with corresponding time durations projected from about 0.05 to 1.5 seconds. Also provide an extended range capability of 35 to 375 watt-seconds; measurement accuracy may be degraded if necessary to obtain this additional range.
5. Display power input, scaled to equivalent mass units in grams, on a digital meter. Hold displayed value until increased by the addition of a following feces increment or until meter reset by the operator.
6. Design system to operate on 28 VDC.
7. System start/stop shall be initiated by the operator; all other functions shall be automatic.
8. Integrate mechanically and electrically with sampling and inertial seat capabilities.

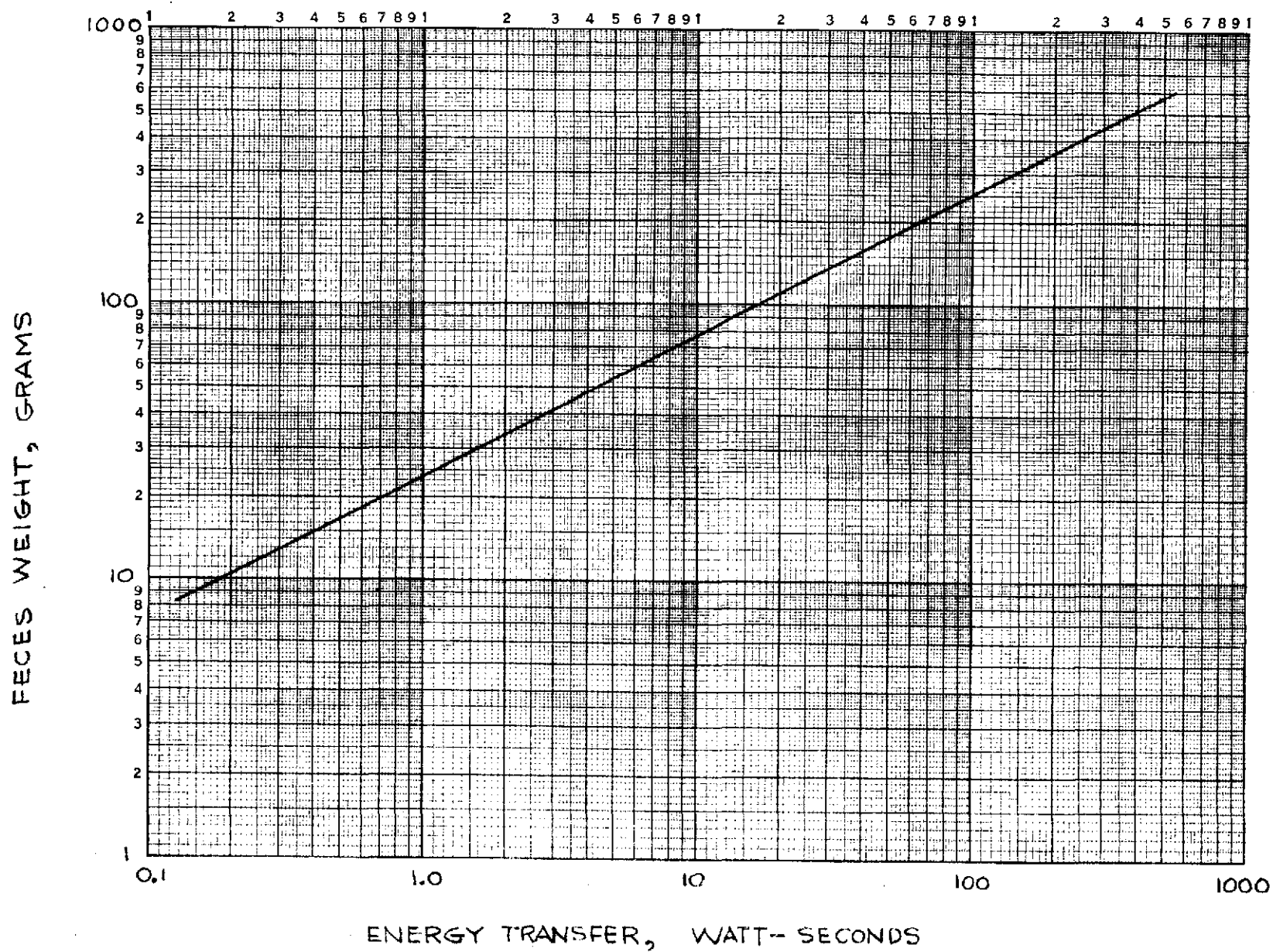


FIGURE 3-1 ENERGY TRANSFER

GENERAL ELECTRICSPACE DIVISION
PHILADELPHIA**PROGRAM INFORMATION REQUEST / RELEASE**

*CLASS. LTR.		OPERATION	PROGRAM	SEQUENCE NO.	REV. LTR.
PIR NO. U		1JL3	XX	1019	
*USE "C" FOR CLASSIFIED AND "U" FOR UNCLASSIFIED					
FROM Ronald S. Young, U2446 X4351			TO Gordon Fogal		
DATE SENT 10/7/74	DATE INFO. REQUIRED	PROJECT AND REQ. NO. ABSS Improved Feses Measurement and Sampling		REFERENCE DIR. NO.	
SUBJECT ABSS FECES MASS MEASUREMENT MICROPROCESSOR SYSTEM					
INFORMATION REQUESTED/RELEASED The attached describes the electronics for the ABSS Feces Mass Measurement breadboard.					
R. Young A. Anderson J. Avery		PAGE NO. 1 OF 47	RETENTION REQUIREMENTS		
			COPIES FOR	MASTERS FOR	
			<input type="checkbox"/> 1 MO.	<input type="checkbox"/> 3 MOS.	
			<input type="checkbox"/> 3 MOS.	<input type="checkbox"/> 6 MOS.	
			<input type="checkbox"/> 6 MOS.	<input type="checkbox"/> 12 MOS.	
			<input type="checkbox"/> MOS.	<input type="checkbox"/> MOS.	
			<input type="checkbox"/>	<input type="checkbox"/> DONOT DESTROY	

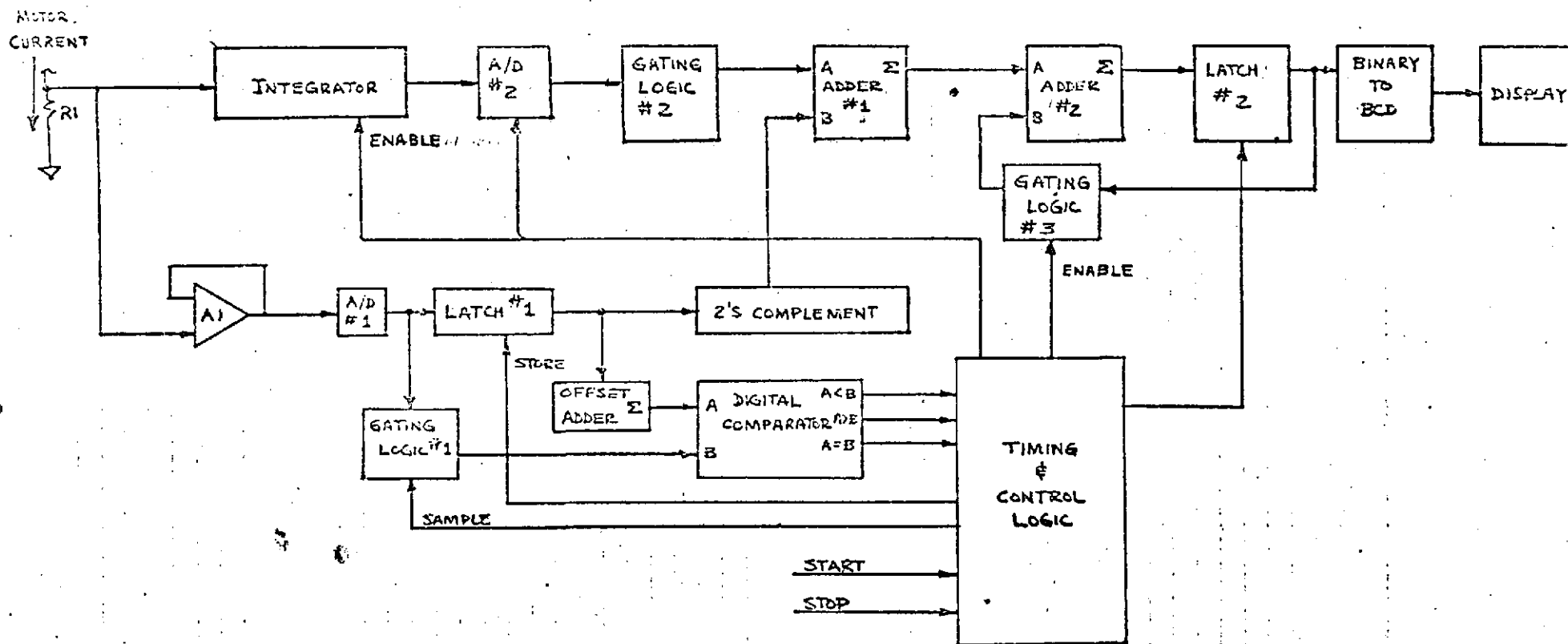
ABSS/FECES MASS MEASUREMENT MICROPROCESSOR SYSTEM

Electronic Design

The ABSS electronics continuously monitors the motor current of a closed-loop servo-amplifier system utilizing a DC shunt motor rotating at a constant speed. The motor current is considered representative of a force placed on the motor. The electromechanical configuration consists of a collector assembly attached to the motor shaft. A mass deposited on the collector, or slinger, assembly results in a change in motor current to maintain constant speed. When the mass was slung off, the motor current returns to its steady-state value.

Figure 1 is a functional block diagram of the ABSS electronics utilizing conventional hard-wired TTL circuitry. The discussion of the block diagram is based on the following assumptions:

1. The motor system servo-amplifier maintains the motor at a constant speed.
2. The change in motor current required to maintain the motor at a constant speed when a force is placed on the shaft is directly related to the value of the force. The integral of this motor current change from its steady-state value as a result of this force is directly proportional to that force. The force in this case would be a mass deposited on the collector assembly attached to the motor shaft and then slung off due to its rotation.
3. A start and stop signal will be externally generated by the user.
4. Measurement of the motor current is accomplished by detecting the voltage developed across the sense resistor, R_1 . Amplifier A1 serves as a gain amplifier for the analog-to-digital converter, A/D 1.



ABSS BLOCK DIAGRAM

FIGURE 1

RE/OUNG
3/27/74

Operational Sequence

1. START command received from external source.
- 2a Timing and control logic issues STORE command to LATCH 1 to store output of A/D 1. This value represents the initial steady-state motor current.
 - b Take 2's complement of LATCH 1 output and send it to ADDER 1.
 - c Add a delta to LATCH 1 output and send it to digital comparator.
 - d Enable GATING LOGIC 1 to continuously present the output of A/D 1 to digital comparator.
3. Timing and control waits for first deposit on the slinger. When this occurs, the motor current will increase and the digital comparator will output an $A > B$ signal.
4. Enable integrator when $A > B$ is received, enable GATING LOGIC 2.
5. Stop integration when $A < B$ signal is received. This indicates that the mass has been slung off the slinger assembly and the current has returned to its initial value.
6. Add GATING LOGIC 2 output and the 2's complement of LATCH 1 output in ADDER 1. This results in the subtraction of the steady-state motor current value and eliminates that offset.
7. Enable GATING LOGIC 3 circuits, which permits any previous values stored at the outputs of LATCH 2 to be added to the output of ADDER 1, which is the current coating.
8. Store output of ADDER 2 to LATCH 2. Binary-to-BCD conversion is performed and the results are displayed as decimal digits.
9. Reset integrator.

10. STOP signal received? If not, go to step 2.

11. If STOP signal received, clear all electronics.

An examination of the block diagram and its operational sequence revealed that the control and measurement requirements were most efficiently implemented by utilizing a microprocessor.

The microprocessor eliminated all the conventional electronics with the exception of the gain amplifier A1, the analog-to-digital converter, A/D 1, and the 4 digit decimal display. The integration function, subtraction of motor current steady-state values, setting of the threshold, direction of when the threshold is exceeded, cumulative addition of previous readings, and the binary-to-BCD conversions are all performed by programs in the microprocessor. All timing control functions and decisions, i.e., detection of mass deposition, start/stop integration, etc., are under program control.

An IMP-16C/200 was selected as the microprocessor. It contains a 16 bit I/O capability. The A/D converter is a 10 bit device, and the digital display has a four digit decimal capability, requiring an input to it of four groups of four binary-coded-decimal (BCD) digits, or 16 bits.

The present design involves a volatile memory system, i.e., memory contents are in RAM and are lost when power is turned off. All special software required for the system will be entered into ROMs (non-volatile) when finalization of all experiment techniques has been achieved and program changes are not required.

Future systems would employ programmable ROMs (PROMS) to permit changes to be made quickly. The programs would be written into a PROM, run with the system and experiment results gathered. If there were changes to be made, a new PROM would be made, the "old" one removed, and the new one plugged in and the experiment would continue under its new operating instructions.

This technique permits the construction of one model whose operation can be changed by substituting one ROM with another ROM.

This achieves a flexibility and economy previously unavailable in hard-wired systems.

The software integration, control, and binary-to-BCD programs and interface hardware were checked out and verified by substituting for the motor current with a known waveform. The control/exp switch was placed in the exp position, and START was depressed. A series of successive rectangular pulses of constant amplitude and pulse width were used as inputs with the resultant readings:

<u>Pulse No.</u>	<u>Readings</u>
1	100
2	200
3	301
4	401
5	502
6	602
7	703
8	804
9	904
10	1005

The accuracy over ten input pulses was 0.5%.

The rectantular pulse was then changed by halving the pulse width and retaining the same amplitude with the following readings:

<u>Pulse</u>	<u>Reading</u>
1	50
2	100
3	150
4	201
5	252
6	303
7	353
8	404
9	454
10	505

The pulse width was kept the same, and the amplitude doubled:

<u>Pulse</u>	<u>Reading</u>
1	100
2	200
3	301
4	402
5	503
6	603
7	704
8	805
9	905
10	1006

A control panel was built to permit programming the microprocessor and provide the START and STOP experiment functions.

The following paragraphs provide the procedures for performing the various control panel operations.

The four digit hexadecimal thumbwheel switches are used to set memory address locations and the data to be entered into memory. The four digit hexadecimal display will display the memory address or the data.

Loading Memory

1. Set the thumbwheel switches to the desired hexadecimal equivalent of the memory address.
2. Press LOAD ADDRESS. The selected hexadecimal address will be displayed.
3. Set the thumbwheel switches to the data value to be loaded.
4. Press LOAD DATA. The data will be displayed, and the memory location will be incremented automatically.
5. Subsequent memory locations may be loaded in consecutive order by setting the thumbwheel switches with the data value to be loaded and pressing LOAD DATA after each setting.

Altering Memory Locations

1. Set the address of the location whose contents are to be changed on the thumbwheel switches, and press LOAD ADDRESS.
2. Set the thumbwheel switches to the new data value, and press LOAD DATA.

Examining Memory Locations

1. Set the thumbwheel switches to the memory address to be examined, and depress LOAD ADDRESS. The selected address will be shown on the display.
2. Press DISPLAY. The contents of the selected address location will be displayed, and the memory location address will be incremented automatically.
3. Subsequent memory locations may be displayed in consecutive order by repeatedly pressing DISPLAY.

The control panel functions are enabled by the control/exp switch in the control position. Placing it in the EXP position enables the experiment program, START and STOP switches and disables the control panel switches. The experiment is enabled by placing control/exp in EXP, pressing CLEAR, and pressing START. The experiment will read and accumulate successive samples. The program may be halted by pressing STOP. The last cumulative value will remain on the display until START is pressed.

Additional information on the IMP-16C/200 may be obtained by referring to the following National Semiconductor publications:

Pub. No. 4200035A	IMP-16C Interfacing Guide
Pub. No. 4200036A Order No. IMP-16P/936A	IMP-16C/200, IMP-16C/300 Microprocessors, IMP-16P Microcomputer Product Description.
Pub. No. 4200021B	IMP-16C Application Manual
Pub. No. 4200002B	IMP-16 Programming and Assembler Manual.

The software is loaded into the IMP-16C via the front panel in the following manner:

1. CONTROL/EXP switch in CONTROL.
2. Press CLEAR.
3. Set thumbwheel switches to 0007.
4. Press LOAD ADDRESS. Address will be on display.
5. Set thumbwheel switches to data to be entered.
6. Press LOAD DATA. Data will be on display.
7. Data may now be entered by setting the thumbwheel switches to the desired word and pressing LOAD DATA. The microprocessor automatically points to the next memory location after each LOAD DATA.

The SLINGER software is a flexible special-purpose program to monitor, measure and display the mass readings made by the SLINGER hardware. The program executes on an IMP-16 microcomputer and is written in the IMP-16 assembly language. The entire program, including some hardware diagnostics, error checking and warning routines and miscellaneous constants occupies approximately 85, 16-bit words of memory.

The functions of the program are:

1. Monitor START/STOP state of system from front-panel push-button;
2. Read, scale and correct the output of the A/D converter;
3. Measure the mass of samples in the SLINGER hardware by integrating the A/D converter output over the period of time for which the output exceeds a preset threshold;
4. Convert and display a cumulative mass measurement on the front panel display.

The overall program flow chart is shown in figure 1. Program start is achieved by the following process:

1. PANEL/EXPERIMENT switch to PANEL;
2. Push CLEAR;
3. PANEL/EXPERIMENT switch to EXPERIMENT;
4. Push START;

The above procedure is only necessary when starting the program after having used the microcomputer for something else (such as inspecting/changing program constants). A given series of measurements may be terminated by pushing the STOP pushbutton. Subsequently pushing the START pushbutton restarts and initializes a new series of measurements.

The program, during most operation is simply monitoring the START/STOP pushbuttons. During a measurement session, the program is primarily monitoring the A/D converter output for when it goes over threshold.

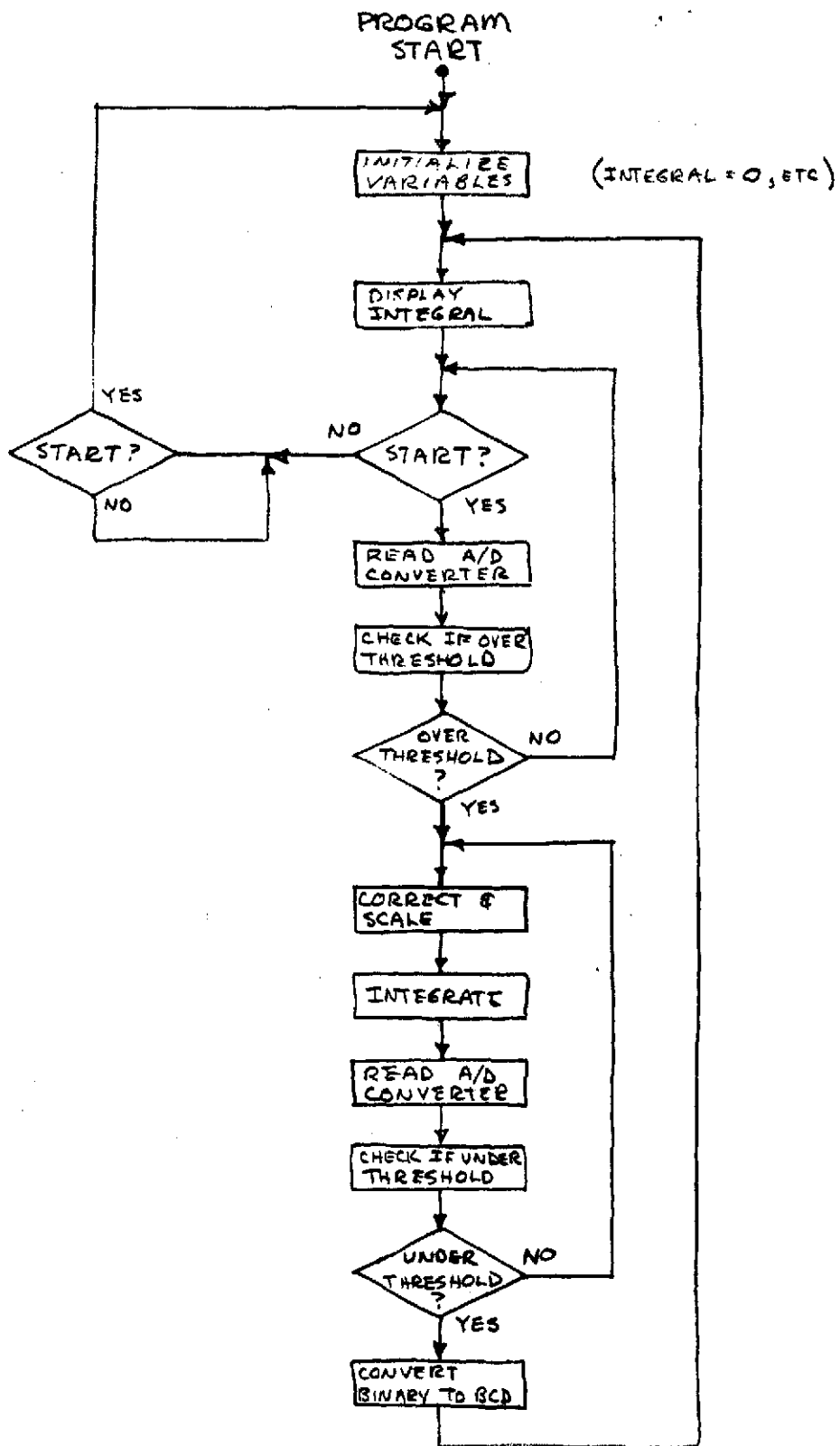


FIGURE 1. SLINGER PROGRAM FLOW CHART

Once the A/D converter output has exceeded threshold, the program continues to read the A/D converter output, but additional operations are performed. Each reading is now taken at precise uniform intervals to ensure that the cumulative addition process is an accurate representation of the integral. Data is scaled and corrected to take into account the effect of non-zero ambient and threshold levels. Each result is added to the previous cumulative sum (integrated). Each reading is also checked to determine if it falls below threshold. When a reading does fall below threshold, the integration process stops, the current cumulative sum is converted from internal binary to BCD and displayed on the front panel. After the display is updated, the program resumes monitoring of the A/D output to detect when it next exceeds threshold.

The program consists of an executive routine and five subroutines.

EXECUTIVE - Monitors panel pushbuttons and calls other subroutines as required for the measurement sequence.

READAD - Initiates A/D conversion, waits for conversion delay, samples A/D converter output, tests for possible bad conversion and subtracts the threshold constant.

INTEGRATE - Scales and corrects the data value read by the A/D converter, adds to previous cumulative sum, waits for integration step-size delay and checks for overflow error.

BINBCD - Converts the cumulative binary sum to a 4-digit BCD representation and checks for overflow.

ERROR - Depending upon subroutine entry point, displays appropriate error message and stops program execution.

WATCH - A diagnostic subroutine to allow continuous monitoring of A/D converter output on front panel display. Threshold is subtracted from the A/D reading before display.

The program requires definition of several internal data constants:

DELAY A/D Converter conversion delay;
THRESH Measurement decision threshold;
STEP Integration step size;
CORCON Correction constant.

The DELAY and STEP constants are adjusted to satisfy dynamic range and accuracy requirements, constrained by the A/D converter conversion time.

THRESH and CORCON are defined by sensitivity and noise immunity considerations.

In addition to the above constants there are several locations in memory in which are stored various internal numbers for diagnostic purpose:

CUMSUM Current value of integral;
ADCONV Most recent A/D converter output (threshold not subtracted);
BINARY Most recent value to be converted to BCD.

A complete listing of the program as assembled by the IMP-16 cross-assembler executing on the GE-635 computer is given in figure 2.

The display on the front panel of the SLINGER is used for both display of data measurement results and error diagnostics:

1. Data Display Initially the display shows 0000. After each sample has been detected and measured, the sample measurement is added to the previous display contents and the cumulative results are updated and displayed;
2. Error Diagnostics There are three detectable error conditions for which and error message is given:

a. CBOF Cumulative Binary Overflow

During integration, if the integral value exceeds the capability of representation by a 16-bit digital word, the program stops with CBOF showing in the display;

b. BCDO Binary Coded Decimal Overflow

If the quantity to be displayed exceeds 9999, the maximum which can be displayed on the 4-digit decimal display, the program

stops with BCDO showing in the display;

c. BADC Bad A/D Conversion

If the A/D converter does not give a "conversion complete" signal within a specified period of time, a bad conversion is assumed.

The program stops with BADC showing in the display.

In all cases of an error diagnostic message, the program is re-initialized and restarted by pushing the START pushbutton.

LINE	ADDRESS	OPERAND	INSTR	OPERAND	COMMENT	HEX
1					TITLE SLINGER	00000010
2					ASECT	00000020
3	0000	0007 A	JMP	EXEC	GO TO EXEC	00000030
4	0007	200E A	JMP	EXEC	GO TO EXEC	00000040
5	0008	0001 A	DELAY	WORD 1	A/D CONV DELAY	00000050
6	0009	0004 A	THRESH	WORD 100	A/D CONV THRESH	00000060
7	000A	0001 A	STEP	WORD 1	INTEGRAT ON TIME STEP	00000070
8	000B	0000 A	CUMSUM	WORD 0	CURRENT CUMSUM	00000080
9	000C	0000 A	ADCONV	WORD 0	MOST RECENT A/D	00000090
10	000D	0000 A	BINARY	WORD 0	MOST RECENT BINARY NO.	00000100
11	000E	3582 A	EXECI	RXOR 1,1	AC1=0	00000110
12	000F	281D A	JSR	HEADAD	A/D CONV STABLE	00000120
13	0010	3582 A	RXOR	0,0	AC0=0	00000130
14	0011	0600 A	DISPLAY	ROUT 0	DISPLAY AC0	00000140
15	0012	1702 A	CHECK	ROC 7, MEASURE	MEASURE F (START) =1	00000150
16	0013	172C A	RECHECK	ROC 7, GOTOSTRT	RECHECK INIT IF START =1	00000160
17	0014	2013 A	JMP	RECHECK	TRY AGAIN	00000170
18	0015	2A1D A	MEASURE	JSR HEADAD	READ A/D	00000180
19	0016	1028 A	ROC	11, GOTOCCHK	IF AC0 NEG, GO TO CHECK	00000190
20	0017	2826 A	PLOP	JSR INTEGRATE	PLOP OCCURRING, INTEGRATE	00000200
21	0018	281D A	JSR	HEADAD	GET NEXT READING FROM A/D	00000210
22	0019	1901 A	ROC	11, PLOPDONE	PLOP DONE IF AC0 NEG	00000220
23	001A	2017 A	JMP	PLOP	PLOP NOT DONE	00000230
24	001B	282E A	PLOPDONE	JSR BINBCD	CONVERT BIN-BCD	00000240
25	001C	2011 A	JMP	DISPLAY	READY TO DISPLAY AND WAIT	00000250
26	001D	0F80 A	READAD	PFLG 0,0	START A/D	00000260
27	001E	808F A	LD	0, DELAY	SET AC0=DELAY	00000270
28	001F	48FF A	CONVDELAY	AISZ 0, -1	DECREMENT AND SKIP	00000280
29	0020	201F A	JMP	CONVDELAY	WAIT SOME MORE	00000290
30	0021	1E2D A	ROC	14, INCOMPL	DELAY OVER, CHECK CONV. COMPL.	00000300
31	0022	0400 A	RN	0	CONV. COMPL., READ IN DATA	00000310
32	0023	A00C A	ST	0, ADCONV	STORE A/D CONV READING	00000320
33	0024	D009 A	SUR	0, THRESH	LESS THRESHOLD	00000330
34	0025	0200 A	RTS	0	RETURN TO CALLER	00000340
35	0026	5CFA A	INTEGRATE	SUR 0, 6	SCALE FACT RT 6 BYTS TO SCALE	00000350
36	0027	88DA A	LD	2, STEP	STEP SIZE IN AC2	00000360
37	0028	4AFF A	STEPDELAY	AISZ 2, -1	DEC, AND SKIP	00000370
38	0029	2028 A	JMP	STEPDELAY	WAIT	00000380
39	002A	205A A	STORE	JMP CORRECT	GO TO CORRECTION ROUTINE	00000390
40	002B	A409 A	ST	1, CUMSUM	STORE CUMULATIVE CUMSUM	00000400
41	002C	1A26 A	ROC	10, OVERFLOW	CHECK CARRY FOR OVERFLOW	00000410
42	002D	0200 A	RTS	0	RETURN, CUMSUM IN AC1	00000420
43	002E	3481 A	BINBCD	RCPY 1,0	AC0=AC1	00000430
44	002F	A00D A	ST	0, BINARY	STORE	00000440
45	0030	D042 A	SUR	0, 510K	CHECK IF GT, 9999	00000450
46	0031	121F A	ROC	2, 10081G	IF GT, 0, TOO BIG FOR BCD	00000460
47	0032	C042 A	ADD	0, 510K	RESTORE OR, G VALUE	00000470
48	0033	4FFF A	LI	3, -1	AC3=-1	00000480
49	0034	4E03 A	LI	2, 3	AC2=3	00000490
50	0035	4E01 A	INCREMENT	AISZ 3, 1	ADD 1 TO AC3	00000500
51	0036	3583 A	RAND	1, 1	DO NOTHING	00000510
52	0037	D242 A	NEXT	SUR 0, P10(2)	SUBTRACT POWER OF 10	00000520
53	0038	1208 A	ROC	2, GOTONCR	IF GT 0, DO AGAIN	00000530
54	0039	0242 A	ADD	0, P10(2)	DIGIT CONV, COMPL.	00000540
55	003A	5F04 A	SHL	3, 4	SHIFT AC3 LEFT 4, NEXT DIGIT	00000550

56	003B	4AFF	A	ALSZ	2,71	AC2=AC2+1, SKIP IF DONE	00000560
57	003C	2037	A	JMP	NEXT	GO TO CONV. NEXT DIGIT	00000570
58	003D	3C00	A	RADD	3,0	AC0=AC0+AC3, CONV. COMPL.	00000580
59	003E	0200	A	RTS		ALL BCD, RETURN BCD IN AC0	00000590
60	003F	2012	A	GOTOCHK1	JMP	CHECK	GO TO CHECK
61	0040	2007	A	GOTOSTRT	JMP	INIT	GO TO INIT
62	0041	2035	A	GOTOINCR	JMP	INCREMENT	GO TO INCREMENT
63	0042	2710	A	SKIP10	WORD	10000	00000630
64	0043	000A	A		WORD	10	00000640
65	0044	0064	A		WORD	100	00000650
66	0045	03E8	A		WORD	1000	00000660
67	0046	BADC	A	BADC	WORD	X'BADC	00000670
68	0047	BCD0	A	BCD0	WORD	X'BCD0	00000680
69	0048	CB0F	A	CB0F	WORD	X'CB0F	00000690
70	0049	0000	A		WORD	0	00000700
71	004A	0000	A		WORD	0	00000710
72	004B	0000	A		WORD	0	00000720
73	004C	0600	A	ERRDR	ROUT	0	00000730
74	004D	0000	A	HALT		HALT	00000740
75	004E	2007	A	JMP	INIT	START OVER	00000750
76	004F	8046	A	INCOMPL	LD	0,BADC	GET BAD CONVERSION FLAG
77	0050	204C	A		JMP	ERROR	00000760
78	0051	8047	A	TOOBIG	LD	0,BCD0	00000770
79	0052	204C	A		JMP	ERROR	00000780
80	0053	8048	A	OVERFLOW	LD	0,CB0F	GET BINARY OVERFLOW FLAG
81	0054	204C	A		JMP	ERROR	00000790
82	0055	201D	A	WATCH	JSR	READAD	WATCH ROUTINE, CALL READAD
83	0056	0A00	A	ROUT	0	DISPLAY AC0	00000800
84	0057	2055	A	JMP	WATCH	DO AGAIN	00000810
85	0058	0000	A		WORD	0	00000820
86	0059	0001	A	CORCON	WORD	X'1	00000830
87	005A	3100	A	CORRECT	RADD	0,1	00000840
88	005B	C459	A		ADD	1,CORCON	00000850
89	005C	2028	A		JMP	STORE	00000860
90				END		GO TO STORE	00000870

***** 0 ERRORS IN ASSEMBLY *****

Slinger Motor

The selection of a motor for the slinger application was based upon the concept that in a zero gravity environment the mass of an object could be determined by measuring the energy transferred to it by a mechanical source. Since the size mass and frequency of measurement were variables and the means of transferring energy was to be the slinger, a constant speed motor was selected to be the energy source.

A permanent magnet, shunt motor was selected as the drive for the slinger assembly. The motor would run at constant speed through a closed loop system employing a power amplifier, a speed tachometer and a feedback network. The mass was assumed to be thrown off at a uniform velocity, therefore, the energy transfer was proportional to the mass. This energy was to be supplied on impact with the slinger rods and the motor would supply periods of impulse torque during this operation.

Motor Torque. The motor will be required to produce a steady-state torque to drive its own inertia, tachometer and slinger as well as to provide the impulse torque to propel the focus mass. Calculation for motor requirements are contained in PIR 1J72-PEM-438. To meet these requirements, a DC Permanent Magnet Motor with low inertia and high peak torque with variable speed was investigated. Variable speed was considered necessary to evaluate different operating conditions. It was also considered necessary to select a motor, amplifier, tachometer which had been designed to operate as a system and no instabilities would be experienced.

The motor which was finally selected is manufactured by Torque Systems Incorporated of Waltham, Massachusetts. The motor will provide:

Peak Torque	- 600 oz. in.
Rated Torque	- 150 oz. in
Torque Sensitivity	- 12.8 per amp
Mech Time Count	- 10 msec
Elect Time Count	- 1.0 msec
Tach Sensitivity	- 3.0 VKRPM

Model No. MT5010-023DA

The amplifier is designed to drive this motor. It will provide:

Watts	- 110
Volts	- +22
Amps	- 5
Response	- 1 KHz/Full Power
Open Loop Gain	- 100 K V/V

The system with amplifier is designated RL5060A-023Ha and has a power supply rated a 40 volts 25 amperes. The system is specified as:

Continuous Torque	- 150 oz in
Peak Torque	- 390 oz in
No Load Speed	- 2800 RPM
Rated Speed	- 2400 RPM

Motor Tach Inertia - $50 \text{ oz in sec}^2 \times 10^{-3}$

This combination will provide a constant speed output with a regulation better than 1% and will meet the requirements of the system.

With a constant speed output, the Torque delivered to the load can be measured by integrated the load current during the slinging operation. The measurement will be the ampere seconds demand while the feces is being slung from the slinger using correction factor provided by the processor.

No load current will be removed due to the integration which will be performed each time a change in current is detected. Since Torque is proportional to current in a permanent magnet motor and K factors can be introduced in the electronics, this measurement was used as the basis for the study.

Calculation of Peak Torque for 5.25" dia slinger.

$$\text{Torque Demand} = \frac{d(Iw)}{dt}$$

I for 300 gram load

$$I = \frac{.3}{14.6} \times \left(\frac{5.25}{2 \times 12} \right) = 10^{-3} \text{ slug-ft.}$$

$$= 2 \times 10^{-3} \text{ for } \frac{dI}{dt} = 1/2$$

$$T = 200 \times \frac{2\pi}{60} \times 2 \times 10^{-3} = 80 \text{ in-oz}$$

Thus, the motor is well capable of providing this Torque demand.

CLASS. LTR.	OPERATION	PROGRAM	SEQUENCE NO.	REV. LTR.
U	1J72	PEM	438	
PIR NO.				
*USE "C" FOR CLASSIFIED AND "U" FOR UNCLASSIFIED				

PROGRAM INFORMATION REQUEST/RELEASE

FROM P. Matheson		TO G. L. Fogal	
DATE SENT 2/8/74	DATE INFO. REQUIRED	PROJECT AND REQ. NO.	REFERENCE DIR. NO.
SUBJECT SLINGER SPEED CONTROL LOOP MODEL			

INFORMATION REQUESTED/RELEASED

1.0 Summary

To aid in selection of torquer and control electronics characteristics, the model of a typical constant speed servo is simulated. Characteristics of a typical torquer, load and processing electronics are selected to show the servo response to an expected slinger load profile. These loop parameters do not represent the selected slinger configuration. They are chosen to show the operation of the simulation, and that it is flexible enough to introduce actual component and loop parameters to determine approximate response characteristics of the hardware.

The selected feces loading profile is of particular concern since torquer sizing and speed control bandpass will be dictated by the expected rate of inertia change (see development of this profile in paragraph 2.2 and 2.3).

2.0 Development

2.1 The servo simulation models a tach feedback speed control loop, D.C. permanent magnet motor and feces loading profile as shown in figure 1. This loading is shown as dI/dt , a function of time and slinger speed. The simulation program is attached as appendix A.

2.2 Motor plus load inertia

Motor plus load inertia ($V(8)$ in figure 1) consists of three parts, two of which are the familiar rotor inertia and unloaded slinger inertia:

$$I_{\text{rotor}} = .125 \times 10^{-4} \text{ sl-ft}^2$$

$$I_{\text{slinger}} = .25 \times 10^{-4} \text{ sl-ft}^2$$

The third inertia term is a function of the instantaneous measure of waste matter on the slinger and as a worst case is assumed to be consistent with the profile of figure 2.

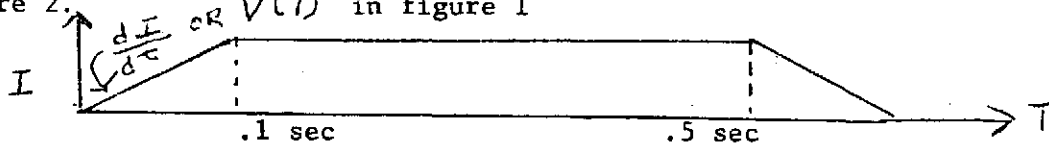


Figure 2 ----- Inertia Profile

Distribution:

A. Anderson ✓
S. Millman

PAGE NO.

1 7
OF

RETENTION REQUIREMENTS

COPIES FOR	MASTERS FOR
<input type="checkbox"/> 1 MO.	<input type="checkbox"/> 3 MOS.
<input type="checkbox"/> 3 MOS.	<input type="checkbox"/> 6 MOS.
<input type="checkbox"/> 6 MOS.	<input type="checkbox"/> 12 MOS.
<input type="checkbox"/> 12 MOS.	<input type="checkbox"/> 18 MOS.
<input type="checkbox"/> 18 MOS.	<input type="checkbox"/> 24 MOS.
<input type="checkbox"/> 24 MOS.	<input type="checkbox"/> 30 MOS.
<input type="checkbox"/> 30 MOS.	<input type="checkbox"/> 36 MOS.
<input type="checkbox"/> 36 MOS.	<input type="checkbox"/> 42 MOS.
<input type="checkbox"/> 42 MOS.	<input type="checkbox"/> 48 MOS.
<input type="checkbox"/> 48 MOS.	<input type="checkbox"/> 54 MOS.
<input type="checkbox"/> 54 MOS.	<input type="checkbox"/> 60 MOS.
<input type="checkbox"/> 60 MOS.	<input type="checkbox"/> 66 MOS.
<input type="checkbox"/> 66 MOS.	<input type="checkbox"/> 72 MOS.
<input type="checkbox"/> 72 MOS.	<input type="checkbox"/> 78 MOS.
<input type="checkbox"/> 78 MOS.	<input type="checkbox"/> 84 MOS.
<input type="checkbox"/> 84 MOS.	<input type="checkbox"/> 90 MOS.
<input type="checkbox"/> 90 MOS.	<input type="checkbox"/> 96 MOS.
<input type="checkbox"/> 96 MOS.	<input type="checkbox"/> 102 MOS.
<input type="checkbox"/> 102 MOS.	<input type="checkbox"/> 108 MOS.
<input type="checkbox"/> 108 MOS.	<input type="checkbox"/> 114 MOS.
<input type="checkbox"/> 114 MOS.	<input type="checkbox"/> 120 MOS.
<input type="checkbox"/> 120 MOS.	<input type="checkbox"/> 126 MOS.
<input type="checkbox"/> 126 MOS.	<input type="checkbox"/> 132 MOS.
<input type="checkbox"/> 132 MOS.	<input type="checkbox"/> 138 MOS.
<input type="checkbox"/> 138 MOS.	<input type="checkbox"/> 144 MOS.
<input type="checkbox"/> 144 MOS.	<input type="checkbox"/> 150 MOS.
<input type="checkbox"/> 150 MOS.	<input type="checkbox"/> 156 MOS.
<input type="checkbox"/> 156 MOS.	<input type="checkbox"/> 162 MOS.
<input type="checkbox"/> 162 MOS.	<input type="checkbox"/> 168 MOS.
<input type="checkbox"/> 168 MOS.	<input type="checkbox"/> 174 MOS.
<input type="checkbox"/> 174 MOS.	<input type="checkbox"/> 180 MOS.
<input type="checkbox"/> 180 MOS.	<input type="checkbox"/> 186 MOS.
<input type="checkbox"/> 186 MOS.	<input type="checkbox"/> 192 MOS.
<input type="checkbox"/> 192 MOS.	<input type="checkbox"/> 198 MOS.
<input type="checkbox"/> 198 MOS.	<input type="checkbox"/> 204 MOS.
<input type="checkbox"/> 204 MOS.	<input type="checkbox"/> 210 MOS.
<input type="checkbox"/> 210 MOS.	<input type="checkbox"/> 216 MOS.
<input type="checkbox"/> 216 MOS.	<input type="checkbox"/> 222 MOS.
<input type="checkbox"/> 222 MOS.	<input type="checkbox"/> 228 MOS.
<input type="checkbox"/> 228 MOS.	<input type="checkbox"/> 234 MOS.
<input type="checkbox"/> 234 MOS.	<input type="checkbox"/> 240 MOS.
<input type="checkbox"/> 240 MOS.	<input type="checkbox"/> 246 MOS.
<input type="checkbox"/> 246 MOS.	<input type="checkbox"/> 252 MOS.
<input type="checkbox"/> 252 MOS.	<input type="checkbox"/> 258 MOS.
<input type="checkbox"/> 258 MOS.	<input type="checkbox"/> 264 MOS.
<input type="checkbox"/> 264 MOS.	<input type="checkbox"/> 270 MOS.
<input type="checkbox"/> 270 MOS.	<input type="checkbox"/> 276 MOS.
<input type="checkbox"/> 276 MOS.	<input type="checkbox"/> 282 MOS.
<input type="checkbox"/> 282 MOS.	<input type="checkbox"/> 288 MOS.
<input type="checkbox"/> 288 MOS.	<input type="checkbox"/> 294 MOS.
<input type="checkbox"/> 294 MOS.	<input type="checkbox"/> 300 MOS.
<input type="checkbox"/> 300 MOS.	<input type="checkbox"/> 306 MOS.
<input type="checkbox"/> 306 MOS.	<input type="checkbox"/> 312 MOS.
<input type="checkbox"/> 312 MOS.	<input type="checkbox"/> 318 MOS.
<input type="checkbox"/> 318 MOS.	<input type="checkbox"/> 324 MOS.
<input type="checkbox"/> 324 MOS.	<input type="checkbox"/> 330 MOS.
<input type="checkbox"/> 330 MOS.	<input type="checkbox"/> 336 MOS.
<input type="checkbox"/> 336 MOS.	<input type="checkbox"/> 342 MOS.
<input type="checkbox"/> 342 MOS.	<input type="checkbox"/> 348 MOS.
<input type="checkbox"/> 348 MOS.	<input type="checkbox"/> 354 MOS.
<input type="checkbox"/> 354 MOS.	<input type="checkbox"/> 360 MOS.
<input type="checkbox"/> 360 MOS.	<input type="checkbox"/> 366 MOS.
<input type="checkbox"/> 366 MOS.	<input type="checkbox"/> 372 MOS.
<input type="checkbox"/> 372 MOS.	<input type="checkbox"/> 378 MOS.
<input type="checkbox"/> 378 MOS.	<input type="checkbox"/> 384 MOS.
<input type="checkbox"/> 384 MOS.	<input type="checkbox"/> 390 MOS.
<input type="checkbox"/> 390 MOS.	<input type="checkbox"/> 396 MOS.
<input type="checkbox"/> 396 MOS.	<input type="checkbox"/> 402 MOS.
<input type="checkbox"/> 402 MOS.	<input type="checkbox"/> 408 MOS.
<input type="checkbox"/> 408 MOS.	<input type="checkbox"/> 414 MOS.
<input type="checkbox"/> 414 MOS.	<input type="checkbox"/> 420 MOS.
<input type="checkbox"/> 420 MOS.	<input type="checkbox"/> 426 MOS.
<input type="checkbox"/> 426 MOS.	<input type="checkbox"/> 432 MOS.
<input type="checkbox"/> 432 MOS.	<input type="checkbox"/> 438 MOS.
<input type="checkbox"/> 438 MOS.	<input type="checkbox"/> 444 MOS.
<input type="checkbox"/> 444 MOS.	<input type="checkbox"/> 450 MOS.
<input type="checkbox"/> 450 MOS.	<input type="checkbox"/> 456 MOS.
<input type="checkbox"/> 456 MOS.	<input type="checkbox"/> 462 MOS.
<input type="checkbox"/> 462 MOS.	<input type="checkbox"/> 468 MOS.
<input type="checkbox"/> 468 MOS.	<input type="checkbox"/> 474 MOS.
<input type="checkbox"/> 474 MOS.	<input type="checkbox"/> 480 MOS.
<input type="checkbox"/> 480 MOS.	<input type="checkbox"/> 486 MOS.
<input type="checkbox"/> 486 MOS.	<input type="checkbox"/> 492 MOS.
<input type="checkbox"/> 492 MOS.	<input type="checkbox"/> 498 MOS.
<input type="checkbox"/> 498 MOS.	<input type="checkbox"/> 504 MOS.
<input type="checkbox"/> 504 MOS.	<input type="checkbox"/> 510 MOS.
<input type="checkbox"/> 510 MOS.	<input type="checkbox"/> 516 MOS.
<input type="checkbox"/> 516 MOS.	<input type="checkbox"/> 522 MOS.
<input type="checkbox"/> 522 MOS.	<input type="checkbox"/> 528 MOS.
<input type="checkbox"/> 528 MOS.	<input type="checkbox"/> 534 MOS.
<input type="checkbox"/> 534 MOS.	<input type="checkbox"/> 540 MOS.
<input type="checkbox"/> 540 MOS.	<input type="checkbox"/> 546 MOS.
<input type="checkbox"/> 546 MOS.	<input type="checkbox"/> 552 MOS.
<input type="checkbox"/> 552 MOS.	<input type="checkbox"/> 558 MOS.
<input type="checkbox"/> 558 MOS.	<input type="checkbox"/> 564 MOS.
<input type="checkbox"/> 564 MOS.	<input type="checkbox"/> 570 MOS.
<input type="checkbox"/> 570 MOS.	<input type="checkbox"/> 576 MOS.
<input type="checkbox"/> 576 MOS.	<input type="checkbox"/> 582 MOS.
<input type="checkbox"/> 582 MOS.	<input type="checkbox"/> 588 MOS.
<input type="checkbox"/> 588 MOS.	<input type="checkbox"/> 594 MOS.
<input type="checkbox"/> 594 MOS.	<input type="checkbox"/> 600 MOS.
<input type="checkbox"/> 600 MOS.	<input type="checkbox"/> 606 MOS.
<input type="checkbox"/> 606 MOS.	<input type="checkbox"/> 612 MOS.
<input type="checkbox"/> 612 MOS.	<input type="checkbox"/> 618 MOS.
<input type="checkbox"/> 618 MOS.	<input type="checkbox"/> 624 MOS.
<input type="checkbox"/> 624 MOS.	<input type="checkbox"/> 630 MOS.
<input type="checkbox"/> 630 MOS.	<input type="checkbox"/> 636 MOS.
<input type="checkbox"/> 636 MOS.	<input type="checkbox"/> 642 MOS.
<input type="checkbox"/> 642 MOS.	<input type="checkbox"/> 648 MOS.
<input type="checkbox"/> 648 MOS.	<input type="checkbox"/> 654 MOS.
<input type="checkbox"/> 654 MOS.	<input type="checkbox"/> 660 MOS.
<input type="checkbox"/> 660 MOS.	<input type="checkbox"/> 666 MOS.
<input type="checkbox"/> 666 MOS.	<input type="checkbox"/> 672 MOS.
<input type="checkbox"/> 672 MOS.	<input type="checkbox"/> 678 MOS.
<input type="checkbox"/> 678 MOS.	<input type="checkbox"/> 684 MOS.
<input type="checkbox"/> 684 MOS.	<input type="checkbox"/> 690 MOS.
<input type="checkbox"/> 690 MOS.	<input type="checkbox"/> 696 MOS.
<input type="checkbox"/> 696 MOS.	<input type="checkbox"/> 702 MOS.
<input type="checkbox"/> 702 MOS.	<input type="checkbox"/> 708 MOS.
<input type="checkbox"/> 708 MOS.	<input type="checkbox"/> 714 MOS.
<input type="checkbox"/> 714 MOS.	<input type="checkbox"/> 720 MOS.
<input type="checkbox"/> 720 MOS.	<input type="checkbox"/> 726 MOS.
<input type="checkbox"/> 726 MOS.	<input type="checkbox"/> 732 MOS.
<input type="checkbox"/> 732 MOS.	<input type="checkbox"/> 738 MOS.
<input type="checkbox"/> 738 MOS.	<input type="checkbox"/> 744 MOS.
<input type="checkbox"/> 744 MOS.	<input type="checkbox"/> 750 MOS.
<input type="checkbox"/> 750 MOS.	<input type="checkbox"/> 756 MOS.
<input type="checkbox"/> 756 MOS.	<input type="checkbox"/> 762 MOS.
<input type="checkbox"/> 762 MOS.	<input type="checkbox"/> 768 MOS.
<input type="checkbox"/> 768 MOS.	<input type="checkbox"/> 774 MOS.
<input type="checkbox"/> 774 MOS.	<input type="checkbox"/> 780 MOS.
<input type="checkbox"/> 780 MOS.	<input type="checkbox"/> 786 MOS.
<input type="checkbox"/> 786 MOS.	<input type="checkbox"/> 792 MOS.
<input type="checkbox"/> 792 MOS.	<input type="checkbox"/> 798 MOS.
<input type="checkbox"/> 798 MOS.	<input type="checkbox"/> 804 MOS.
<input type="checkbox"/> 804 MOS.	<input type="checkbox"/> 810 MOS.
<input type="checkbox"/> 810 MOS.	<input type="checkbox"/> 816 MOS.
<input type="checkbox"/> 816 MOS.	<input type="checkbox"/> 822 MOS.
<input type="checkbox"/> 822 MOS.	<input type="checkbox"/> 828 MOS.
<input type="checkbox"/> 828 MOS.	<input type="checkbox"/> 834 MOS.
<input type="checkbox"/> 834 MOS.	<input type="checkbox"/> 840 MOS.
<input type="checkbox"/> 840 MOS.	<input type="checkbox"/> 846 MOS.
<input type="checkbox"/> 846 MOS.	<input type="checkbox"/> 852 MOS.
<input type="checkbox"/> 852 MOS.	<input type="checkbox"/> 858 MOS.
<input type="checkbox"/> 858 MOS.	<input type="checkbox"/> 864 MOS.
<input type="checkbox"/> 864 MOS.	<input type="checkbox"/> 870 MOS.
<input type="checkbox"/> 870 MOS.	<input type="checkbox"/> 876 MOS.
<input type="checkbox"/> 876 MOS.	<input type="checkbox"/> 882 MOS.
<input type="checkbox"/> 882 MOS.	<input type="checkbox"/> 888 MOS.
<input type="checkbox"/> 888 MOS.	<input type="checkbox"/> 894 MOS.
<input type="checkbox"/> 894 MOS.	<input type="checkbox"/> 900 MOS.
<input type="checkbox"/> 900 MOS.	<input type="checkbox"/> 906 MOS.
<input type="checkbox"/> 906 MOS.	<input type="checkbox"/> 912 MOS.
<input type="checkbox"/> 912 MOS.	<input type="checkbox"/> 918 MOS.
<input type="checkbox"/> 918 MOS.	<input type="checkbox"/> 924 MOS.
<input type="checkbox"/> 924 MOS.	<input type="checkbox"/> 930 MOS.
<input type="checkbox"/> 930 MOS.	<input type="checkbox"/> 936 MOS.
<input type="checkbox"/> 936 MOS.	<input type="checkbox"/> 942 MOS.
<input type="checkbox"/> 942 MOS.	<input type="checkbox"/> 948 MOS.
<input type="checkbox"/> 948 MOS.	<input type="checkbox"/> 954 MOS.
<input type="checkbox"/> 954 MOS.	<input type="checkbox"/> 960 MOS.
<input type="checkbox"/> 960 MOS.	<input type="checkbox"/> 966 MOS.
<input type="checkbox"/> 966 MOS.	<input type="checkbox"/> 972 MOS.
<input type="checkbox"/> 972 MOS.	<input type="checkbox"/> 978 MOS.
<input type="checkbox"/> 978 MOS.	<input type="checkbox"/> 984 MOS.
<input type="checkbox"/> 984 MOS.	<input type="checkbox"/> 990 MOS.
<input type="checkbox"/> 990 MOS.	<input type="checkbox"/> 996 MOS.
<input type="checkbox"/> 996 MOS.	<input type="checkbox"/> 1000 MOS.

This assumes that the full 300 gram load does not have to be handled instantaneously by the slinger mechanism. Instead, the load is applied at a constant rate with an equilibrium period after .1 second where application rate becomes equal to sling rate. The resulting worst case increase in motor plus load inertia can be calculated as:

$$\frac{\Delta I}{\Delta t} \times .1 \text{ SEC} = .2 \times 10^{-3} \text{ SL-FT}^2$$

In the simulation program motor plus load inertia is calculated as a function of time and given the variable V(8).

2.3 Load Torque

The inertia profile in Figure 2 is scaled from the total inertia associated with 300 grams located at the outer edge of the slinger. Runs have been made for two inertia levels, one for an 8 inch diameter and one for a 5.25 inch diameter slinger.

$$I_{\text{LOAD}} (8" \text{ dia}) = mr^2 = \frac{.3}{14.6} \times \left(\frac{1}{3}\right)^2 = 2.28 \text{ SL-FT}^2 \times 10^{-3}$$

$$I_{\text{LOAD}} (5.25" \text{ dia}) = \frac{.3}{14.6} \times \left(\frac{5.25}{2 \times 12}\right)^2 = 10^{-3} \text{ SL-FT}^2$$

If one assumes the inertia has to be slung within .5 seconds and the rate of deposit is constant, an expression for $\frac{dI}{dt}$ is;

$$\frac{2.28 \times 10^{-3}}{.5} = 4.56 \times 10^{-3} \text{ SL-FT}^2/\text{SEC} \quad ; (2 \times 10^{-3} \text{ FOR } 5.25" \text{ SLINGER})$$

Now we can express the torque required to do this as:

$$T = \frac{\partial(I\omega)}{\partial t} = \omega \frac{\Delta I}{\Delta t} \quad \text{ASSUMING A CONSTANT SPEED}$$

$$\begin{aligned} T_{\text{DEMAND}} &= 2000 \times \frac{2\pi}{60} \times 4.56 \times 10^{-3} = .958 \text{ FT-#} = 184 \text{ IN-OZ} \\ &= 80 \text{ IN-OZ (FOR } 5.25" \text{ SLINGER)} \end{aligned}$$

Finally, the step in torque due to this dI/dt step will cause speed change transients, and a more accurate model of load torque can be obtained (shown in Figure 1) by multiplying dI/dt by actual slinger speed.

2.4 Motor Characteristics

The motor loop in Figure 1 consists of torque scale factor K_M (set at .266 ft-# /volt) and back EMF constant K_b (set at .0907 v/rad/sec). A fixed running torque friction level is also introduced (shown as .025 ft-#). These characteristics are representative of a 150 in-oz torquer which is too large for the present slinger design (5.25 in). New characteristics will be introduced when the motor is selected.

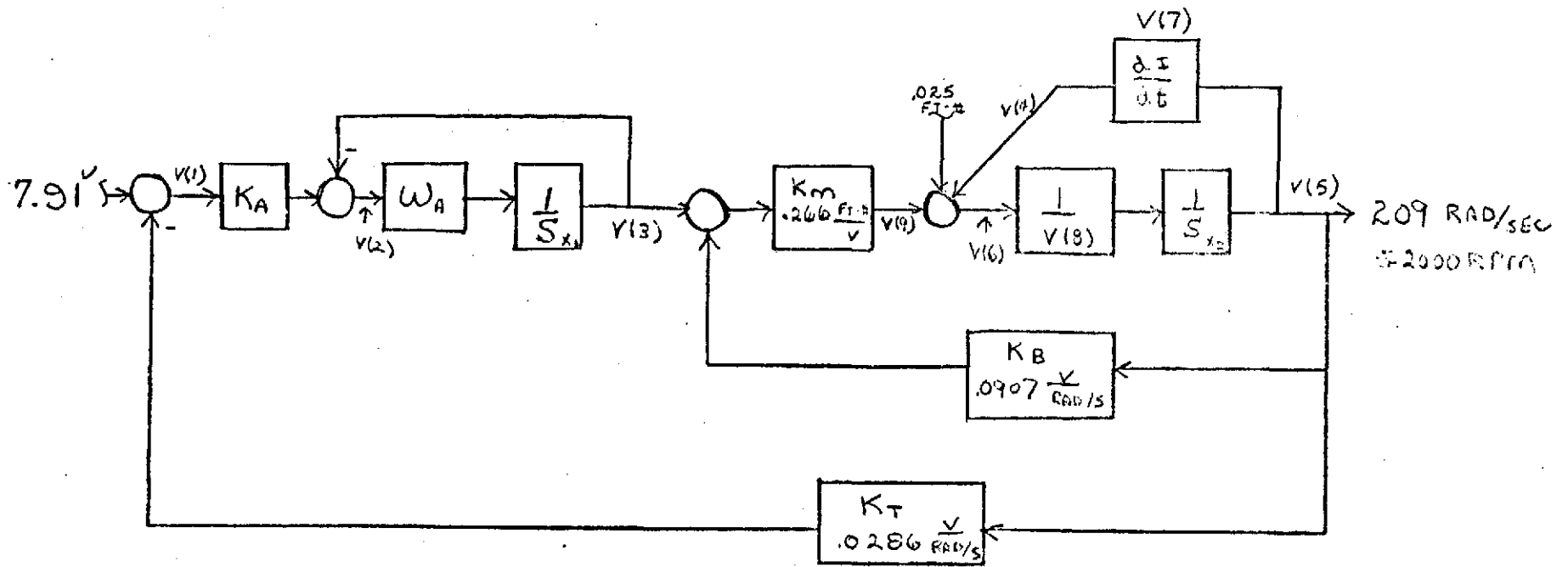


FIGURE 1 -- SLINGER SIMULATION MODEL

2.5 Speed Control Loop

Tach feedback speed control is represented in Figure 1 by a tachometer scale factor K_T (.0286 v/rad/sec), electronic gain K_A and electronics filter frequency (W_A). Speed is set to 2000 rpm by a fixed input voltage level (set at 2.91V). At present it is felt that adequate speed control can be attained by this simple loop, with K_A and W_A adjustable to allow for experimentation with loop bandpass and gain for best accuracy in the mass calculation.

3.0 Preliminary Results

Figure 3 shows loop speed response with different values of K_A and W_A for the loading profile obtained with the 8 inch diameter slinger. The program settles in the first five seconds and the load is applied from 5.0 to 5.5 seconds (see program listing in Appendix A). Rate changes peak at the beginning and end of this sequence due to the step input of applied torque, worst than actual since there will be some torque shaping in actual hardware applications. Results of these three cases show that the wide bandpass loop gives best speed response and peak torque does not increase much with bandpass in this range. Figure 4 shows the speed characteristic using the same simulation parameters as the 10 rad loop in Figure 3 except the torque loading profile for the 5.25 inch slinger is applied. In this case, speed changes are only 6% and peak torque is 91 in-oz.

FIGURE 3 -- SPEED CHARACTERISTIC FOR
AN 8 INCH DIA. SLINGER

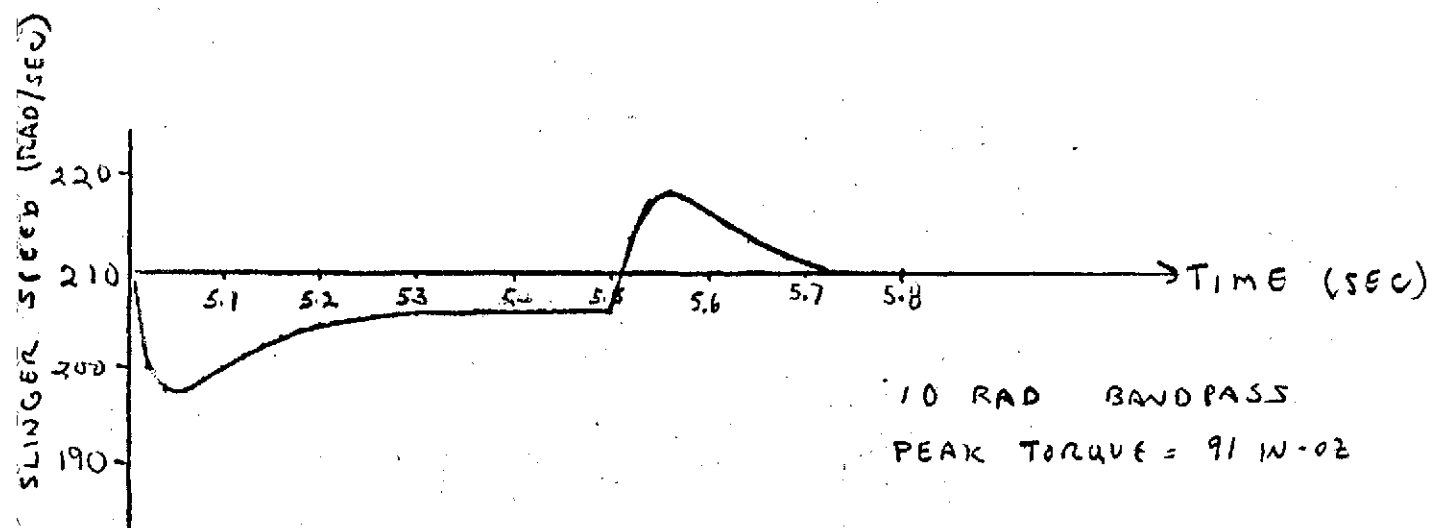
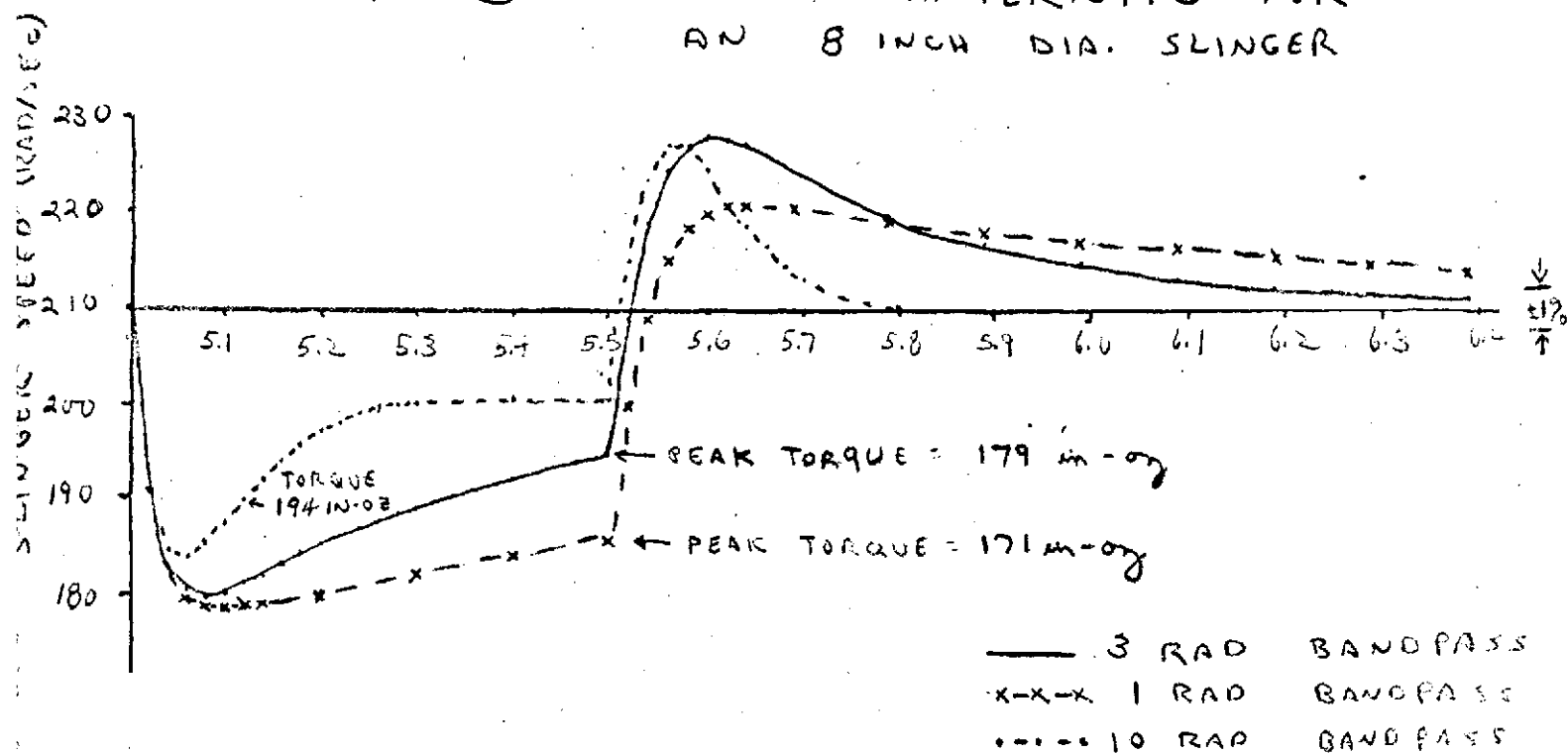


FIGURE 4 -- SPEED CHARACTERISTIC
FOR A 5.25 INCH DIA. SLINGER

APPENDIX A

Page 6

GE: VFSTC HYBRID COMPUTER FACILITY

FORTRAN VERSION 4, LEVEL 3/A

```
1 C SLINGER MODEL 31 JAN
2 C MAIN PROGRAM
3 COMMON IXI,IXS,IS(6),V(20),P(15)
4 DIMENSION X(7),XD(7),REL(7),ABS0(7),TS(107)
5 NAMELIST/INPUT/P
6 NAMELIST/RKMI/ABS0,REL,CI, NCIP,FINTIM
7 READ(5,INPUT)
8 READ(5,RKMI)
9 T = 0.
10 IP = 0
11 X(1) = 19.1
12 X(2) = 209
13 DB 40 I = 3,7
14 40 X(I) = 0.0
15 DB 50 I = 1,20
16 50 V(I) = 0.
17 DB 60 I = 1,107
18 60 TS(I) = 0.0
19 N = 2
20 HMINT = 1.E-7
21 NP = NCIP = 1
22 20 CALL RKMI(T,N,X,XD,CI,HMINT,REL,ABS0,TS,IP)
23 IF(T.GT. 4.9 .AND. T.LT. 5.71) NP=9
24 90 NP = NP + 1
25 IF(NP.LT. NCIP) GO TO 20
26 NP = 0
27 WRITE(6,30) T,(V(I),I=1,11)
28 IF(T.LT. FINTIM) GO TO 20
29 30 FORMAT(12E11,4)
30 STOP
31 END
```

GE: VFSTC HYBRID COMPUTER FACILITY

FORTRAN VERSION 4, LEVEL 3/A

```
1 C SLINGER MODEL 31 JAN
2 C DERIV SUB-PROGRAM
3 SUBROUTINE DERIV(T,X,XD,IE)
4 COMMON IX1,IXS,IS(6),V(20),P(15)
5 DIMENSION X(1),XD(1)
6 V(7) = 0.
7 V(8) = P(3)
8 IF(T .GE. 5.0 .AND. T .LE. 5.1) GO TO 10
9 IF(T .GT. 5.1 .AND. T .LT. 5.5) GO TO 20
10 IF(T .GE. 5.5 .AND. T .LE. 5.6) V(8)=P(3)+P(4)*(5.6-T)
11 GO TO 30
12 10 V(7) = P(4)
13 V(8) = P(3) + P(4)*(T-5.0)
14 GO TO 30
15 20 V(7) = P(4)
16 V(8) = P(3) + .1*P(4)
17 30 V(3) = X(1)
18 V(5) = X(2)
19 V(9) = 192*.266*(V(3)-.0907*V(5))
20 V(1) = 7.91 - V(5)*.0286
21 V(2) = V(1)*P(1)-V(3)
22 V(4) = V(5)*V(7)
23 V(6) = .266*(V(3)-.0907*V(5))-.025*V(4)
24 XD(1) = P(2)*V(2)
25 XD(2) = V(6)/V(8)
26 RETURN
27 END
```

GENERAL ELECTRIC

SPACE DIVISION
PHILADELPHIA

PROGRAM INFORMATION REQUEST / RELEASE

CLASS. LTR.	OPERATION	PROGRAM	SEQUENCE NO.	REV. LTR.
PIR NO. U	1451	SLR	001	
*USE "C" FOR CLASSIFIED AND "U" FOR UNCLASSIFIED				

FROM	J.E. Avery, Mgr. Computer Systems Eng'g Rm U-8010, X-7243	TO	Gordon Fogal
------	---	----	--------------

DATE SENT	DATE INFO. REQUIRED	PROJECT AND REQ. NO.	REFERENCE DIR. NO.
9-18-74			

SUBJECT	Set-up of SLINGER Threshold and Correction Constants
---------	--

INFORMATION REQUESTED/RELEASED

The digital threshold and correction constants for the SLINGER must be manually set and reset fairly frequently until an adaptive threshold capability is included. This PIR documents the procedures necessary to calculate and store the proper values of THRESH (threshold) and CORCON (correction constant) for the current version of SLINGER hardware and software.

The basic measurement sequence for the SLINGER is shown in simplified functional form in figure 1. The calculation and storage procedures, as well as a hexadecimal-decimal conversion aid, are included on the following pages.

DISTRIBUTION:	J. Avery	U-8010 (5)	R. Sergio	U-2446	PAGE NO. 1 OF 4	RETENTION REQUIREMENTS	
	G. Fogal	U-1240				COPIES FOR	MASTERS FOR
	R. Farrell	U-8010				<input type="checkbox"/> 1 MO.	<input type="checkbox"/> 3 MOS.
	R. Young	U-2446				<input type="checkbox"/> 3 MOS.	<input type="checkbox"/> 6 MOS.
						<input type="checkbox"/> 6 MOS.	<input type="checkbox"/> 12 MOS.
						<input type="checkbox"/> 1 MOS.	<input type="checkbox"/> 1 MOS.
						<input type="checkbox"/>	<input type="checkbox"/> DON'T DESTROY

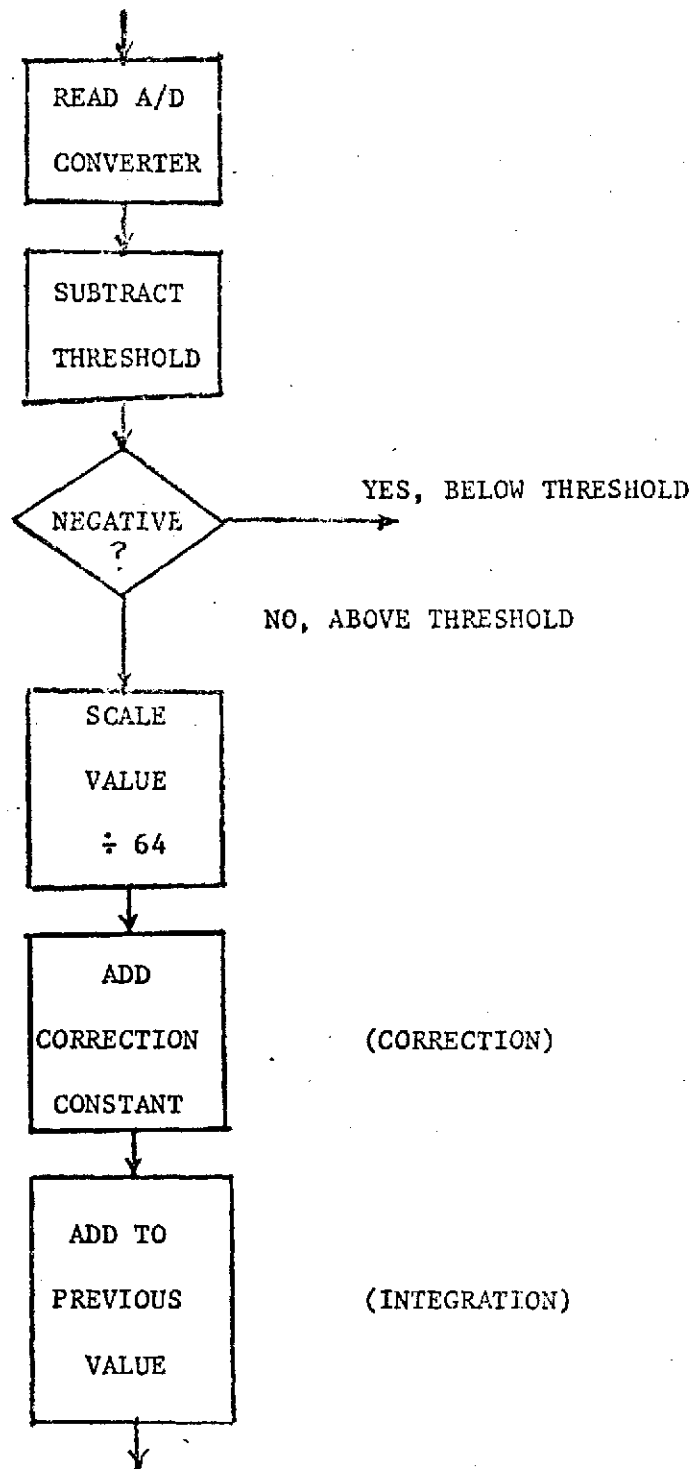


FIGURE 1 SIMPLIFIED MEASUREMENT PROCEDURE

I. Determine ambient, steady-state output of A/D converter

A. Set threshold equal to zero

1. experiment/panel switch to PANEL
2. push CLEAR button
3. set switch to 0009
4. push LOAD ADDRESS button (0009 appears in display)
5. push DISPLAY button (current THRESH value appears)
6. push LOAD ADDRESS button (0009 appears)
7. set switch to 0000
8. push LOAD button (0000 appears)
9. set switch to 0009
10. push LOAD ADDRESS button (0009 appears)
11. push DISPLAY button (0000 should appear)

B. Watch instantaneous A/D reading

1. set switch to 0055
2. push LOAD ADDRESS button (0055 appears)
3. push EXECUTE switch
4. experiment/panel switch to EXPERIMENT
5. push START button

At this point, a quickly changing NON-ZERO reading should appear in the display. Verify that it is reading correctly by loading the motor slightly, the readings should increase. If readings do not increase, or if the steady-state value is 0000 on display, the analog circuitry must be adjusted.

6. estimate average steady-state value, "A"
7. estimate peak value, a value which is never exceeded, "P".

II. Compute and store new values of THRESH and CORCON

A. Compute required values THRESH and CORCON

1. convert "A" and "P" to decimal values "a", "p" (see enclosed hexadecimal-

decimal conversion).

2. choose a value "t" which is to be the threshold value THRESH. "t" must be equal to or greater than "p". A higher "t" increases noise immunity but sacrifices accuracy. A lower "t" increases accuracy but loses noise immunity.

$$t \geq p$$

3. choose a value "c" which is to be the correction constant CORCON.

$$c = \frac{t-a}{64} \quad (\text{round to nearest integer})$$

4. convert "t" and "c" to hexadecimal values "T" and "C" (THRESH and CORCON) using the enclosed decimal-hexadecimal conversion.

B. Load new values of THRESH and CORCON.

1. experiment/panel switch to PANEL
2. push CLEAR button
3. set switch to 0009
4. push LOAD ADDRESS button (0009 appears)
5. set switch to value "T"
6. push LOAD button ("T" appears)
7. set switch to 0009
8. push LOAD ADDRESS button (0009 appears)
9. push DISPLAY button ("T" should appear)
10. set switch to 0059
11. push LOAD ADDRESS button (0059 appears)
12. set switch to value "c"
13. push LOAD button ("c" appears)
14. set switch to 0059
15. push LOAD ADDRESS button (0059 appears)
16. push DISPLAY button ("c" should appear)

III. At this point the new values have been set and stored and the SLINGER may be

exercised operationally. A notation of the new values and the date changed and by whom should be made.

HEXADECIMAL AND DECIMAL INTEGER CONVERSION TABLE

	8		7		6		5		4		3		2		1
Hex	Decimal	Hex	Decimal	Hex	Decimal	Hex	Decimal	Hex	Decimal	Hex	Decimal	Hex	Decimal	Hex	Decimal
0	0	0	0	0	0	0	0	0	0	0	0	0	0	0	0
1	268,435,456	1	16,777,216	1	1,048,576	1	65,536	1	4,096	1	256	1	16	1	1
2	536,870,912	2	33,554,432	2	2,097,152	2	131,072	2	8,192	2	512	2	32	2	2
3	805,306,368	3	50,331,648	3	3,145,728	3	196,608	3	12,288	3	768	3	48	3	3
4	1,073,741,824	4	67,108,864	4	4,194,304	4	262,144	4	16,384	4	1,024	4	64	4	4
5	1,342,177,280	5	83,886,080	5	5,242,880	5	327,680	5	20,480	5	1,280	5	80	5	5
6	1,610,612,736	6	100,663,296	6	6,291,456	6	393,216	6	24,576	6	1,536	6	96	6	6
7	1,879,048,192	7	117,440,512	7	7,340,032	7	458,752	7	28,672	7	1,792	7	112	7	7
8	2,147,483,648	8	134,217,728	8	8,388,608	8	524,288	8	32,768	8	2,048	8	128	8	8
9	2,415,919,104	9	150,994,944	9	9,437,184	9	589,824	9	36,864	9	2,304	9	144	9	9
A	2,684,354,560	A	167,772,160	A	10,485,760	A	655,360	A	40,960	A	2,560	A	160	A	10
B	2,952,790,016	B	184,549,376	B	11,534,336	B	720,896	B	45,056	B	2,816	B	176	B	11
C	3,221,225,472	C	201,326,592	C	12,582,912	C	786,432	C	49,152	C	3,072	C	192	C	12
D	3,489,660,928	D	218,103,808	D	13,631,488	D	851,968	D	53,248	D	3,328	D	208	D	13
E	3,758,096,384	E	234,881,024	E	14,680,064	E	917,504	E	57,344	E	3,584	E	224	E	14
F	4,026,531,840	F	251,658,240	F	15,728,640	F	983,040	F	61,440	F	3,840	F	240	F	15
	8		7		6		5		4		3		2		1

TO CONVERT HEXADECIMAL TO DECIMAL

1. Locate the column of decimal numbers corresponding to the left-most digit or letter of the hexadecimal; select from this column and record the number that corresponds to the position of the hexadecimal digit or letter.
2. Repeat step 1 for the next (second from the left) position.
3. Repeat step 1 for the units (third from the left) position.
4. Add the numbers selected from the table to form the decimal number.

To convert integer numbers greater than the capacity of table, use the techniques below:

HEXADECIMAL TO DECIMAL

Successive cumulative multiplication from left to right, adding units position.

Example: $D34_{16} = 3380_{10}$

$$\begin{array}{r}
 D = 13 \\
 \times 16 \\
 \hline
 208 \\
 3 = +3 \\
 \hline
 211 \\
 \times 16 \\
 \hline
 3376 \\
 4 = +4 \\
 \hline
 3380
 \end{array}$$

EXAMPLE	
Conversion of Hexadecimal Value	D34
1. D	3328
2. 3	48
3. 4	4
4. Decimal	3380

TO CONVERT DECIMAL TO HEXADECIMAL

1. (a) Select from the table the highest decimal number that is equal to or less than the number to be converted.
(b) Record the hexadecimal of the column containing the selected number.
(c) Subtract the selected decimal from the number to be converted.
2. Using the remainder from step 1(c) repeat all of step 1 to develop the second position of the hexadecimal (and a remainder).
3. Using the remainder from step 2 repeat all of step 1 to develop the units position of the hexadecimal.
4. Combine terms to form the hexadecimal number.

DECIMAL TO HEXADECIMAL

Divide and collect the remainder in reverse order.

Example: $3380_{10} = D34_{16}$

$$\begin{array}{r}
 16 \overline{) 3380} \quad \text{remainder} \\
 \underline{16 \overline{) 211}} \quad 4 \\
 \underline{16 \overline{) 13}} \quad 3 \\
 \quad \quad D
 \end{array}$$

EXAMPLE	
Conversion of Decimal Value	3380
1. D	<u>-3328</u>
	52
2. 3	<u>-48</u>
	4
3. 4	<u>-4</u>
4. Hexadecimal	D34

CALCULATION OF MOTOR TORQUE EFFECT

Analytical

Based on the preliminary derivation and analysis of the electro-mechanical portion of the mass measurement system, the following results have been obtained:

- o If the motor speed is constant, the relationship between the motor current and torque is linear and of the form $f(x) = ax+b$.
- o The magnitude of the torque is a function of the following variables: time, radius, angular acceleration, and mass. Further, the solution is exponential with the mass being contained in the exponent.
- o There is non-linearity in the relationship between the motor current and the mass as shown by Eq's (1.22) and (2.14).
- o The preliminary model indicates that the relationship to be established is the energy transfered by the motor to the mass in order to accelerate the mass of the disk.
- o Finally, only the peak torque allows a linear relationship between torque and motor current where the mass is the primary constant of porportionality.

Based on the model for the prime mover portion of the mass measurement system, the dynamic performance equations will be examined and the electromechanical transfer function derived. Once the transfer function has been obtained, the system performance will be examined for linearity and sensitivity. Due to the nature of the system, the derivation will be performed in three portions: (1) the electronic; (2) the mechanical and (3) the electromechanical.

The electrical model for a D.C. shunt motor is shown in Figure (1).

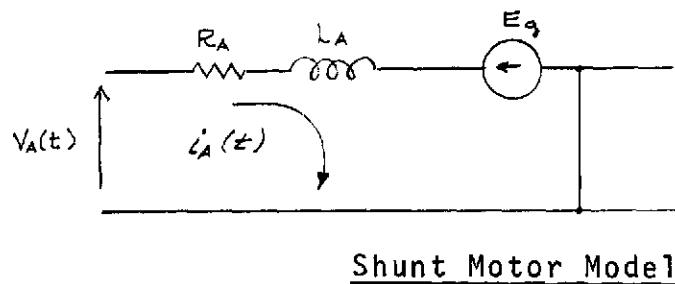


Figure (1)

where:

$V_A(t)$ = the applied armature voltage

R_A = the armature resistance

L_A = the armature inductance

E_g = the back or counter EMF

$i_A(t)$ = the armature current.

The general equation for this circuit may be written as:

$$\text{Eq (1.1)} \quad V_A(t) = \frac{L_A di_A}{dt} + R_A i_A(t) + E_g$$

However, the back or counter EMF is a voltage that is dependent on the motor speed and the magnetic flux which may be expressed as:

$$\text{Eq (1.2)} \quad V_E = K_E \cdot \emptyset \cdot \omega_M$$

where:

K_E = a constant of porportionality

\emptyset = the magnetic flux

ω_M = the angular velocity of the motor.

But, the magnetic flux is constant for a permanent magnet D.C. motor so Eq (1.3) may be written as:

$$\text{Eq (1.3)} \quad E_G = K_V \cdot \omega_M$$

where:

$$E_G = V_E$$

$$K_V = K_E \cdot \emptyset$$

Substitution of Eq (1.3) into Eq (1.1) yields:

$$\text{Eq (1.4)} \quad V_A(t) = \frac{L_A di_A}{dt} + R_A \cdot i_A(t) + K_V \cdot \omega_M$$

Employing the La Place transformation Eq (1.4) becomes:

$$\text{Eq (1.5)} \quad V_A(s) = sL_A + R_A \cdot I_A(s) + K_V \cdot \omega$$

so that the motor impedance may be expressed as:

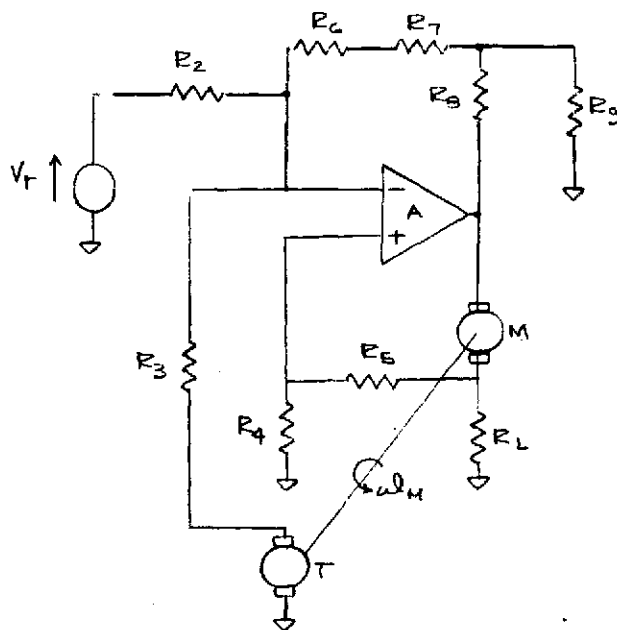
$$\text{Eq (1.6)} \quad Z_M(s) = (sL_A + R_A)$$

Since

$$\text{Eq. (1.7)} \quad Z_M(s) = \frac{V_A(s) - K_V \cdot \omega_M}{I_A(s)}$$

so that Eq (1.5) and Eq (1.6) define the motor.

However, the overall configuration must be examined in order to establish the parametric relationships. The prime mover system relationship and configuration is shown in Figure (2) and the electrical equivalent in Figure (3).



System Configuration

Figure (2)

where:

V_r = a reference voltage

T = the D.C. tachometer generator

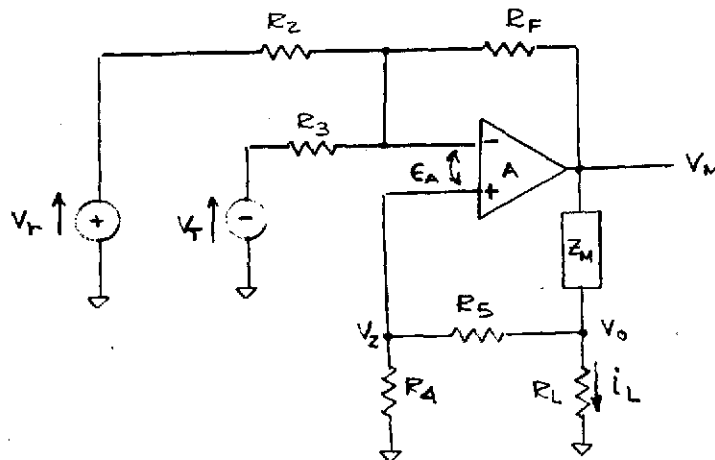
M = the D.C. shunt motor

R_L = the load or sense resistor

R_x = the external resistances

A = the operational amplifier.

and:



System Electrical Equivalent

Figure (3)

where:

V_r = a reference voltage

V_T = the tachometer generator output voltage

A = the amplifier input summing point voltage

V_M = the output voltage of the amplifier

R_F = the equivalent feedback resistance

V_o = the system output voltage

V_z = the voltage at the non-inverting terminal

i_L = the load current

R_x = the external resistances

z_M = the motor impedance

R_L = the load or sense resistance.

Examination of the feedback loop in Figure (3) shows that resistance multiplication is employed so that the equivalent feedback resistance may be expressed as:

$$\text{Eq. (1.8)} \quad R_F = \frac{(R_6+R_7)(R_8+R_9)}{R_9}$$

so that the general transfer function for the operational amplifier may be written as:

$$\text{Eq. (1.9)} \quad \frac{V_r - V_2 - A}{R_2} + \frac{V_T - V_2 - A}{R_3} = \frac{V_2 + A - V_M}{R_F}$$

which may be rewritten as:

$$\text{Eq. (1.10)} \quad \frac{V_r - V_2}{R_2} + \frac{-V_T - V_2}{R_3} - \frac{(R_3 R_F + R_2 R_F + R_2 R_3) \epsilon_A}{R_2 \cdot R_3 \cdot R_F} = \frac{V_2 - V_M}{R_F}$$

If the contribution due to ϵ_A is neglected and Eq (1.10) is simplified, the following results:

$$\text{Eq. (1.11)} \quad V_M = \left[\frac{R_2 R_3 + R_2 R_F + R_3 R_F}{R_2 \cdot R_3} \right] V_2 - \left[\frac{R_F}{R_2 R_3} \right] [R_3 V_r - R_2 V_T]$$

Further, it can be shown that the relationship between the output voltage V_M and the voltage at the non-inverting term V_2 can be expressed as:

$$\text{Eq. (1.12)} \quad V_2 = \frac{R_L \cdot R_4}{R_L (R_4 + R_5) + Z_M (R_L + R_4 + R_5)} V_M$$

so that substitution of Eq (1.12) into Eq (1.11) and simplification yields:

$$\text{Eq. (1.13)} \quad \left[\frac{R_F}{R_2 R_3} \right] [R_3 V_r - R_2 V_T] = \left[\frac{R_2 R_3 + R_2 R_F + R_3 R_F}{R_2 R_3} \frac{R_L \cdot R_4}{R_L (R_4 + R_5) + Z_M (R_L + R_4 + R_5)} - 1 \right] V_2$$

and multiplication By (-1) yields:

$$\text{Eq. (1.14)} \quad \left[\frac{R_F}{R_2 R_3} \right] [R_2 V_T - R_3 V_r] = \left[1 - \frac{R_L R_4}{R_2 R_3} \frac{R_2 R_3 + R_2 R_F + R_3 R_F}{R_L (R_4 + R_5) + Z_M (R_L + R_4 + R_5)} \right] V_M$$

Examination of Figure (3) reveals that the applied armature voltage for the motor may be written as:

$$\text{Eq. (1.15)} \quad V_A(t) = V_M(t) - V_O(t)$$

so that

$$\text{Eq (1.16)} \quad V_O(t) = V_A(t) - V_M(t)$$

Employing the La Place transform of Eq (1.16) and substitution of Eq (1.5) yields:

$$\text{Eq (1.17)} \quad V_O(s) = [SLA + RA] I_A(s) + KV \cdot \omega_M - V_M(s)$$

If the tachometer generator is examined, the electromechanical transfer function may be defined as:

$$\text{Eq. (1.18)} \quad V_T = K_G \cdot \omega_M$$

where:

V_T = the tachometer generator output voltage

K_G = a constant of porportionality

ω_M = the angular velocity of the motor.

substitution of Eq (1.18) into Eq (1.14) yields:

$$\text{Eq. (1.19)} \quad \left[\frac{R_F}{R_2 R_3} \right] \left[R_2 K_e u_{1M} - R_3 V_r \right] = \left[1 - \frac{R_L R_4}{R_2 R_3} \cdot \frac{R_2 R_3 + R_2 R_F + R_3 R_F}{R_L (R_4 + R_5) + Z_M (R_L + R_4 + R_5)} \right] V_M$$

Eq. (1.17) and Eq (1.19) are the characteristic equations for the prime mover portion of the mass measurement system. The overall relationship is obtained by solving Eq (1.19) for V_M and substitution into Eq (1.17). It will be shown that the dependent variable $V_o(s)$ is a function of $I_A(s)$.

Finally, the relationship between the torque and the armature current is given by:

$$\text{Eq (1.20)} \quad T(s) = K_T \cdot I_A(s)$$

where:

$T(s)$ = the torque placed on the motor

K_T = a constant of proportionality

$I_A(s)$ = the armature current.

So that substitution of Eq (1.20) into Eq (1.17) yields:

$$\text{Eq. (1.21)} \quad V_o(s) = \left[\frac{S L_A + R_A}{K} \right] T(s) \quad V_M(s) + K_V \cdot u_{1M}$$

so that the transfer function is expressed as:

$$\text{Eq (1.22)} \quad V_o(s) = \left[\frac{S L_A + R_A}{K_T} \right] T(s) - \left[\frac{R_F}{R_2 R_3} \right] \left[R_2 K_e u_{1M} - R_3 V_r \right]$$

$$\left[1 - \frac{R_L R_4}{R_2 R_3} \cdot \frac{R_2 R_3 + R_2 R_F + R_3 R_F}{R_L (R_4 + R_5) + Z_M (R_L + R_4 + R_5)} \right] - 1$$

$$+ K_V \cdot u_{1M}$$

Eq (1.22) is the electrical parametric equation for the electronic portion of the prime mover portion of the mass measurement system. It should be obvious that the independent variable is torque and the dependent variable is the output voltage. This equation completes the electrical derivation and dictates that the mechanical portion examine the torque and its relationship to mass and angular velocity.

In its present form, Eq (1.22) is a first order linear differential equation with a complimentary and particular solution. Further, the solution to this form of equation is exponential which for a first order expansion is linear.

After a preliminary investigation of the mechanical aspects of the transducer portion of the system, it was concluded that a precise mathematical model could not be derived under the existing economic conditions. However, a satisfactory first order model can be derived with a limited number of assumptions and will adequately describe the system behavior.

Initially, a description of the system may prove useful in understanding the events, the validity of the assumptions, and the modeling of the events. At some arbitrary time t_0 , a mass is dropped from a fixed height without any external forces other than the downward force due to some type of gravity, it will be assumed that this mass will possess no angular momentum when it initially contacts the plate. Once the mass contacts the plate, a torque is created due to the $-z$ force which causes the disk to oscillate with respect to the z axis. This oscillation as well as the effects initially

upon contact. Under these assumptions, the total mass is concentrated at one point on the disk so that a torque is created, and in the instant of time the mass is stationary. As the disk rotates, the velocity changes in direction so that the mass is accelerated. Once the linear force exceeds the static friction, the mass begins to move outward in the direction of the velocity vector with a defined momentum. As the mass moves outward, the velocity increases with the increased radius so that the momentum increases. Consequently, the torque increases due to the increase in the momentum.

At some point, the mass will be positioned so that a maximum torque will be exerted and this point is when the effective mass is located at the radius of the disk. Since there are not constraints on the body, the mass will leave the disk. If the entire mass leaves the disk simultaneously, the torque will drop to zero due to the absence of a force. However, for this situation to occur, the entire mass must be present at the outer edge simultaneously. Due to the very nature of the mass, this situation cannot occur. If it is assumed that the entire mass is on the plate prior to any mass being tossed off, the following statement is valid. The torque may be considered in a piece wise fashion where it is initially a function of the radius and then a function of the mass and the radius. Further, it will be assumed that the mass is cylindrical with a uniform density

ρ .

Initially, the general torque equation must be derived from the point when the mass is on the plate. By definition, the torque may be expressed as:

$$\text{Eq. (2.1)} \quad T = r \cdot F$$

where:

T = the torque

r = the distance from the torque

F = the force creating the torque.

Eq. (2.1) is based on torque being defined as the moment of force or the product of the force and the perpendicular distance from the line of action of the force to the center of rotation as shown in Figure (1).



Vector Representation of Torque

Figure (1)

so that Eq (2.1) may be proven in the following manner.

The torque is a vector given by the cross-product of the force vector and the position vector which is:

$$\text{Eq (2.2)} \quad \vec{T} = \vec{r} \times \vec{F}$$

However, Eq (2.2) may be expressed as:

$$\text{Eq (2.3)} \quad \vec{T} = r \cdot F \sin \theta$$

where ϕ = the angle between the position and force vectors.
 Moreover, by definition $\phi = \pi/2$ so that Eq (2.3) becomes:

$$\text{Eq (2.4)} \quad T = r \cdot F$$

which proves Eq (2.1).

From Newton's second law, the force may be expressed as the rate of change of momentum so that:

$$\text{Eq. (2.5)} \quad F = \frac{d(m \cdot v)}{dt}$$

where:

F = the force

m = the effective mass

v = the linear velocity.

So that Eq (2.5) may be written as:

$$\text{Eq (2.6)} \quad F = m \frac{dv}{dt} + v \frac{dm}{dt}$$

However, the problem is one of a rotating body and the relationship between linear velocity and angular velocity is given by:

$$\text{Eq (2.7)} \quad v = r \frac{d\theta}{dt} + \theta \frac{dr}{dt}$$

where:

r = the radius of rotation

θ = the angular displacement

v = the linear velocity.

Substitution of Eq (2.7) into Eq (2.6) yields:

$$\text{Eq (2.8)} \quad F = m d \left[\frac{r d\theta/dt + \theta dr/dt}{dt} \right] + \left[\frac{r d\theta}{dt} + \theta \frac{dr}{dt} \right] \frac{dm}{dt}$$

However, by definition

$$\text{Eq (2.9)} \quad \frac{d\theta}{dt} = \omega$$

where ω = angular velocity

so that Eq (2.9) may be written as:

$$\text{Eq (2.9)} \quad F = m \frac{d(r\omega + \theta dr/dt)}{dt} + (r\omega + \theta dr/dt) \frac{dm}{dt}$$

and differentiation yields:

$$\text{Eq (2.10)} \quad F = m \frac{d(r\omega)}{dt} + m \frac{d(\theta dr/dt)}{dt} + (r\omega) \frac{dm}{dt} + \theta \frac{dr}{dt} \frac{dm}{dt}$$

and simplification yields:

$$\text{Eq (2.11)} \quad F = m \cdot \omega \frac{dr}{dt} + m r \frac{d\omega}{dt} + m \frac{dr}{dt} \frac{d\theta}{dt} + m \theta \frac{d^2 r}{dt^2} + (r\omega) \frac{dm}{dt} + \theta \frac{dr}{dt} \frac{dm}{dt}$$

so that employing Eq (2.9) yields

$$\text{Eq (2.12)} \quad F = m \omega \frac{dr}{dt} + m r \frac{d\omega}{dt} + m \omega \frac{dr}{dt} + m \theta \frac{d^2 r}{dt^2} + r \omega \frac{dm}{dt} + \theta \frac{dr}{dt} \frac{dm}{dt}$$

However, if only the tangential components are employed, Eq (2.12) becomes:

$$\text{Eq (2.13)} \quad F = m \omega \frac{dr}{dt} + m r \frac{d\omega}{dt} + r \omega \frac{dm}{dt}$$

So that substitution of Eq (2.13) into Eq (2.4) yields:

$$\text{Eq (2.14)} \quad T = mrw\frac{dr}{dt} + mr^2\frac{dw}{dt} + r^2w\frac{dm}{dt}$$

which is the general torque equation.

Based on the assumption that the entire mass contacts the plate prior to any mass being thrown off, the mass does change with time so that:

$$\text{Eq (2.15)} \quad \frac{dm}{dt} = 0$$

and, therefore, equation (2.14) becomes:

$$\text{Eq. (2.16)} \quad T = M_T r w \frac{dr}{dt} + M_T r^2 \frac{dw}{dt}$$

where: M_T = the effective mass located at a distance r from the center.

If Eq (2.16) is examined with respect to time, the torque is a function of the effective location of the mass and there is no change in radius with respect to a change in time so that:

$$\text{Eq. (2.17)} \quad \frac{dr}{dt} = 0$$

and equation (2.16) may be expressed as:

$$\text{Eq (2.18)} \quad T(t_i) = M_T r^2 \frac{dw}{dt} \quad t_i \leq T(t_i) \leq t_p$$

Moreover, the magnitude of the rate of change of angular velocity may be treated as a constant so that

$$\text{Eq (2.19)} \quad T(t_i) = M\alpha r_i^2$$

Consequently, the instantaneous torque at any time is:

$$\begin{aligned} \text{Eq. (2.20)} \quad T(t_1) &= M_T \alpha r_1^2 & r_1 > 0 \\ T(t_2) &= M_T \alpha r_2^2 & r_1 < r_2 < r_3 \\ T(t_3) &= M_T \alpha r_3^2 & r_2 < r_3 < r_4 \\ &0 \\ &0 \\ &0 \\ T(t_n) &= M_T \alpha r_n^2 & r_{n-1} < r_n \leq r_{\text{disk}} \end{aligned}$$

Further, the examination of Eq (2.20) shows that the root loci of the torque to be parabolic and the overall function exponential. Finally, at some instant of time t_p , the effective mass will be located at a maximum distance from the center of action so that the peak torque is:

$$\text{Eq (2.21)} \quad T(t_p) = M_T r_{\text{max}}^2 \alpha$$

where:

$T(t_p)$ = the peak torque

M_T = the effective mass

r_{max} = the maximum distance from the center of action

α = the angular acceleration which is constant.

If it is assumed that the relationship between the radius and time is linear:

$$\text{Eq (2.22)} \quad r(t) = (r_c)(t^2) \quad K, \text{ where } K = \text{constant.}$$

Then the first half of the graph in Appendix A should model the system while all the mass is on the disk. Then Eq (2.16) may be written as:

$$\text{Eq (2.23)} \quad T(t) = Mr_c \cdot t \cdot \omega_r + Mr_c^2 \cdot t^2 \alpha$$

which yields:

$$\text{Eq (2.24)} \quad T(t) = MTr_c^2 t (\omega + t \cdot \alpha)$$

for

$$t_1 \leq T(t) \leq t_p$$

Examination of the second portion of the torque becomes extremely difficult. During this time, the mass is being thrown off the disk as a function of time so that Eq (2.14) must be employed in total form.

However, if it is assumed that the effective mass changes about a point then torque is:

$$\text{Eq (2.25)} \quad T(t) = mr^2 \frac{d\omega}{dt} + r^2 \omega \frac{dm}{dt}$$

and since dm/dt is a complex function, the only expression is:

$$\text{Eq. (2.26)} \quad T(t) = Mr^2 \frac{d\omega}{dt} + r^2 \omega f(M)$$

If the mass follows a parabolic curve, the second half of the graph describes the system.

GENERAL ELECTRICSPACE DIVISION
PHILADELPHIA**PROGRAM INFORMATION REQUEST / RELEASE**

CLASS. LTR.		OPERATION	PROGRAM	SEQUENCE NO.	REV. LTR.
U		1R60	74	129	
*USE "C" FOR CLASSIFIED AND "U" FOR UNCLASSIFIED					
FROM G. L. Fogal, Bioengineering Programs Room #U-1240, VFSC Extension - 5636			TO File		
DATE SENT 9/19/74	DATE INFO. REQUIRED	PROJECT AND REQ. NO. ABSS Improved Feces Measurement and Sampling	REFERENCE DIR. NO.		
SUBJECT Mass Measurement Breadboard Test Results					
INFORMATION REQUESTED/RELEASED					
1.0 <u>SUMMARY</u> The mass measurement breadboard demonstrated the feasibility of the concept and established the major factors influencing measurement error. These major factors are slinger blade configuration and slinger rotational velocity. Refinement of the slinger design will be required to achieve the $\pm 2\%$ maximum error measurement goal.					
2.0 <u>BACKGROUND</u> The feces mass measurement breadboard design was based on previous General Electric funded effort. In brief, feces mass is determined by measuring the incremental power input to the slinger element of the ABSS Solids Subsystem feces collection capability. By operating the slinger motor at constant rpm, the incremental power input, i.e. energy transferred to the feces as the feces passes thru the slinger, is proportional to feces mass.					
3.0 <u>BREADBOARD DESIGN</u> Figure 3-1 shows the mass measurement breadboard model. The breadboard consists of the slinger and slinger motor assembly mounted on a test structure, a power supply and tach feedback speed control loop and microprocessor assembly. The microprocessor integrates a voltage proportional to the incremental instantaneous power input and displays the result on a digital display. PIR 1JL3-1019 describes the breadboard electronics.					
4.0 <u>TEST RESULTS</u> A mix of dry dog food (plain Gainesburgers) and peanut butter (cream style) in about a 4 to 1 ratio (respectively) with water added to bring the moisture content up to about 75%, was used as a simulated fecal material. The weight of each sample used was determined to the nearest tenth of a gram using a Mettler scale. Sample size, slinger rpm and slinger configuration were varied as discussed in Sections 4.1 and 4.2. As noted in PIR 1JL3-1019, the microprocessor program was checked, using known electrical inputs (to simulate the power input pulse), to assure desired performance. Thus variations in test results will be caused by the effects of sample size, slinger rpm and slinger configuration. The integration threshold was set as low as possible for each slinger type and rpm combination. In general, the higher the rpm, the higher the threshold setting required. Also, the scale factor was held constant, thus the meter reading value is comparable for all test conditions.					
cc: A. Andersen G. L. Fogal R. W. Murray R. Young J. Mangialardi		PAGE NO. 1 OF 17	RETENTION REQUIREMENTS COPIES FOR <input type="checkbox"/> 1 MO. <input type="checkbox"/> 3 MOS. <input type="checkbox"/> 6 MOS. <input type="checkbox"/> 12 MOS. <input type="checkbox"/> MOS. <input type="checkbox"/> DO NOT DESTROY		

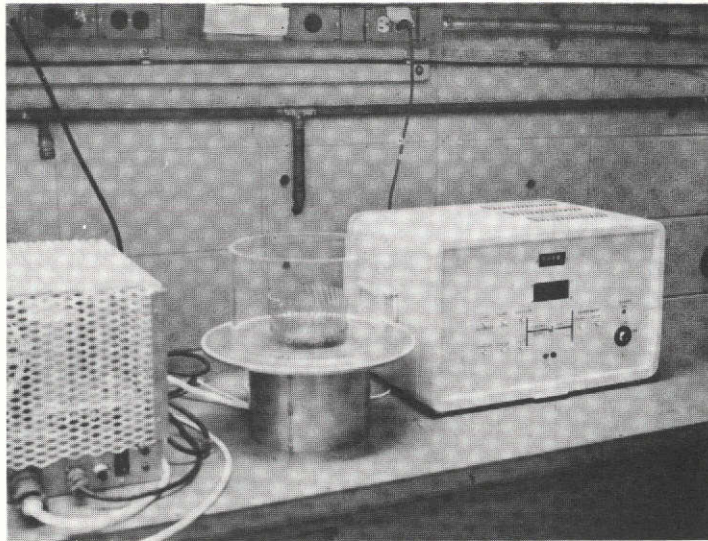


Figure 3-1(a) Mass Measurement Breadboard (from Left to Right, 28 VDC Power Supply and Motor Speed Control Electronics, Slinger/Motor Assembly, Microprocessor and Control and Readout Console)

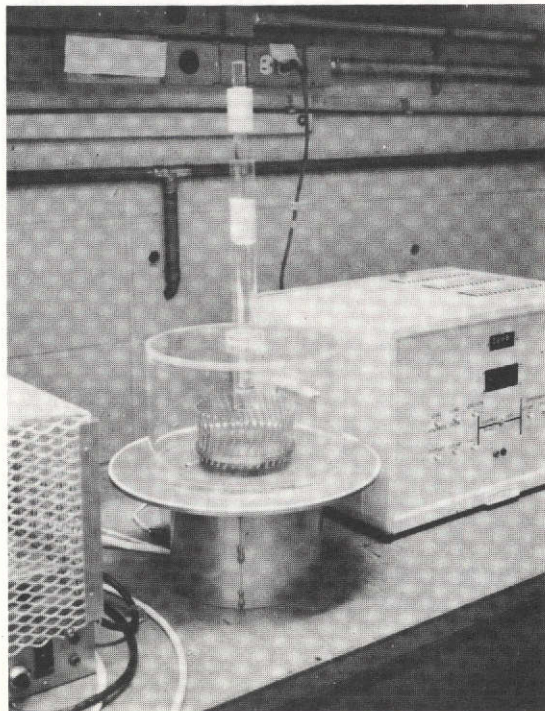


Figure 3-1(b) Mass Measurement Breadboard with Ejection Device for Applying 1.0 Inch O.D. Cylindrical Samples

4.1 Slinger Configuration

The effect of slinger configuration on mass measurement accuracy was evaluated. Three slinger configurations were used, see Figures 4-1 thru 4-3. Examination of the data, Figures 4-4 thru 4-6, indicates that the type 1 slinger exhibits the minimum error band. For this configuration, the error ranges from about $\pm 3.5\%$ for 250 gram samples up to about $\pm 6\%$ for 100 gram samples and about $\pm 8\%$ for 50 gram samples.

4.2 Slinger RPM

The effect of slinger RPM is shown in Figures 4-6 thru 4-9 for the type 1 slinger. As can be seen, measurement accuracy for the type 1 slinger appears best at about 1500 rpm.

4.3 Sample Configuration

The shape of the sample can be expected to vary from a roughly spherical blob to a long cylinder. This shape variation or sample impact rate (in grams per second of sample traversing the slinger) drastically changes the shape of the power pulse being integrated. Figures 4-10 and 4-11 illustrate this point for 100 gram simulated feces samples (using Mark II Brush Recorder). However, referring to Figures 4-4 thru 4-9, the effect of sample configuration does not appear significant.

4.4 Sample Moisture Content

Sample moisture content may vary from very dry to essentially liquid. The preceeding discussion covered the use of simulated feces samples having a moisture content range of 60 to 75%. Figure 4-12 shows the results for liquid samples using the type 1 slinger at 1500 rpm. Liquid sample conditions result in lower readings than for comparable solid spherical or cylindrical samples. This is probably due to the slinger tines being less effective (in transferring energy to the sample) for water than for solids. This further emphasises the importance of slinger configuration (blade size, number, shape) on mass measurement accuracy.

For the results shown in Figure 4-12, water was poured onto the slinger from a beaker at the maximum rate possible (by upending the beaker). The corresponding power profiles for 100 gram size liquid samples are shown in Figure 4-13. Figure 4-14 shows the power profiles for slower rates (of pouring liquid onto the slinger). Note that the incremental area under the power profile is essentially equal for Figures 4-13 and 4-14. Thus, as with solid samples, the incremental power input is independent, as it theoretically should be, of rate of sample weight thru the slinger (at least over the range investigated).

4.5 Sample/Slinger Impact Point

In normal laboratory testing, the sample is dropped onto the rotating plate portion of the slinger. Friction between the sample and rotating plate cause the sample to be accelerated radially outward into the path of the

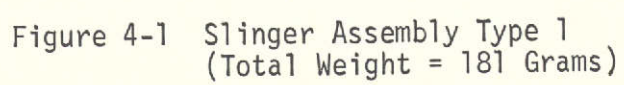
slinger "tines" or blades. The amount of energy for accomplishing this radial movement of the sample will depend on the location of the sample/slinger impact point. An impact point near the center of the rotating plate will require more energy than an impact point near the edge of the plate.

In the tests represented by Figures 4-4 thru 4-9, the impact point of the spherical samples was relatively random whereas the cylindrical samples were injected for an initial impact with the center of the plate. Referring to the Figures, the effect of impact point cannot be discerned and thus may be negligible compared to other error sources. Significantly, from visual observation of larger size cylindrical samples, after the initial portion of the sample contacts the rotating plate and is accelerated outward into the slinger tines, the action of the tines "draws" the remainder of the sample into the tines without the sample contacting the rotating plate. Thus the radial motion component of energy would be less than for a spherical sample, yet Figures 4-4 thru 4-9 show no apparent bias in this direction.

To further explore this situation, a test was performed wherein the sample impacted the slinger at the apex of the slinger plate and tines, see Figure 4-15. Results compared with samples impacting the slinger plate first did not reveal significant differences.

4.6 Residual

At the conclusion of each test series, the slinger assembly exhibits a build-up of sample. This residual appears to remain relatively constant after an initial build-up period. Table 4-1 shows the magnitude of the residual. As might be expected, the residual is less at higher slinger speeds and reduced number of slinger tines. This residual does not effect the mass measurement accuracy since the constant slinger speed eliminates the effect of slinger moment of inertia. This latter is illustrated by Figures 4-4 and 4-6 wherein the slinger moment of inertia for Figure 4-4 is considerably larger than that for Figure 4-6. A reduction in residual by surface treatment or change in blade shape or by other means may be necessary if feces sampling downstream of the slinger is contemplated.



C-2

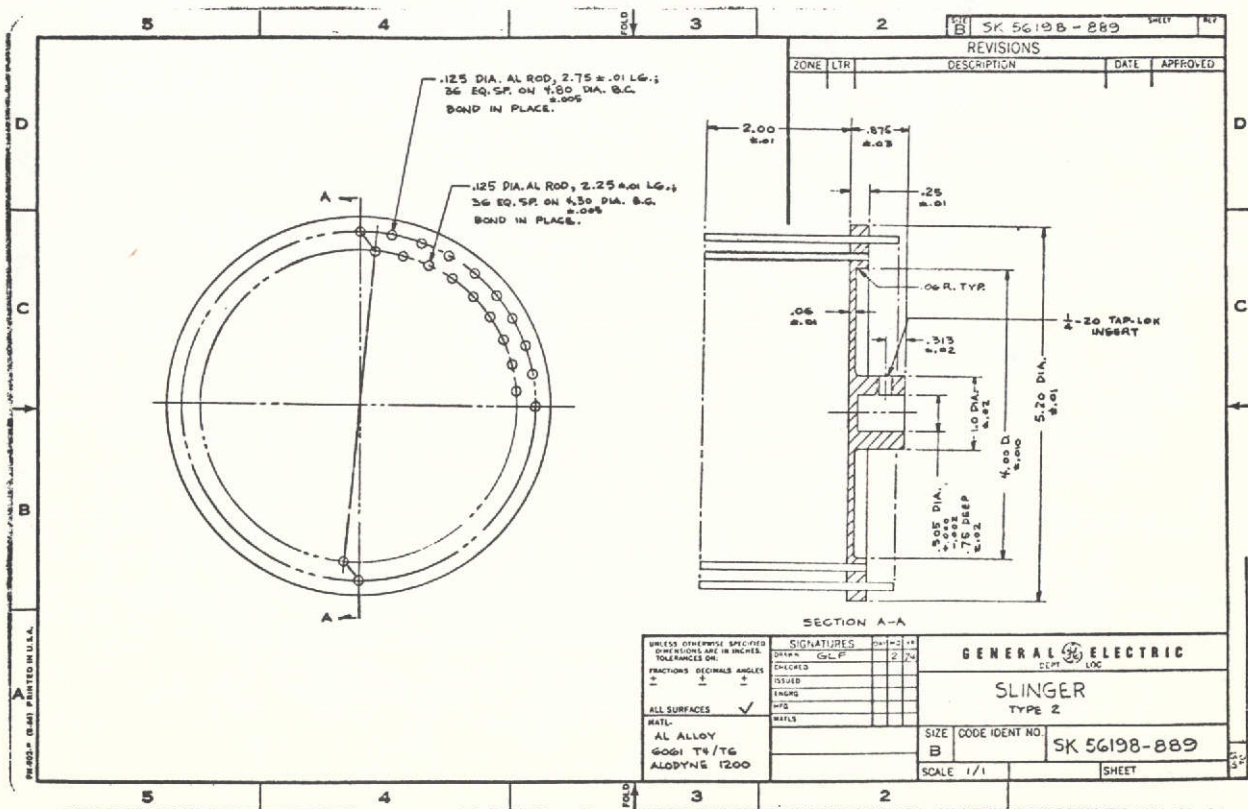
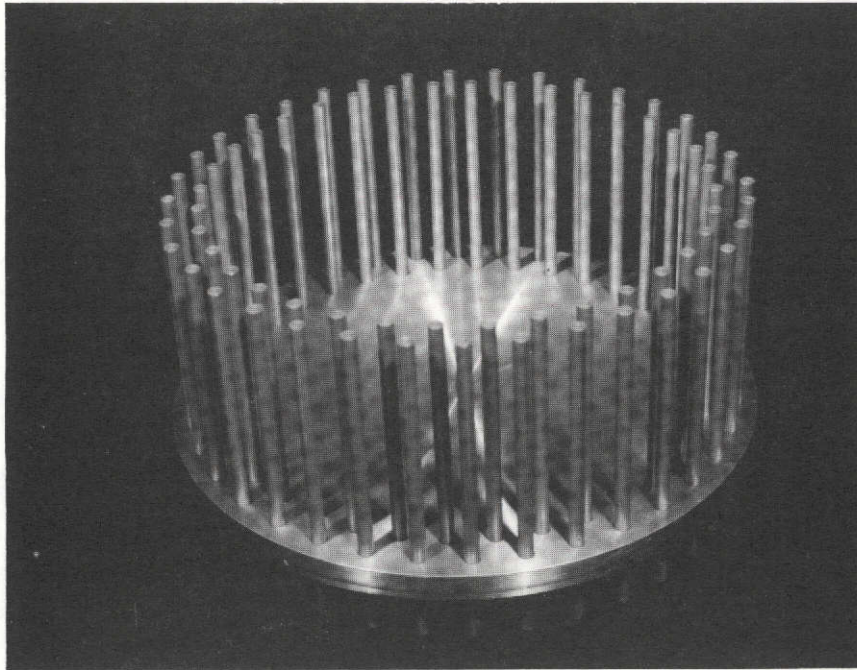




Figure 4-3 Slinger Assembly Type 3
(Total Weight = 308 Grams)

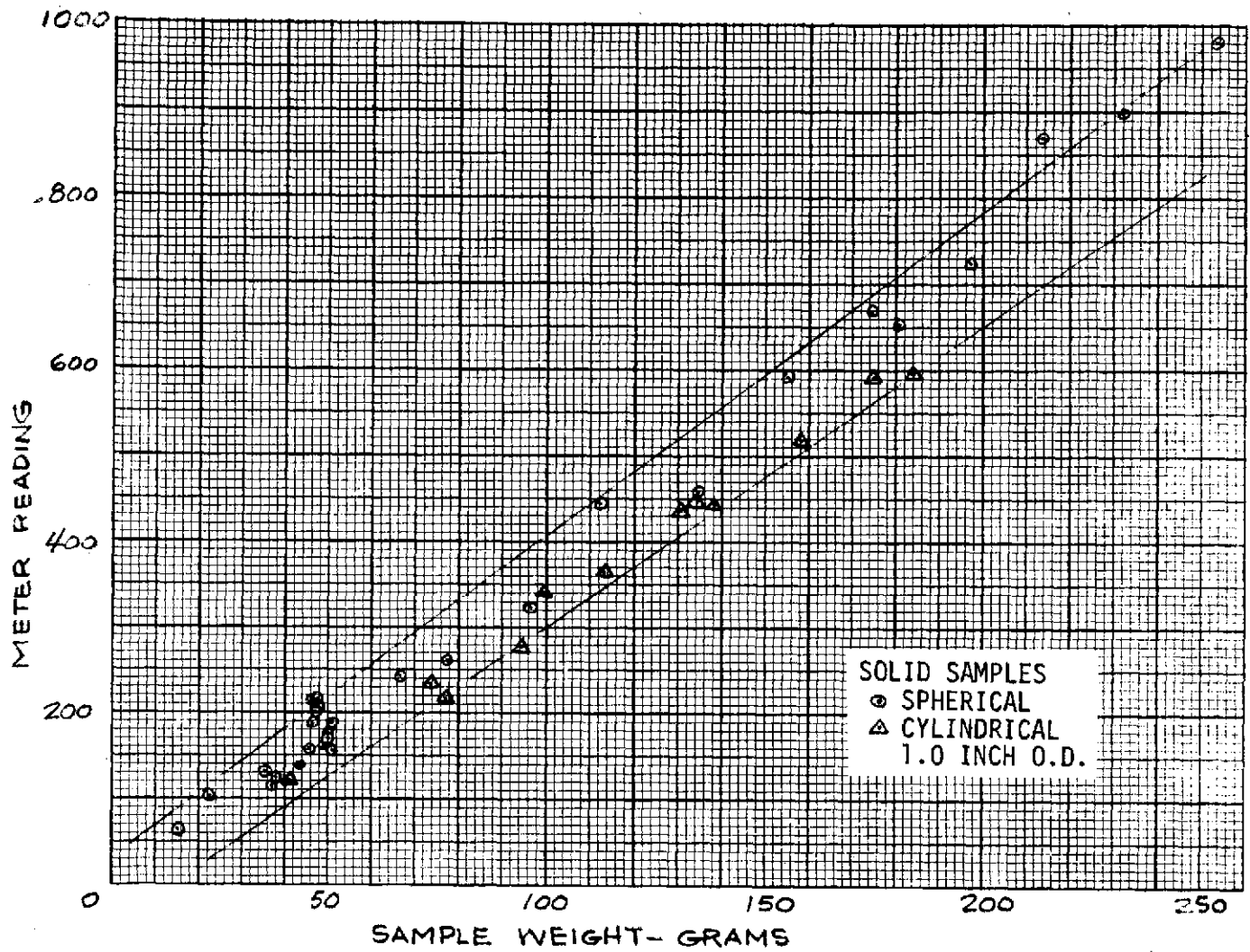


Figure 4-4 Measurement Data, Type 2 Slinger at 1500 rpm

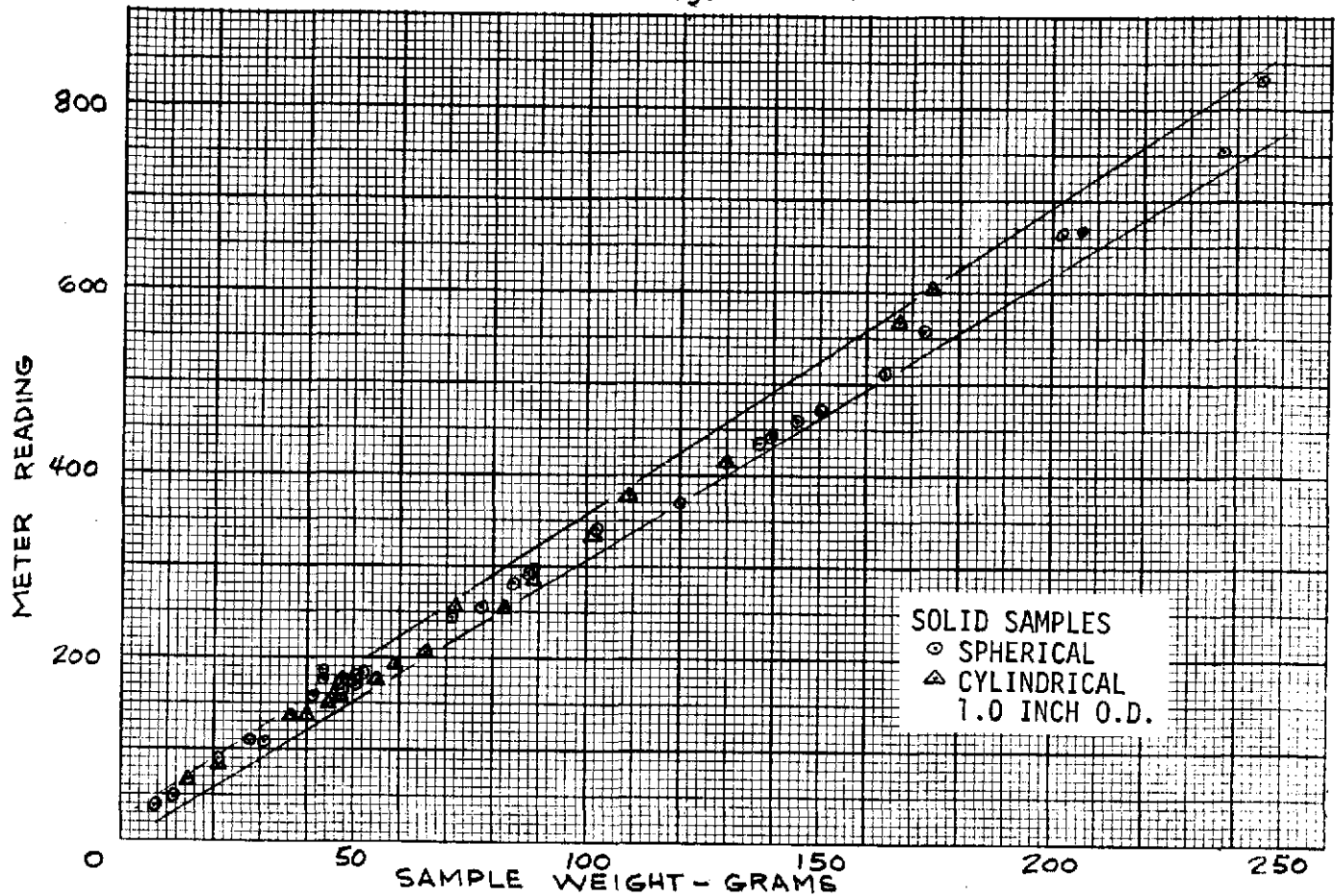


Figure 4-5 Measurement Data, Type 3 Slinger at 1500 rpm

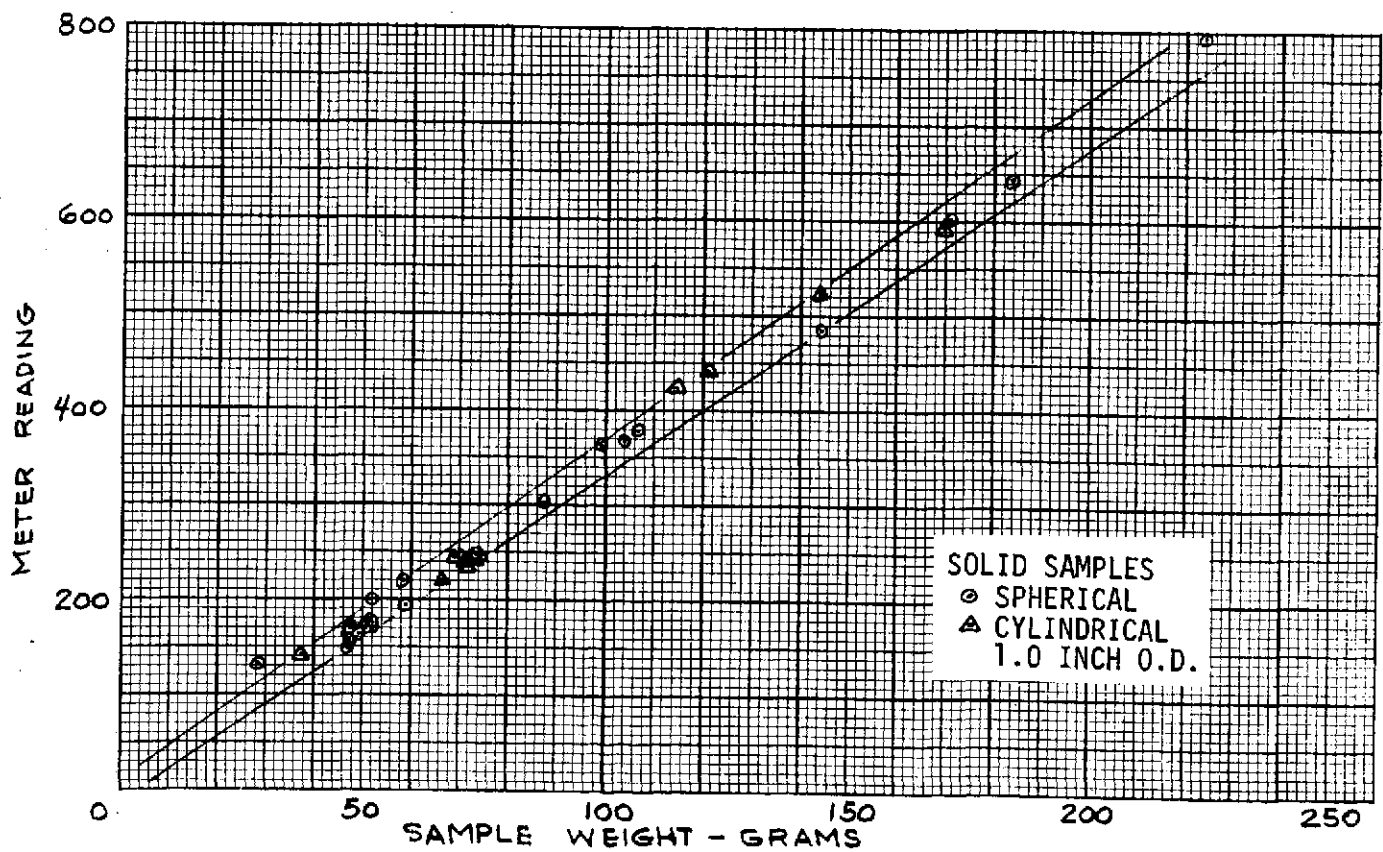


Figure 4-6 Measurement Data, Type 1 Slinger at 1500 rpm

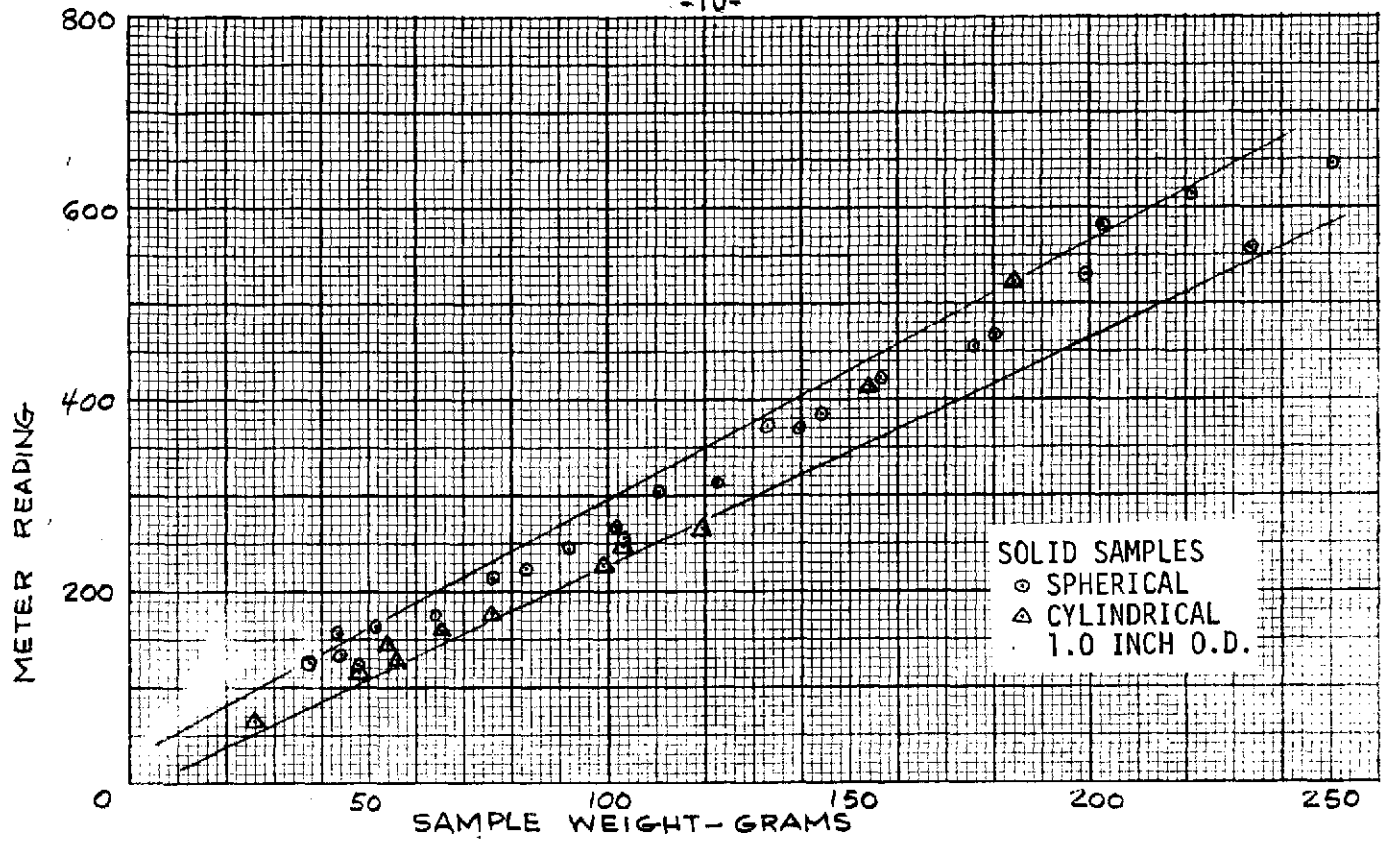


Figure 4-7 Measurement Data, Type 1 Slinger at 1000 rpm

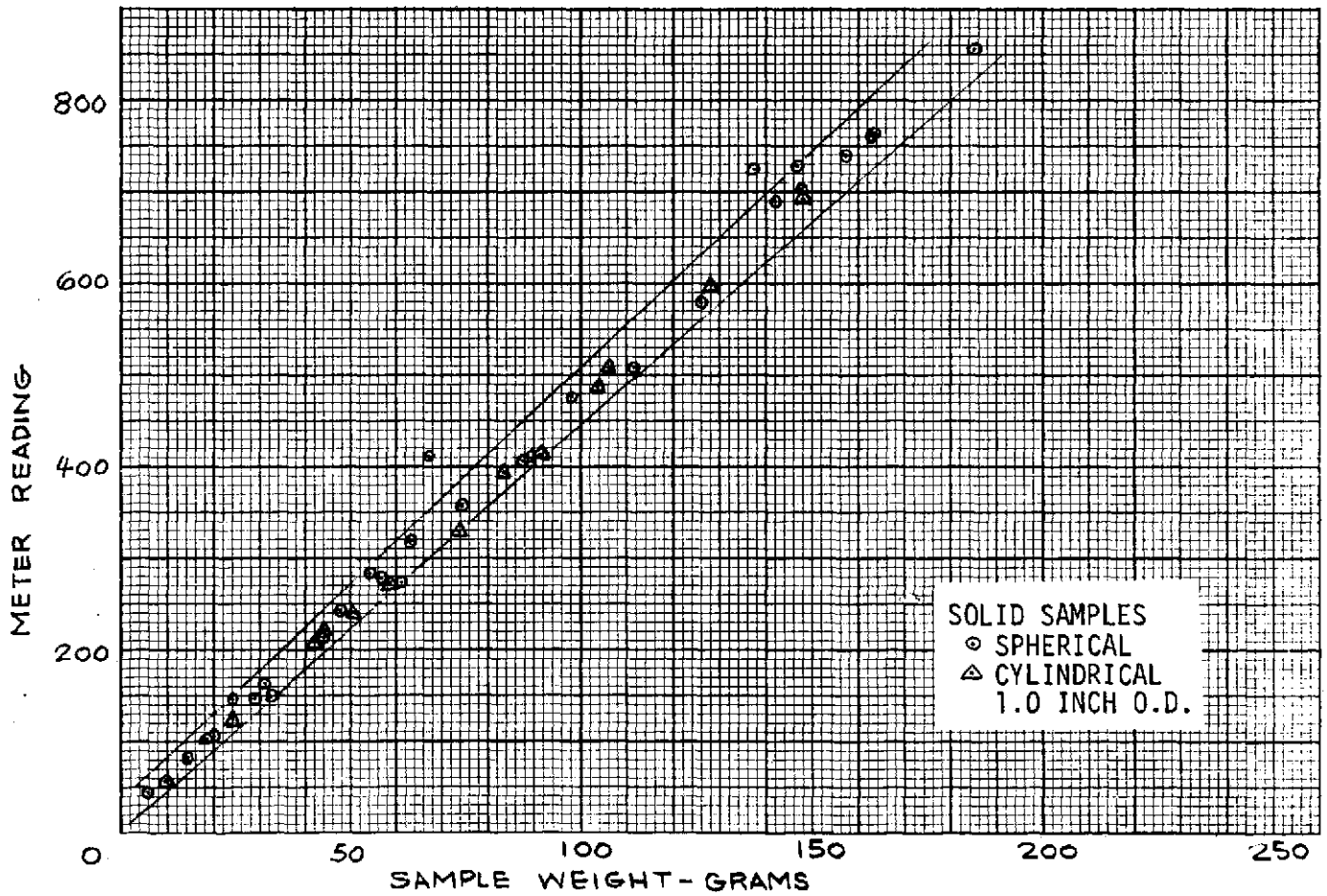


Figure 4-8 Measurement Data, Type 1 Slinger at 2000 rpm

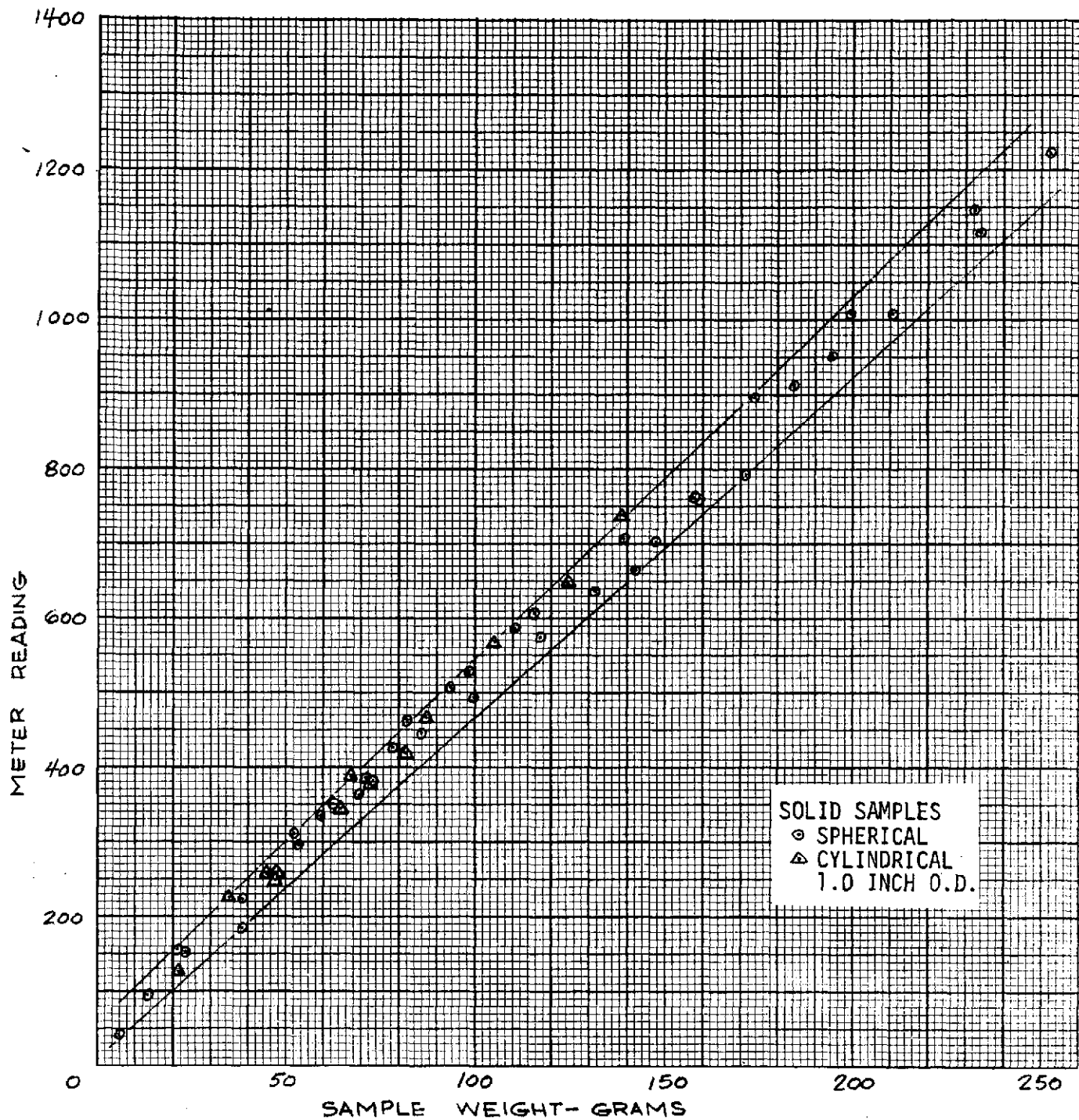


Figure 4-9 Measurement Data, Type 1 Slinger at 2500 rpm

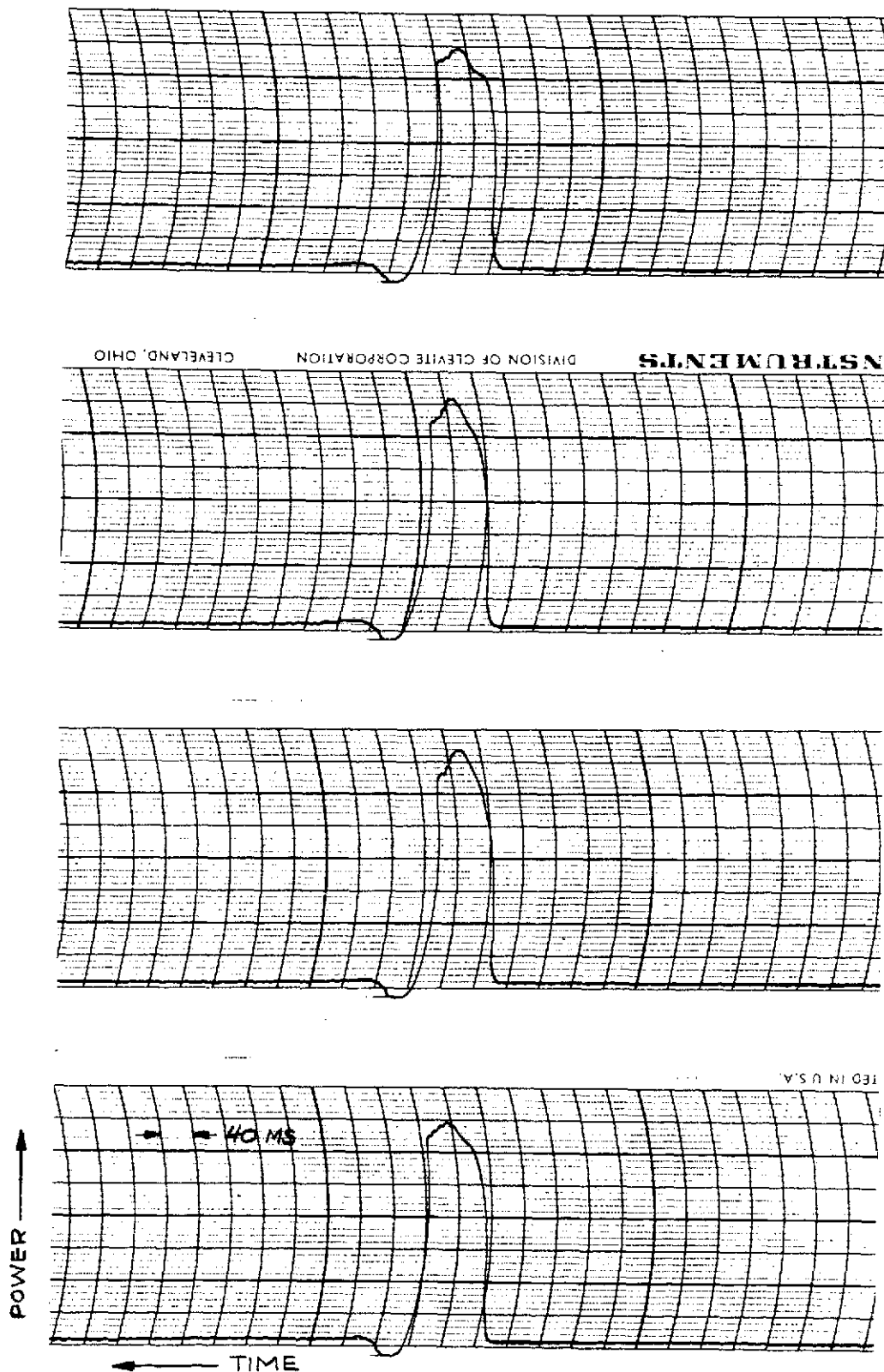


Figure 4-10 Power Input Profile for 100 Grain Size Simulated Feces Samples (Approximately Spherical Shape). Type 1 Slinger @ 1500 rpm; chart paper speed 125 mm/sec., 0.2 Volts/Line.

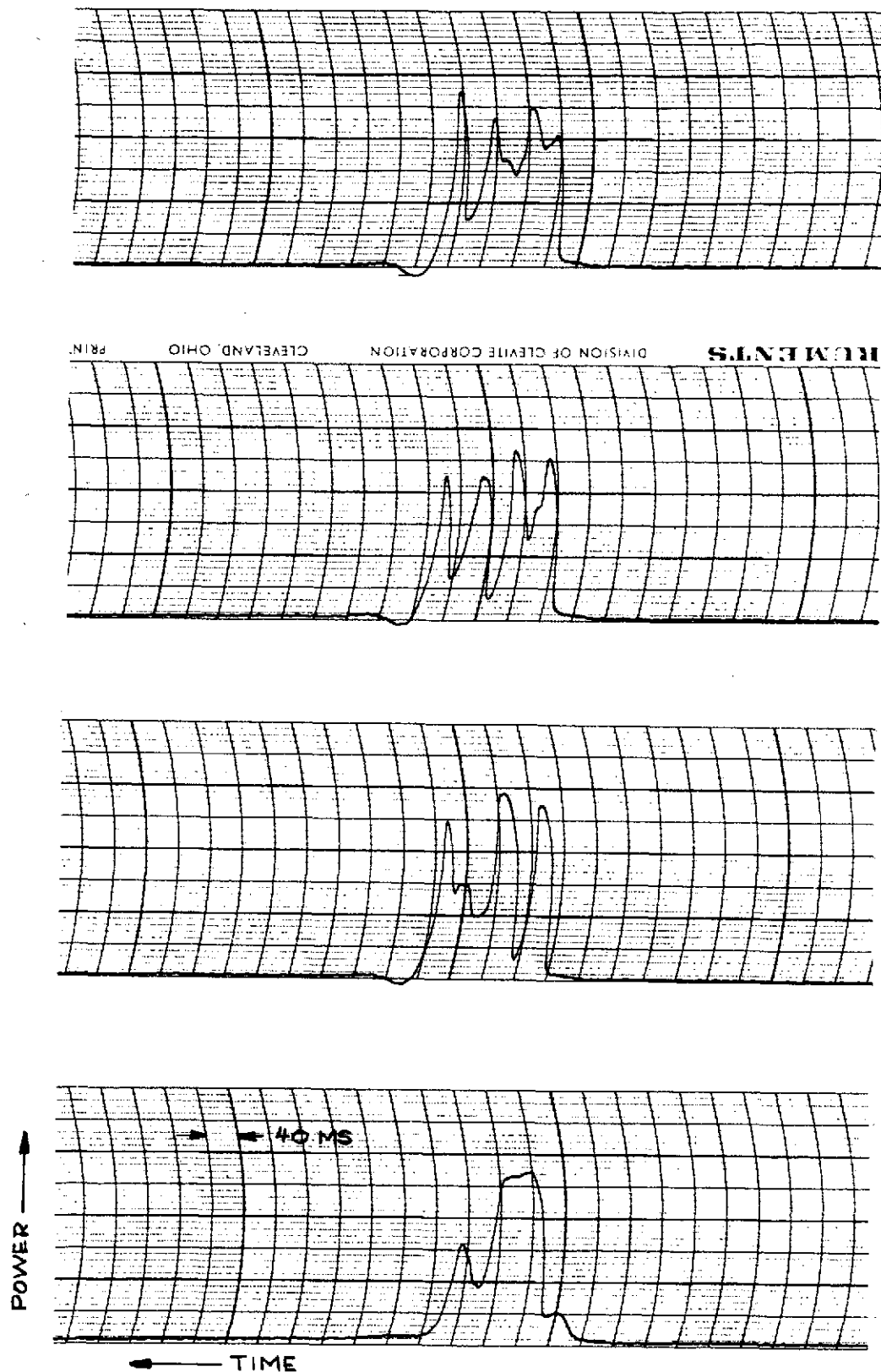


Figure 4-11 Power Input Profile for 100 Gram Size Simulated Feces Samples (1 Inch O.D. Cylindrical Shape). Type 1 Slinger @ 1500 rpm; Chart Paper Speed 125 mm/sec., 0.2 Volts/Line.

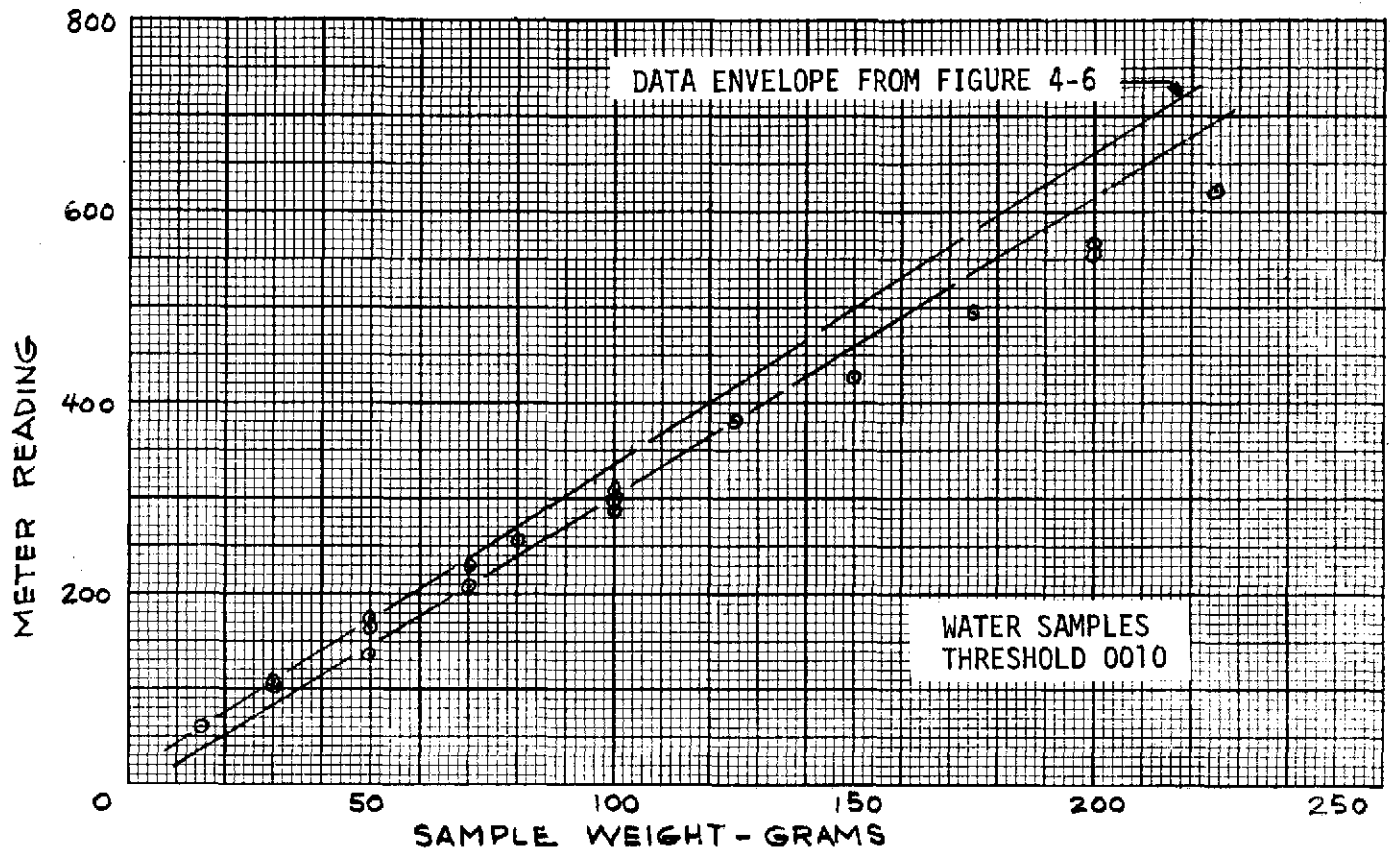


Figure 4-12 Measurement Data, Type 1 Slinger at 1500 rpm

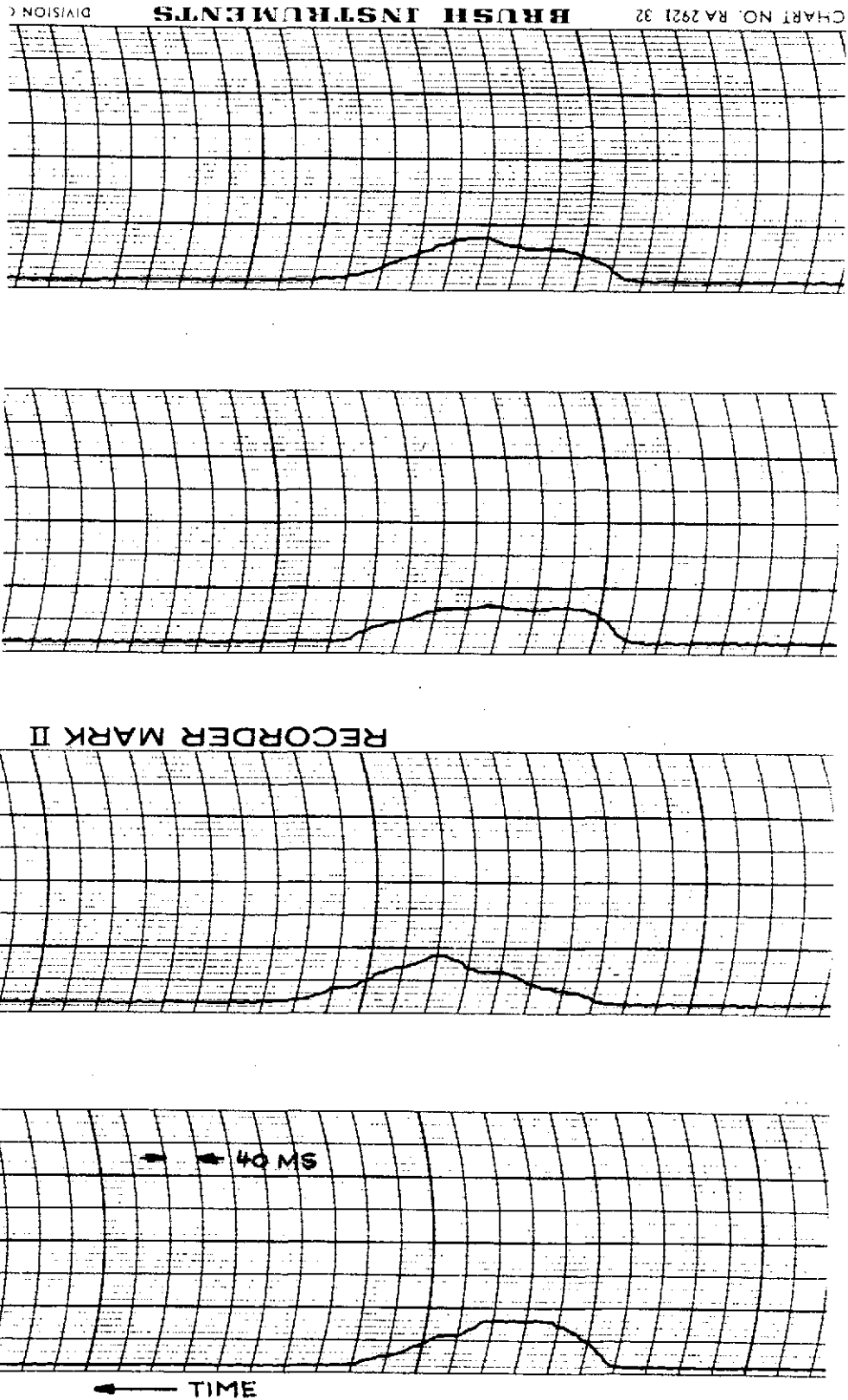


Figure 4-13 Power Input Profile for 100 Gram Size Liquid Samples (Water). Type 1 Slinger @ 1500 rpm; Chart Paper Speed 125 mm/sec., 0.2 volts/line.

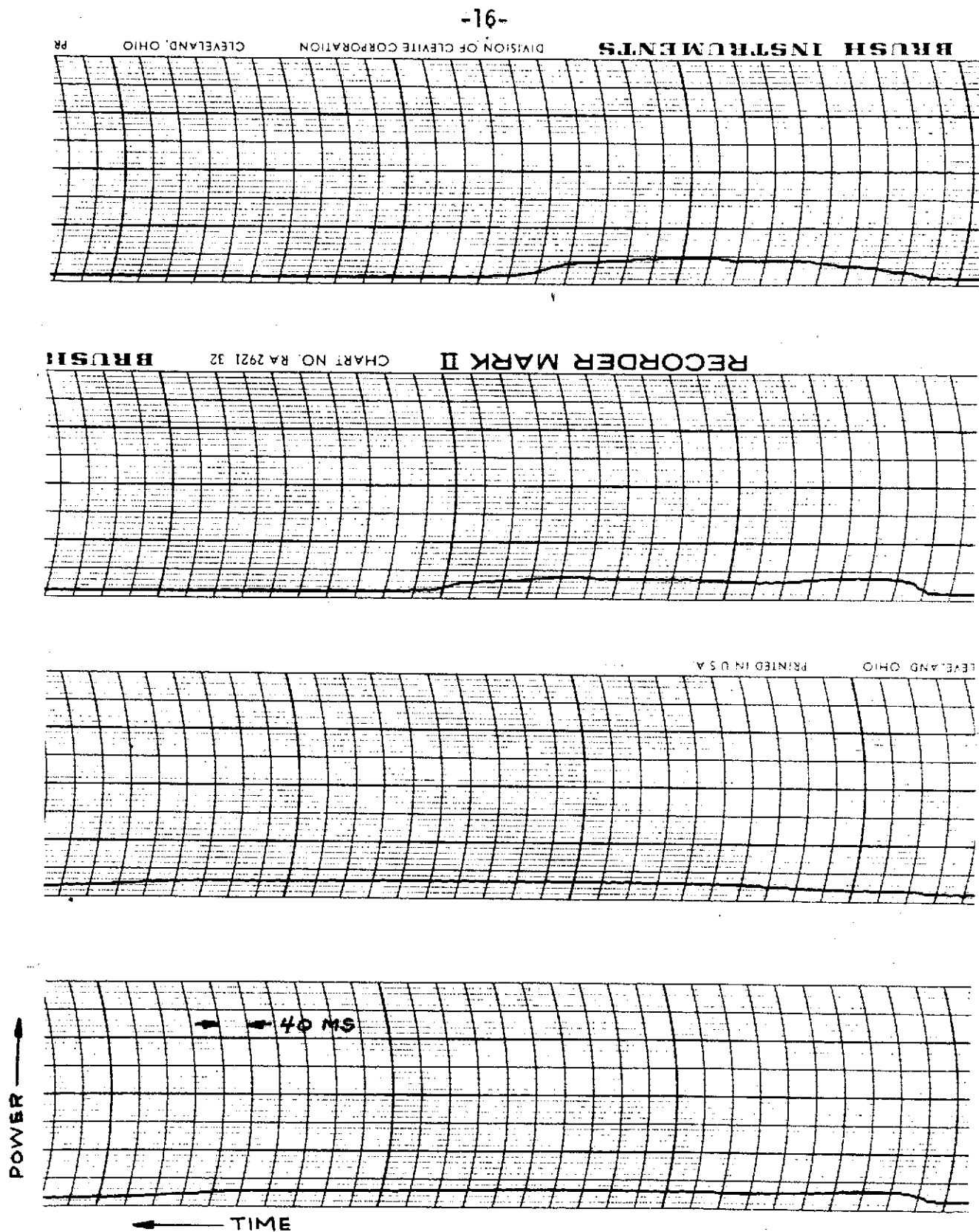


Figure 4-14 Power Input Profile for 100 Gram Size Liquid Samples (Water).
Type 1 Slinger @ 1500 rpm; Chart Paper Speed 125 mm/sec.,
0.2 Volts/Line.

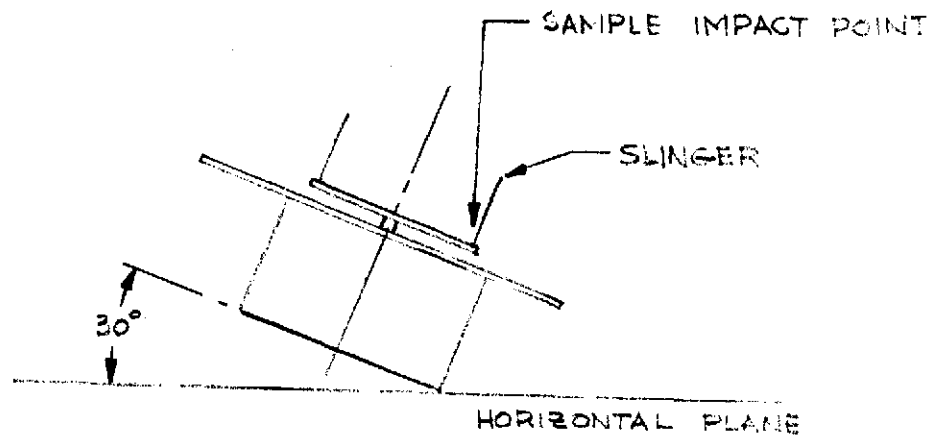


Figure 4-15 Breadboard Model Impact Point Test Orientation

Table 4-1 Residual

Slinger Type	Slinger rpm	Residual grams
1	1500	4.4
2	1500	11.9
3	1500	4.0
1	1000	8.0

GENERAL ELECTRIC

SPACE DIVISION
PHILADELPHIA

PROGRAM INFORMATION REQUEST / RELEASE

*CLASS. LTR. U	OPERATION 1R60	PROGRAM 74	SEQUENCE NO. 130	REV. LTR.
PIR NO. —				
*USE "C" FOR CLASSIFIED AND "U" FOR UNCLASSIFIED				

FROM: G. L. Fogal, Bioengineering Programs
Room U1240, VFSC, X5636

TO: File

DATE SENT 9/24/74	DATE INFO. REQUIRED	PROJECT AND REQ. NO. ABSS Improved Feces Measurement and Sampling	REFERENCE DIR. NO.
----------------------	---------------------	---	--------------------

SUBJECT

FECES SAMPLING B/B TEST RESULTS

INFORMATION REQUESTED/RELEASED

- 1.0 SUMMARY - The feces sampling breadboard demonstrated the mechanical feasibility of collecting only a percentage of the total fecal material input. In combination with an in place feces mass measurement capability, this approach would result in a significant reduction in sample refrigerated storage volume requirements. Unfortunately, based on test results with three types of slingers, the distribution of fecal material from the slinger is not uniform which results in a wide dispersion in the size of the collected samples. This latter negates the sampling approach and implies the need for collecting the total defecation. Additional effort expended on improving the distribution from the slinger is needed to revive this concept, i.e. collecting a percentage of the total defecation.
- 2.0 BACKGROUND - The sampling concept designed and evaluated for the ABSS Solids Subsystem was based on collecting the entire fecal discharge from each individual defecation. Details of this design and evaluation are included in the ABSS Final Report, GE Report No. 74SD4208-Part II. The requirement for collecting the total fecal discharge from each defecation derived from the need to determine the mass of the fecal material and not for purposes of analysis. As established by PIR 1R62-72-107, "Biological Requirements/Recommendations for the ABSS" (included in Appendix section 7.5, GE Report 74SD-4208, Part I), the quantity of feces required for analysis purposes is relatively a small portion of a normal defecation. For example, 20 grams is sufficient for determining moisture content, electrolyte and nitrogen concentrations and fatty acid content.
- 3.0 REVISED SAMPLING REQUIREMENTS - Assuming the successful development of the GE real time feces mass measurement concept into practical hardware, the need for collecting the total fecal discharge is no longer a necessary adjunct to the sampling requirement. Thus sampling requirement can be revised as follows:

"The ABSS shall be capable of providing, at user option, a representative fecal sampling from each defecation. The fecal sample shall be collected in a user identifiable sample container. The sample container shall not degrade subsequent chemical analyses or moisture content determinations. The sample size shall be a minimum 20 grams for average and larger discharges and 20% of the total fecal mass for below average size discharges."
- 4.0 SAMPLING CONCEPT - The above revised sampling requirements permit the use of a modified version of the ABSS Solids Subsystem sampling concept. Rather than completely encircling the slinger assembly, only a portion of the feces distribution area needs to be covered by the collection strip to obtain a reduced size sample. Figure 1 illustrates the relative location of slinger and sampling element. This approach results in some

copy to: J. K. Mangialardi
R. W. Murray
G. L. Fogal (3)

PAGE NO.	RETENTION REQUIREMENTS	
	COPIES FOR	MASTERS FOR
	<input type="checkbox"/> 1 MO.	<input type="checkbox"/> 3 MOS.
	<input type="checkbox"/> 3 MOS.	<input type="checkbox"/> 6 MOS.
	<input type="checkbox"/> 6 MOS.	<input type="checkbox"/> 12 MOS.
	<input type="checkbox"/> MOS.	<input type="checkbox"/> MOS.
	<input type="checkbox"/>	<input type="checkbox"/> DO NOT DESTROY

1 OF 13

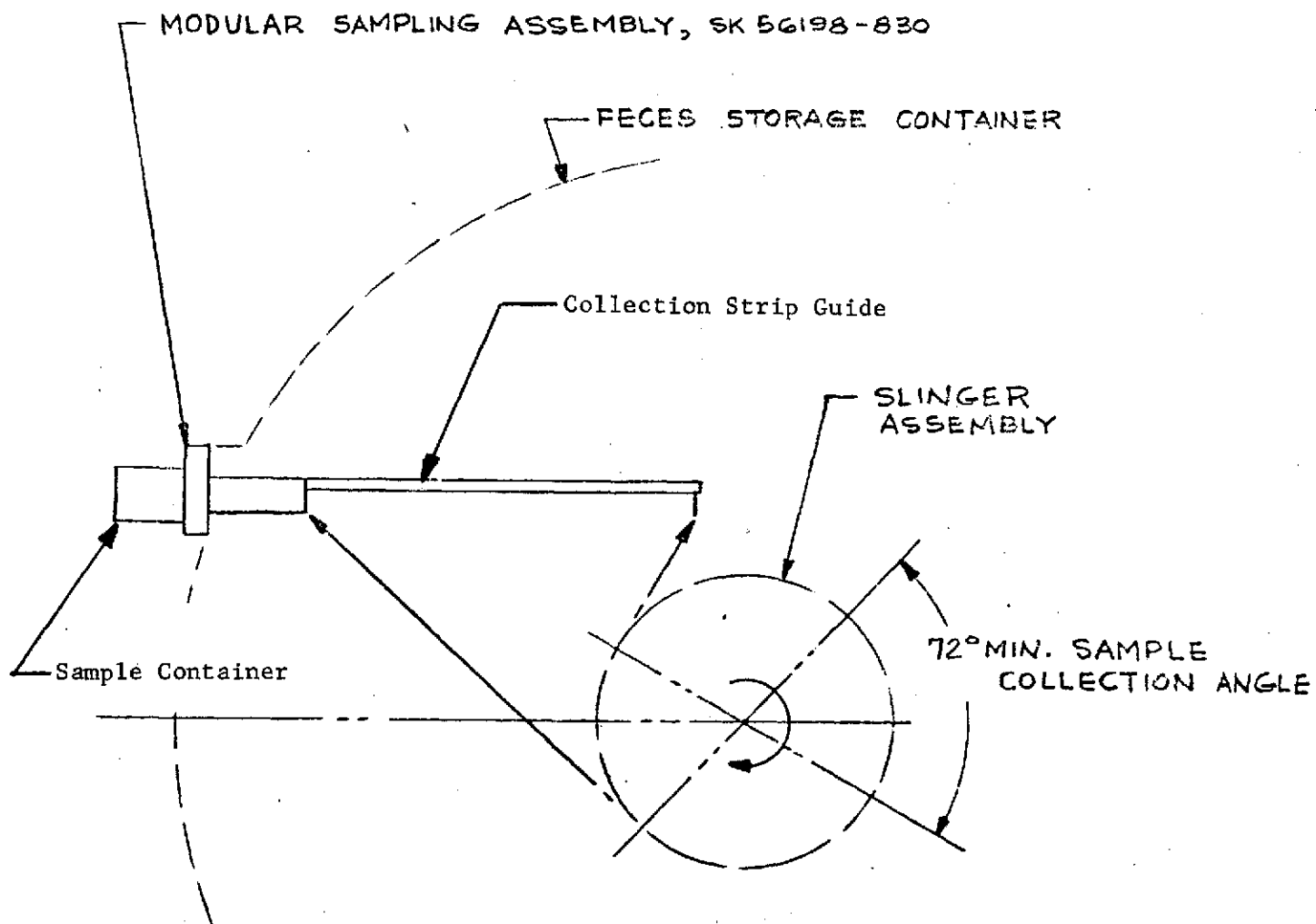


FIGURE 1 MODIFIED FECES SAMPLING CONCEPT

reduction in hardware complexity and a significant reduction in sample container volume. This latter is important in minimizing S/C refrigerated sample storage requirements.

Figures 2 and 3 show the feces sampling breadboard model. The assembly consists of a slide valve and collection strip guide secured to a mounting plate which in turn interfaces with the feces deactivation and storage container. The mounting plate also provides a recess for locating the sample container. As shown, operation (insertion and withdrawal of the collection strip) is performed manually. If desired the basic design is readily adaptable to a motorized drive for automatic operation. Also mechanical interlocks can be included so that

- (a) the slide valve cannot be opened without a sample container in place,
- (b) the sample container cannot be removed unless the slide valve is closed and
- (c) the slide valve cannot be closed unless the sample collection strip is retracted back into the sample container.

This interlock capability (or equal) is necessary to prevent inadvertent exposure of the feces storage container interior to the S/C ambient.

The sample container is shown in Figures 4 and 5. Referring to Figure 5, the collection strip (.006 stainless steel) is stored within the sample container housing with all but a small portion wrapped around a cylindrical roll. Rotating the reel forces the collection strip out of the sample container housing. Rotating the reel in the opposite direction retracts the collection strip. As the collection strip is retracted (and assuming a fecal sample had been collected), the fecal solids are largely scraped from the collection strip and collect in the sample collection recess in the container housing. This process continues until the end of the collection strip closes-off the sample collection recess. The maximum amount of feces which can be collected as a sample is limited by the size of the sample collection recess. For the breadboard model, this recess will accommodate a maximum of 2 in ³ of sample (about 25 grams of normal composition feces). The sample container is designed primarily for collecting fecal samples of roughly normal composition. Collection of diarrhetic type fecal samples can be accomplished but will be limited in size. Note the three recessed areas located at the end of the collection strip. In zero g operation, these recessed areas will retain an estimated 5 gms of diarrhetic type feces (in addition to any sample retained along the length of the collection strip). This quantity is adequate for chemical analyses.

EVALUATION

Mechanical Operation - Using the assembly of Figure 2, the collection strip was extended and retracted without difficulty. As expected with retraction, torque is small as compared to the torque required for extension (4.5 in lbs). Mechanical operation was also checked for two alternate configurations wherein the teflon bushing was replaced by 0.125 dia. stainless steel rollers (18 secured at both ends to form a crude roller bearing) in one case and by a plain al bushing in the other case. Neither of these two alternates was satisfactory; in both cases extension of the collection strip could not be accomplished due to the excessive torque required (caused by the friction between rollers/al bushing and collection strip).

Sample Collection - Two factors are important in sample collection. These are (a) the quantity collected for a given size defecation and (b) the composition of the collected sample as compared to the total defecation. It should be noted that neither of the factors are relevant if the total defecation were being collected. After examining

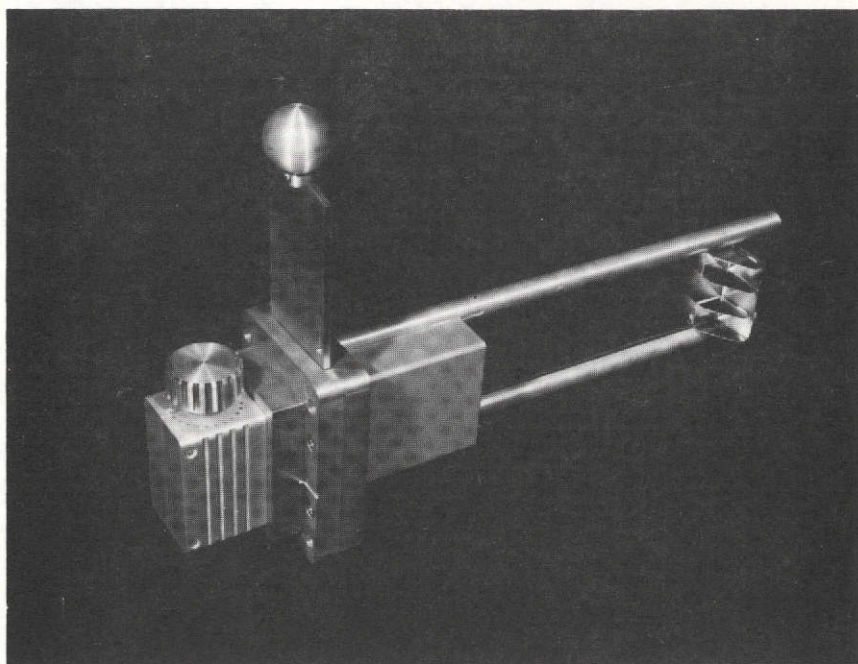


Figure 2 (a) Feces Sampling Breadboard
Collection Strip Deployed

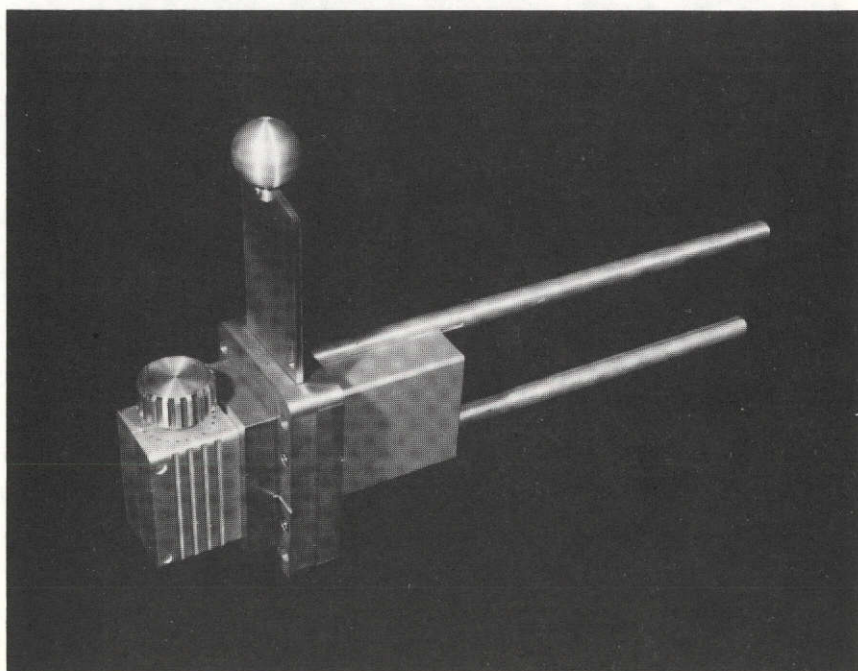


Figure 2 (b) Feces Sampling Breadboard

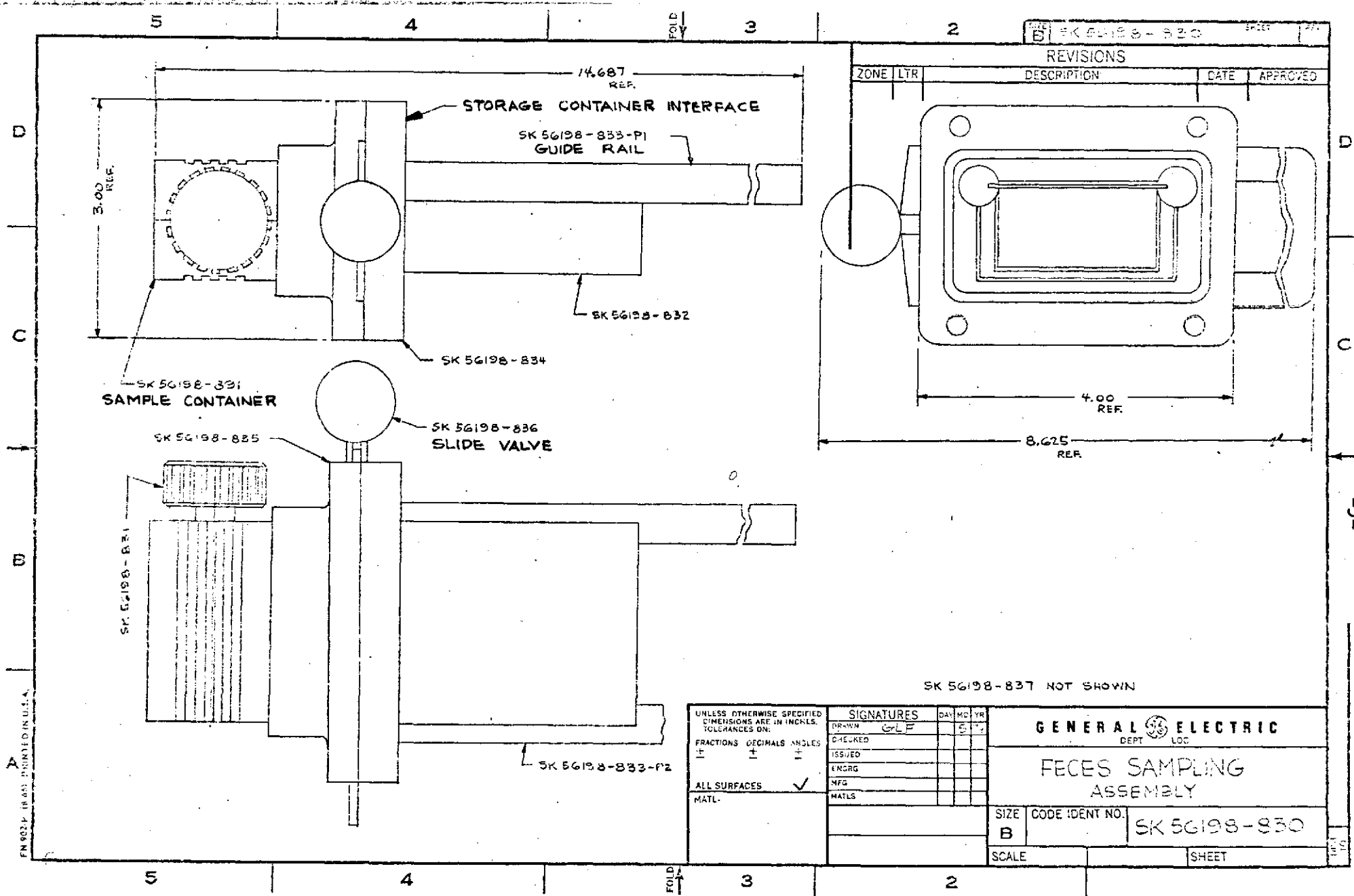


Figure 3 Feces Sampling Assembly

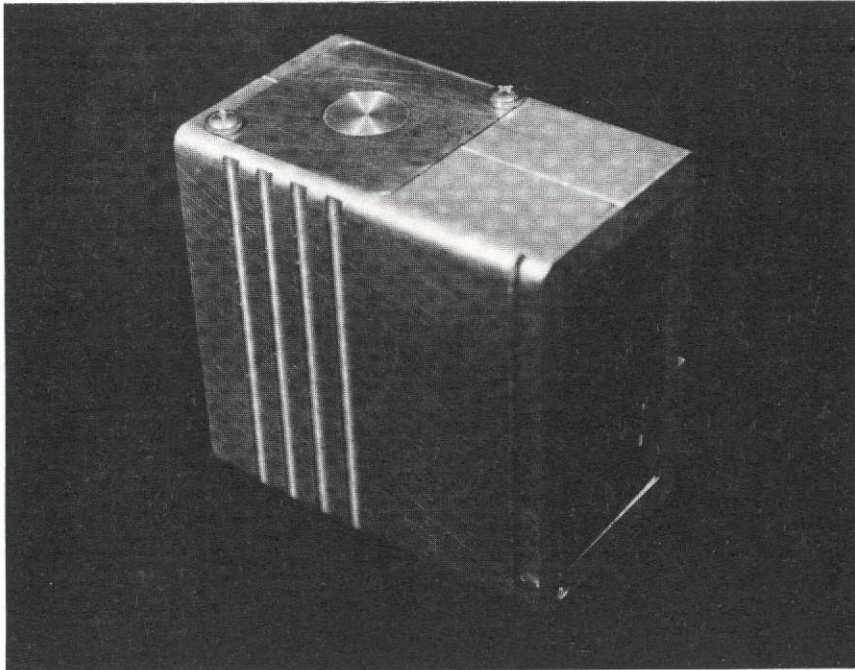


Figure 4 Sample Container

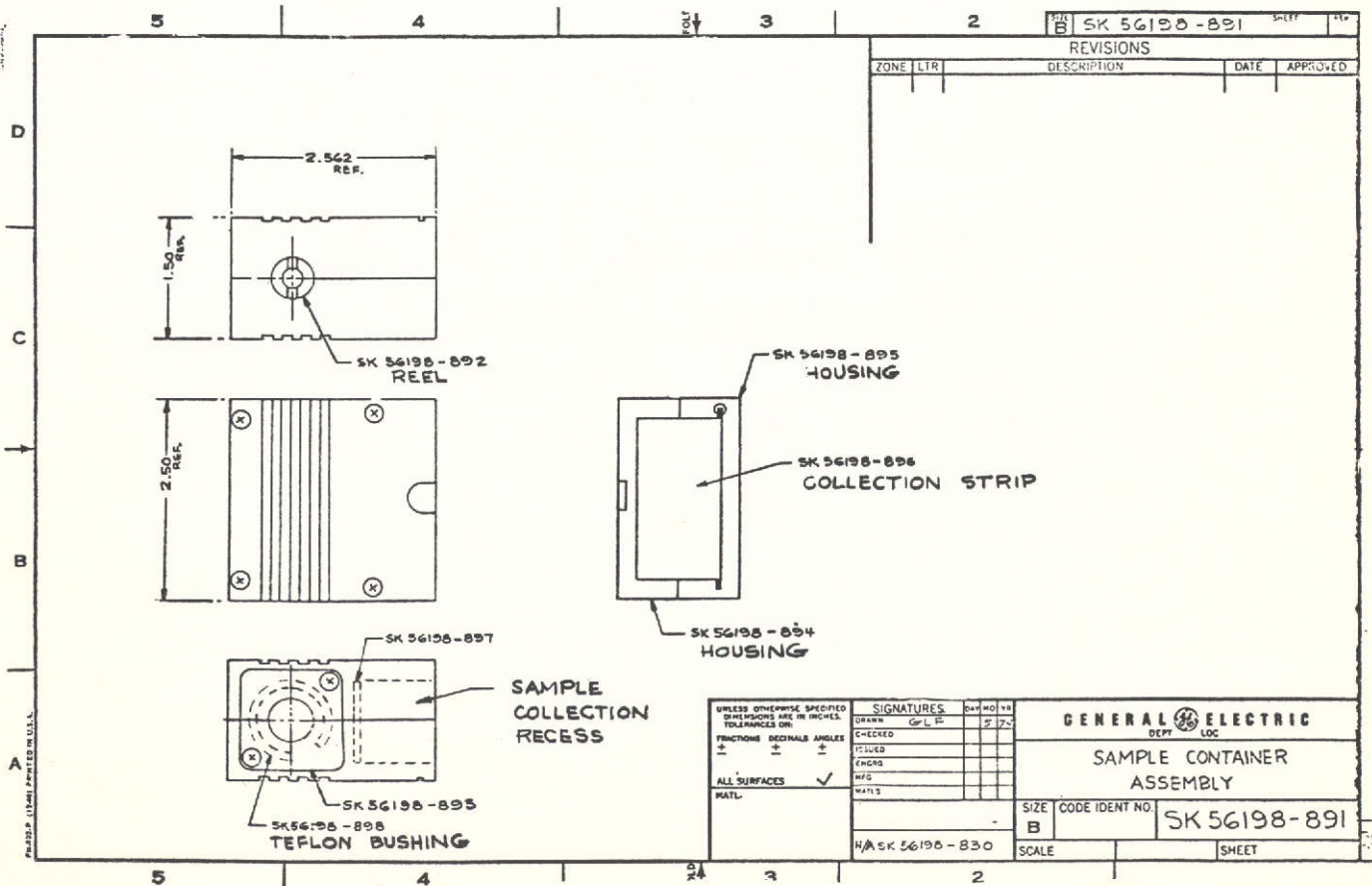


Figure 5 Sample Container Assembly Drawing

each of these factors, it is apparent that if the incoming fecal material is uniformly distributed by the slinger, the quantity collected will be consistent and the composition will be a replica of the total. For example, assume a bolus is divided into two parts with one part of composition X and one of composition Y. Assuming a perfectly uniform distribution by the slinger, the collection strip will collect Z% of composition X and Z% of composition Y. The sample collected will then be Z% of the total defecation (X+Y) and of the same composition. Whether the bolus is in one or more parts (two in the example) does not change the end result for the idealized situation. In a real situation, a minimum quantity (on the order of 10-20 grams of fecal material may be required to achieve complete distribution (about the axis of the slinger). Thus changes in composition within the 10-20 gram minimum would not be perfectly reflected in the collected sample. Fortunately, large and abrupt composition changes along the length of the bolus are unlikely.

Thus the slinger rather than the feces sampling hardware assembly (see Figure 2) is the key element in attaining an effective feces sample. A number of slinger configurations were evaluated as shown in Figures 6 thru 8.

Figure 9 shows the test setup and pseudo collection strip for collecting 28.2% (theoretical) of each simulated defecation. A dog food/peanut butter mix (4 parts Gainesburgers to 1 part creamy style peanut butter mixed with water to desired consistency) was used as simulated fecal material. Test results are summarized in Figures 10 thru 15 with conclusions as follows:

- a. Slinger configuration (type), slinger rpm and sample shape have only a minor influence on the size distribution of collected samples.
- b. The smaller the input mass, the larger the dispersion of the collected sample about the theoretical value.
- c. Some sample was always collected.
- d. The dispersion in collected sample size negates the usefulness of the partial sample (% of total defecation) approach.

.0 RECOMMENDATIONS - Additional effort on improving the distribution of fecal material leaving the slinger is required for the concept (collection of a % of the total defecation) to be useful for other than limited test applications. Until this distribution improvement is accomplished, collection of the total fecal discharge is recommended.

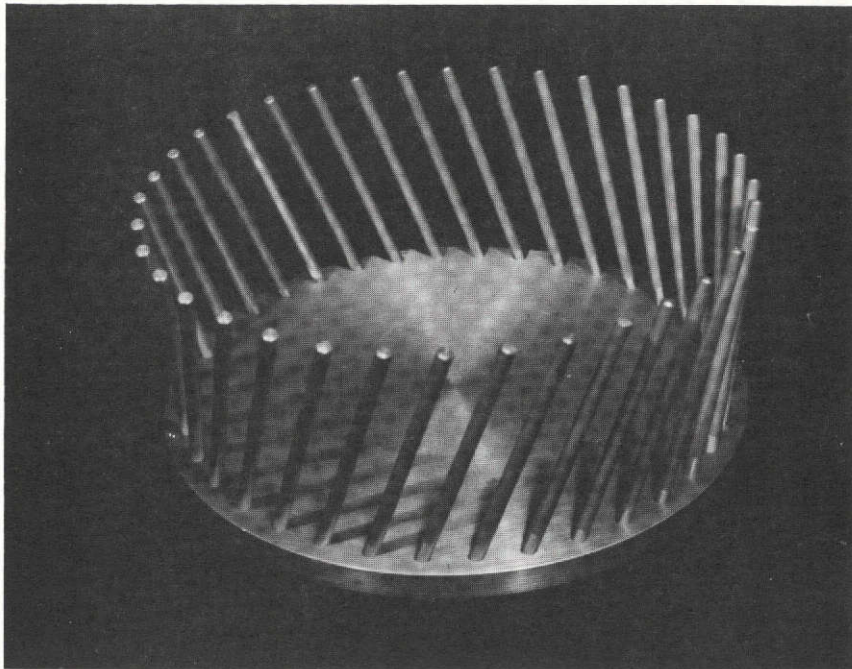


Figure 6 Type 1 Slinger Assembly (GESK56198-890)

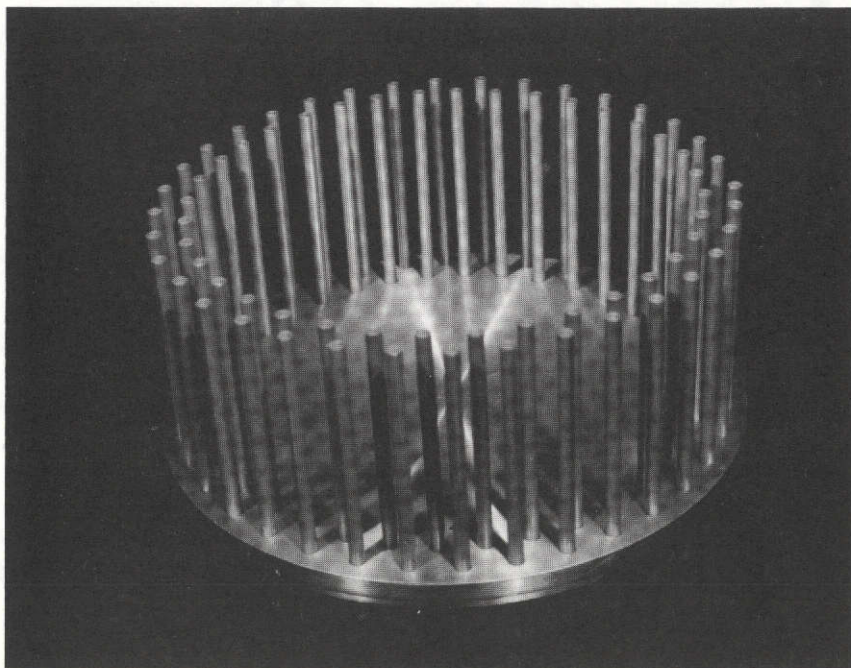


Figure 7 Type 2 Slinger Assembly (GESK56198-889)

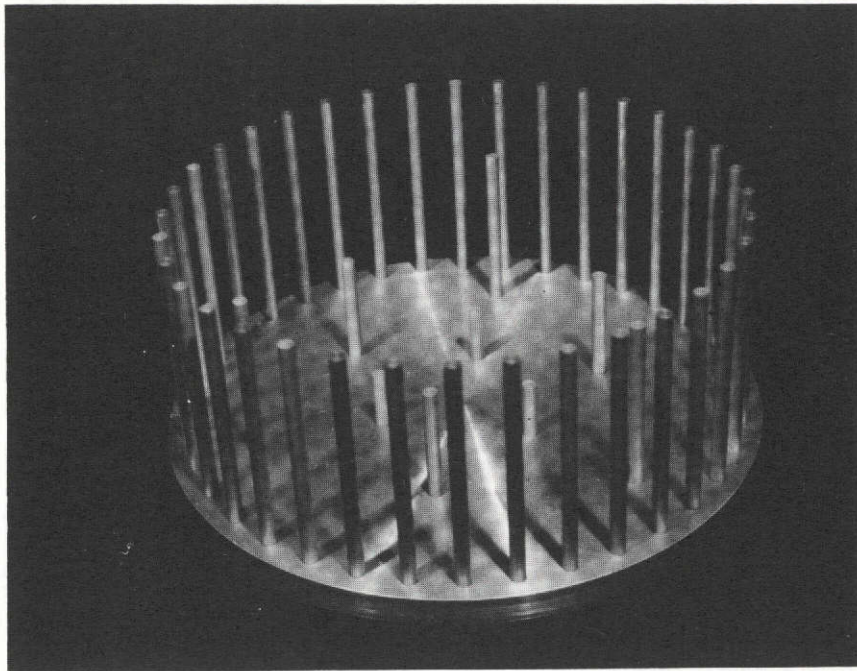


Figure 8 Type 3 Slinger Assembly (GESK56198-888)

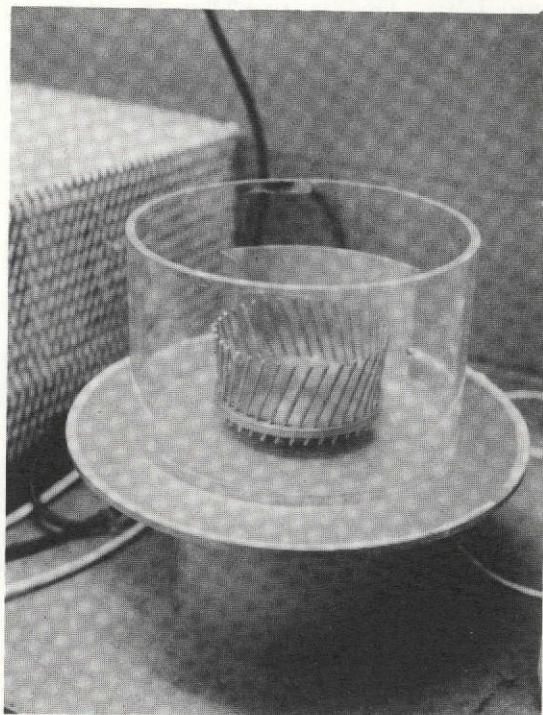


Figure 9(a) Test Set-Up

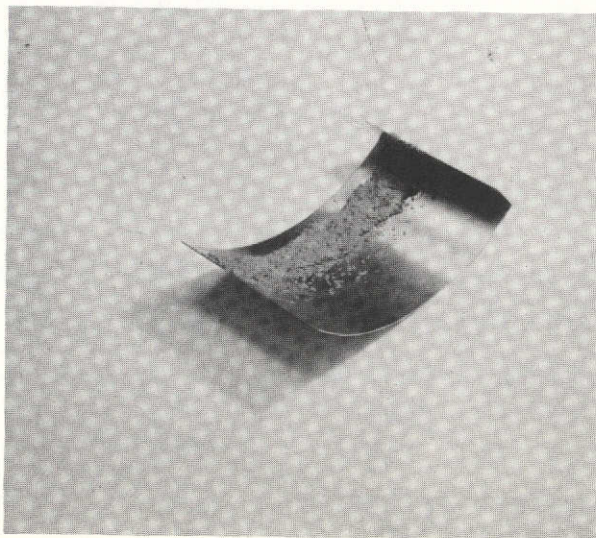


Figure 9(b) Simulated Collection Strip
(With Collected Sample)

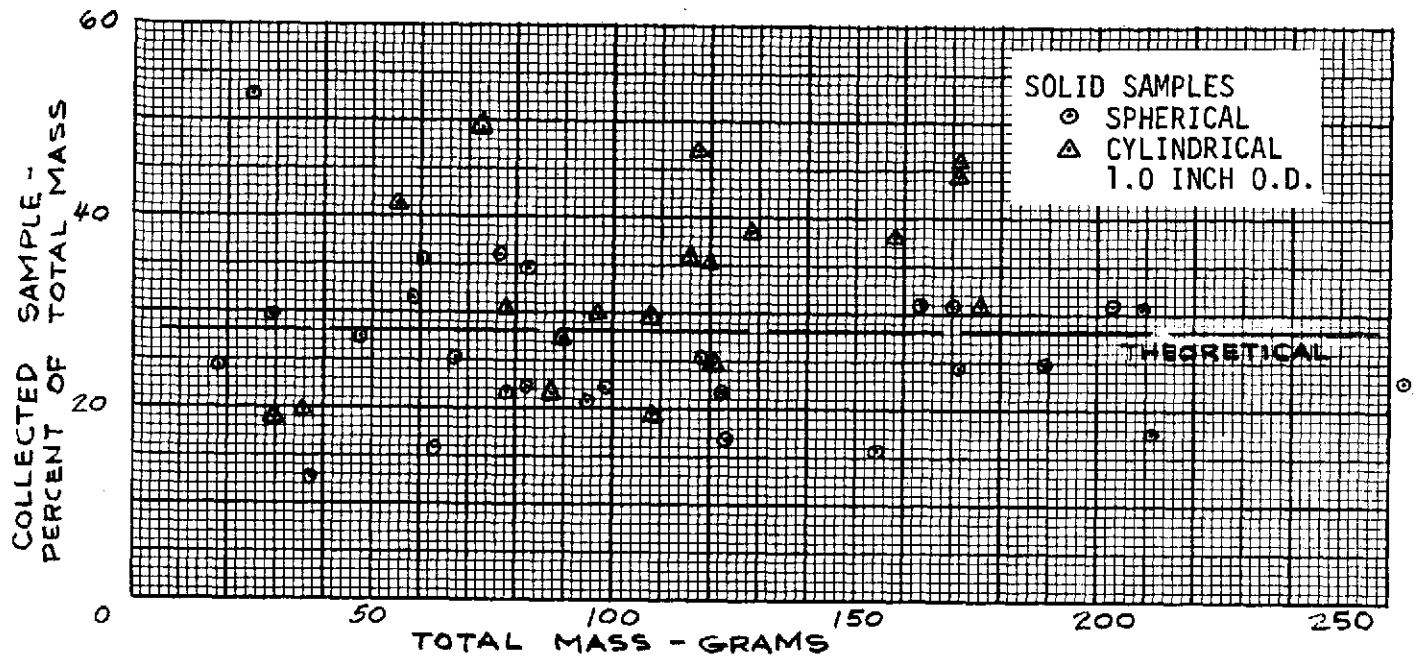


Figure 10 Collection Capability,
Type 2 Slinger at 1500 rpm

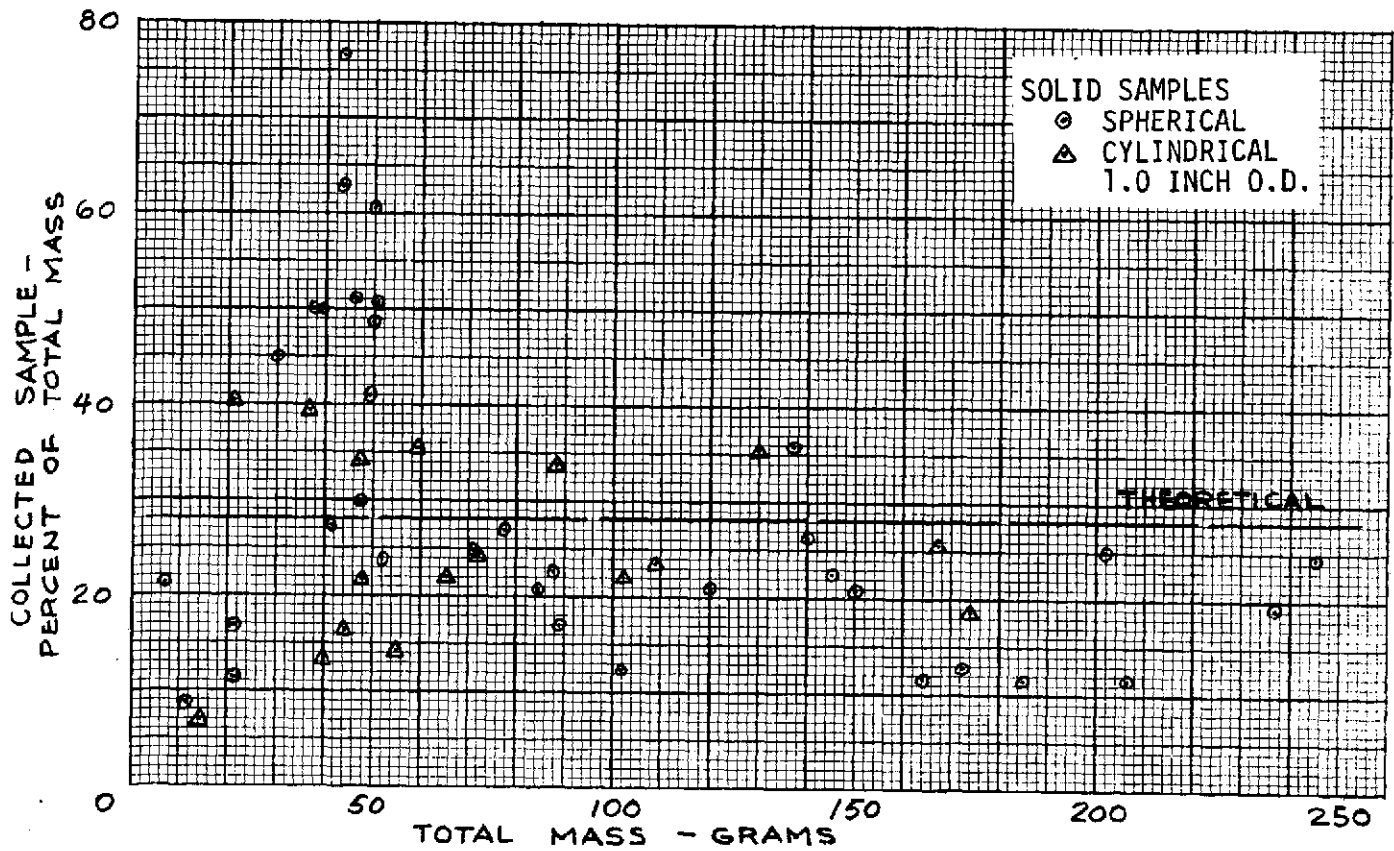


Figure 11 Collection Capability,
Type 3 Slinger at 1500 rpm

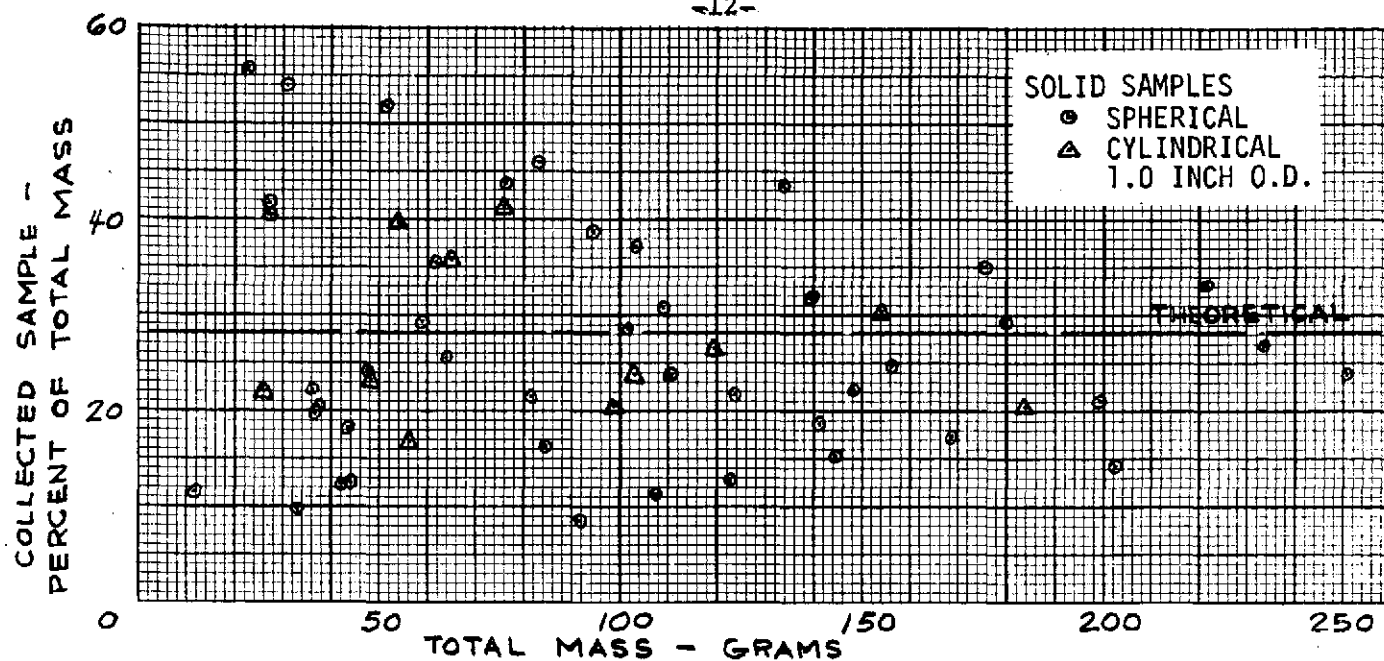


Figure 12 Collection Capability,
Type 1 Slinger at 1000 rpm

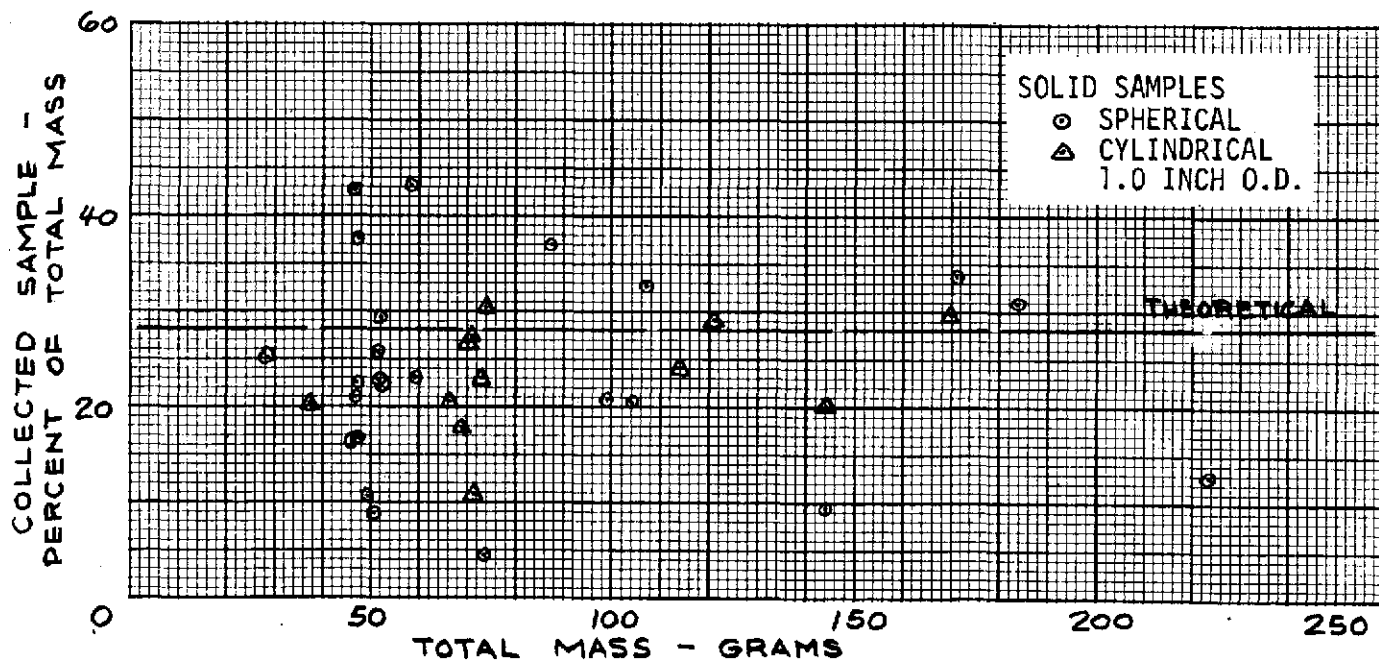


Figure 13 Collection Capability,
Type 1 Slinger at 1500 rpm

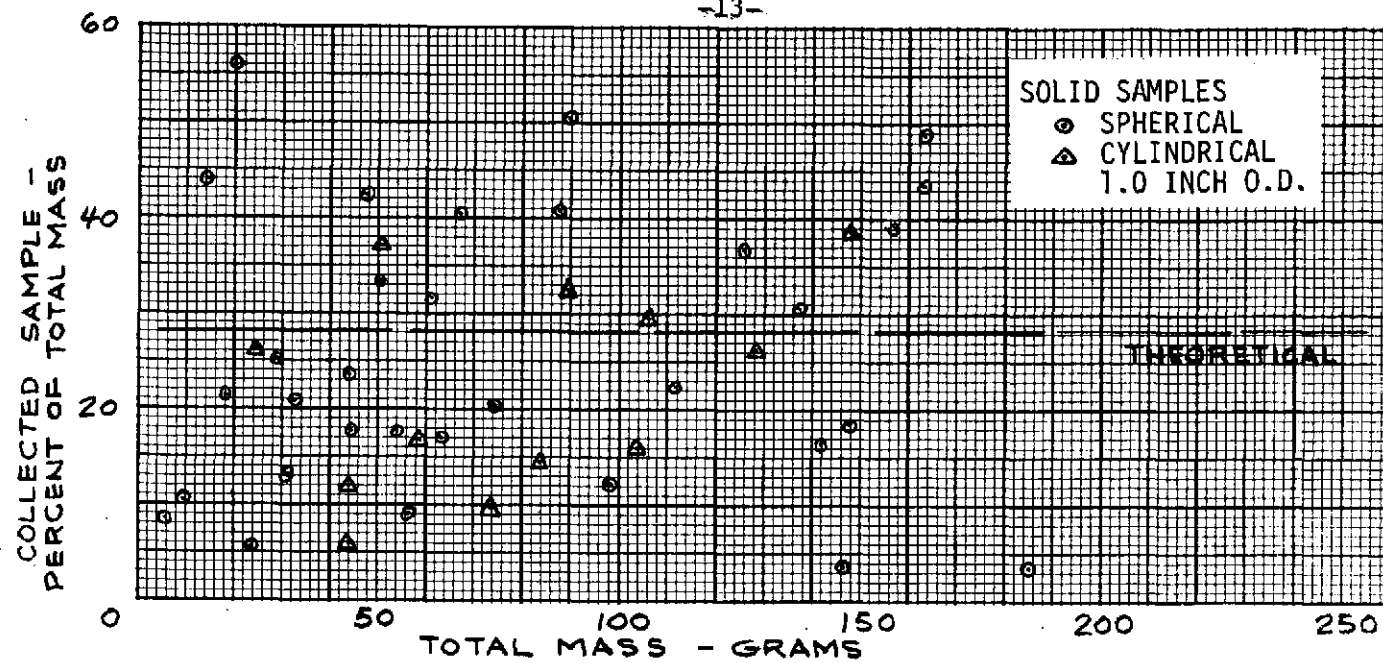


Figure 14 Collection Capability
Type 1 Slinger at 2000 rpm

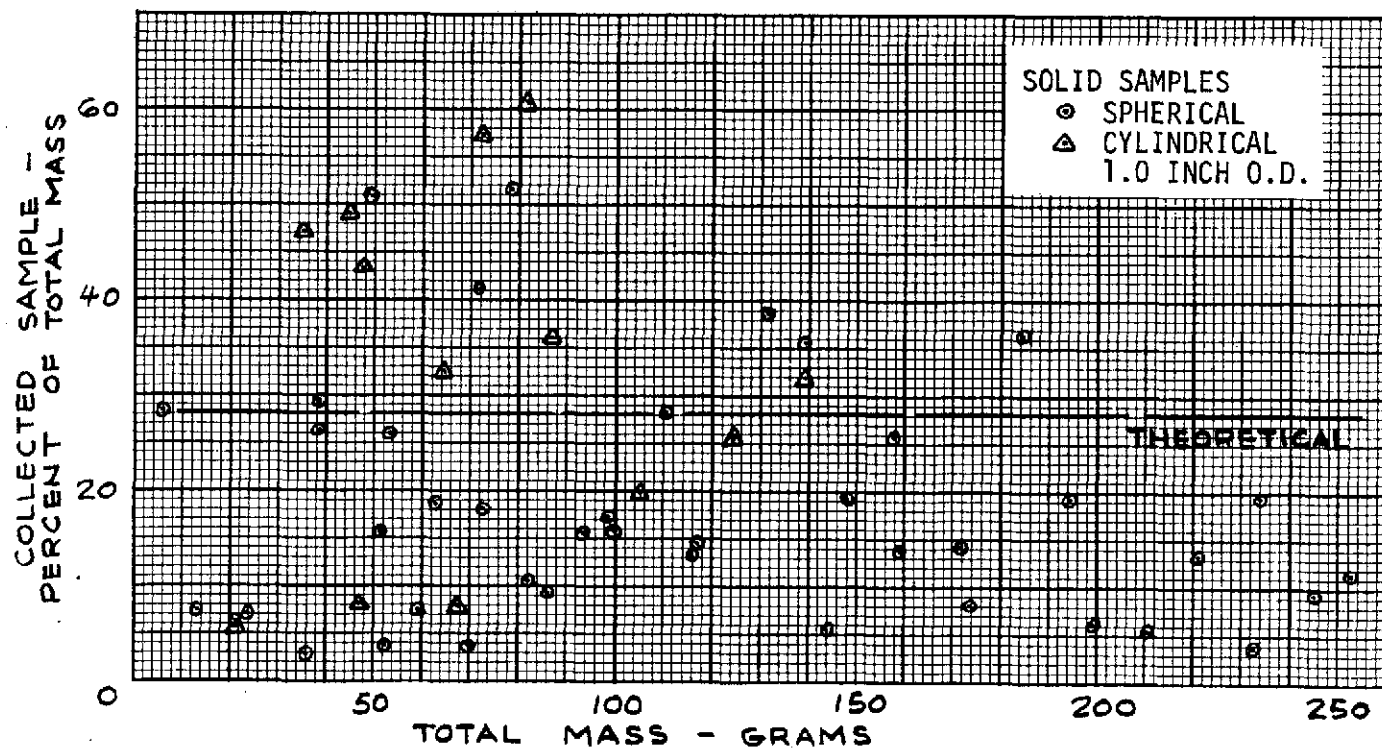


Figure 15 Collection Capability,
Type 1 Slinger at 2500 rpm

GENERAL ELECTRIC

SPACE DIVISION
PHILADELPHIA

PROGRAM INFORMATION REQUEST / RELEASE

*CLASS. LTR.	OPERATION	PROGRAM	SEQUENCE NO.	REV. LTR.
PIR NO. U	— 1R60 —	74	— 132	
*USE "C" FOR CLASSIFIED AND "U" FOR UNCLASSIFIED				

FROM J. K. Mangialardi, Environmental Engineering, Room U1243, VFSC	TO G. Fogal, Program Manager
---	------------------------------

DATE SENT 10/1/74	DATE INFO. REQUIRED	PROJECT AND REQ. NO. ABSS Improved Feces Measurement and Sampling	REFERENCE DIR. NO.
----------------------	---------------------	--	--------------------

SUBJECT Improved ABSS Feces Sampling

INFORMATION REQUESTED/RELEASED

1.0 SUMMARY

The Automated Biowaste Sampling System (ABSS) solids subsystem was designed to collect total samples of fecal solids or solid/liquid mixtures for the purpose of mass measurement, moisture content and other analyses if required. The collection was accomplished by means of a long stainless steel strip which could be automatically fed in and out of an otherwise typical "Dry-John." The checkout of the original equipment proved the feasibility of the total sampling concept and pointed out areas of improvements.

This document reviews the general ABSS sampling requirements, the ABSS Design, and the proposed changes based on the additional tests conducted as part of the ABSS improvement program and described in this report. The most significant change permits the collection and retention of liquid mixtures even in a one "G" environment. This feature could not be demonstrated with the previous ABSS sample collection strip. Other significant improvements are the storage of the sample collection strip in a cassette type container, the use of a single track to move the strip to and around the slinger and the general improvement of the air flow pattern and clearances around and below the slinger. A demonstration model has been built to show the feasibility of the concept. A description of the model, its operation and the basic shop drawings are attached as part of the test report.

2.0 BACKGROUND

Several design concepts relating to automatic sampling of fecal material for medical research have been considered and developed in conjunction with past Air Force or NASA sponsored programs. Only two significant approaches have ever been designed, built, and tested to any extent as part of a solid waste management system. Both are applicable to "Dry-John" type systems which use a high speed slinger to shred the biowaste material in a storage container with subsequent air or vacuum drying.

The first design was aimed at the collection of a small sample only. It consisted of a probe inserted thru an air lock near the top of the container and required a relatively significant amount of operating time before and after use. The device was actually used on a successful 4 man - 90 day test conducted by NASA and the Air Force in 1969.

The second design was developed as part of the Automated Biowaste Sampling System for Medical Research (ABSS) under NASA contract NAS1-11443. In the ABSS the basic biochemical sampling requirements were expanded to include information related to mass

cc: S. Hunt R. Murray C. Cerone	PAGE NO. 1 OF 28	RETENTION REQUIREMENTS	
		COPIES FOR	MASTERS FOR
		<input type="checkbox"/> 1 MO.	<input type="checkbox"/> 3 MOS.
		<input type="checkbox"/> 3 MOS.	<input type="checkbox"/> 6 MOS.
		<input type="checkbox"/> 6 MOS.	<input type="checkbox"/> 12 MOS.
		<input type="checkbox"/> MOS.	<input type="checkbox"/> MOS.
		<input type="checkbox"/>	<input type="checkbox"/> DO NOT DESTROY

measurement and moisture content for the solid biowaste material. This was accomplished by using a relatively long and narrow collection strip which automatically winds and unwinds itself from a position of temporary storage outside the "Dry-John" container to a position of collection around the slinger inside the container, thru a manual slide valve. The system was designed, built and tested during 1973. The tests indicated that the concept was feasible and that, as to be expected with any new design, further development was required mainly to improve the physical retention of the collected sample. This report describes some of the additional work done in this area including the design and test of a working model of a flight prototype.

3.0 SAMPLING REQUIREMENTS

The basic requirements controlling the design of the ABSS sampling system and the additional work described in this report are.

3.1 The primary goal of the sampling system is to collect and retrieve a total sample of feces or vomitus without significantly affecting the normal operation of the waste collection system when sampling is not required.

3.2 The sampling system shall be capable of collecting and retaining individual defecations ranging in mass up to 400 gms (110 gms average) or a maximum diarrhetic liquid/solid mix of 500 gms. The capacity for vomitus collection shall also be 500 gms maximum.

3.3 Cross contamination from sample to sample shall not exceed 1%.

3.4 The system shall be designed for zero gravity operation and shall be demonstrated under normal earth gravity conditions.

3.5 The sample containers shall not degrade subsequent chemical or microbiological analyses or moisture content determinations.

3.6 The system is to be designed for a high degree of automatic operation. User involvement should be limited to a one step installation and activation and a one step deactivation and removal of the sample container.

3.7 The sample container shall provide the information for automatic serialization and recording of the event.

3.8 The hardware shall be configured to provide both a functional and attractive appearance representative of a possible flight configuration. It need not be optimized for minimum size, weight or power input.

4.0 SAMPLING CONCEPT

The proposed sampling concept is based on the present ABSS design with significant improvements in the collection strip design, housing configuration and general mode of operation. A brief description of the ABSS sampling design is a necessary basis for a discussion of the proposed changes.

4.1 ABSS Design

The essential components of the ABSS sampling design are shown in Figure 1. The container assembly is not much different from the previous "Dry-John" units except for the addition of the side sample inlet valve and a set of tracks running from the valve to and around the slinger. On the external side of the valve is the sampling container and the drive mechanism. The sampling container consists of an aluminum housing with a set of sprockets driving the collection strip from the protective

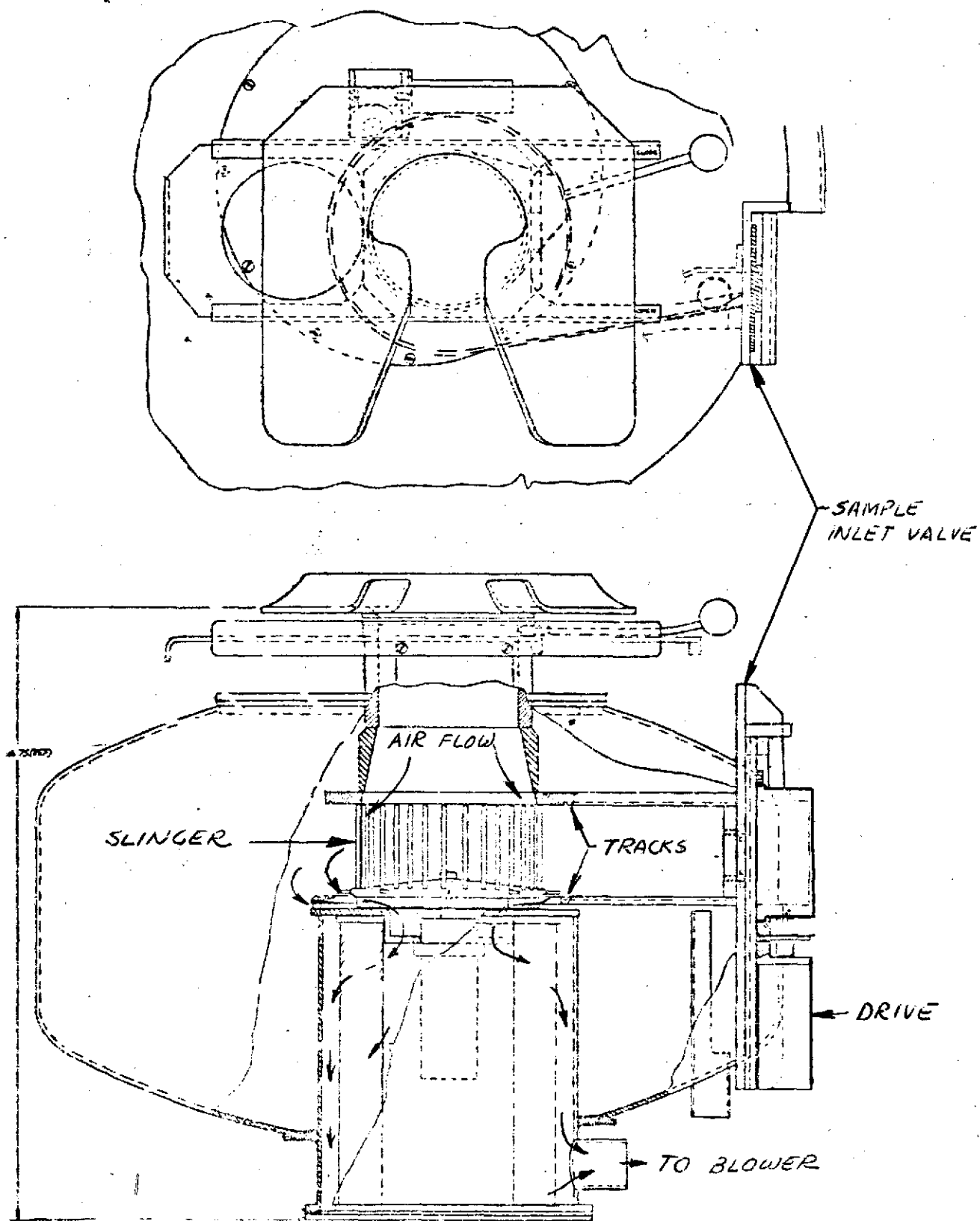


FIGURE 1 - ABSS SOLIDS SUBSYSTEMS
OPERATING MODEL .

flexible sleeving into the container and back. The collection strip consists of a stainless steel foil 2.5" high x 28" long x .006" thick with perforations along the edges for engagement to the sprockets in the housing. The sprockets are connected to the drive mechanism through a slot and key. Figure 2 shows the ABSS sampling container.

The original concept called for the collection strip to wind into a box or cassette for handling and storage. However, due to design restraints imposed at the time, the straight run into a flexible sleeve was used to replace the cassette idea.

Although the number of tests performed on the ABSS solids sampling system was relatively limited, there was sufficient evidence to draw conclusion that the concept is feasible and can be made to work satisfactorily if:

1. The distance between the slinger tines and the surface of the collection is increased.
2. Additional development is done to improve the retention capability of the collection strip.

The increase in distance between the collector and the slinger is needed to allow sufficient room for local build up on the surface of the collection strip. Laboratory and zero "g" tests have shown that most of each bolus intersected by the slinger tines is centrifuged in a relatively narrow band covering about half of the possible 360° spread, in a direction tangent to the slinger exit points and perpendicular to the axis of rotation. A good illustration of sample localization is shown in Figure 3 from some of the tests described in Paragraph 5.0.

Excessive build up may cause stalling of the slinger and loss of sample material with consequent excessive fouling up of the sampling mechanism such as the tracks, the sample inlet valve, etc.

The need to improve the retention capability for the collection strip was indicated by the occasional total loss of a sample due to poor adhesion to the smooth surface of the collection strip. Initial efforts to improve the surface texture by the addition of a layer of large open pore foam material failed as the foam was ripped off the collection strip this time due to poor bond between the foam and the stainless steel strip. It also became obvious that even with the use of the foam layer it would be nearly impossible to demonstrate the capability of dry and/solids mixtures retention such as might occur in the case of vomitus or diarrhea.

4.2 Proposed Design

The proposed design retains the concept of the self winding strip moving in and out of the container to collect and retrieve a total sample, as in the original ABSS design. However, in order to improve the system performance the following significant changes are proposed.

1. Redesign the collection strip to minimize loss of sample material and to make possible the collection and retention of liquid/solids mixtures in a one "G" field as well as zero "G".
2. Package the collection strip in a cassette type container.
3. Increase the clearance between the slinger and the collection strip from a nominal 6.34 dia. to 8.00 dia. to minimize interference and improve the air flow path.

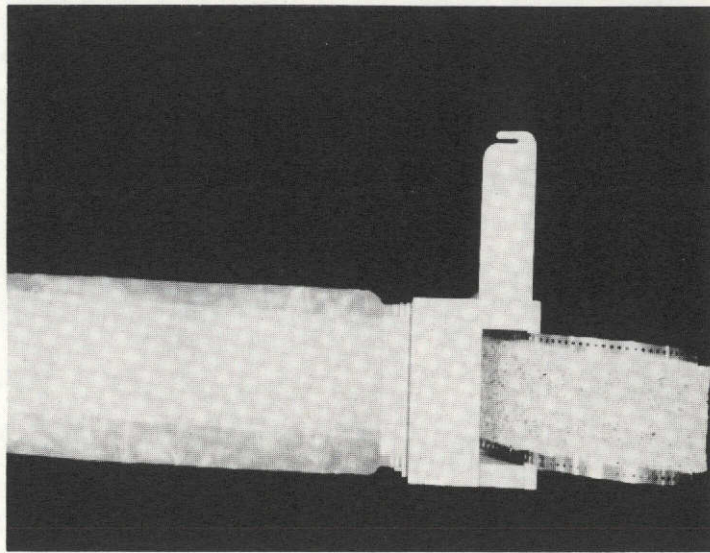


FIGURE 2 - ABSS SAMPLE CONTAINER

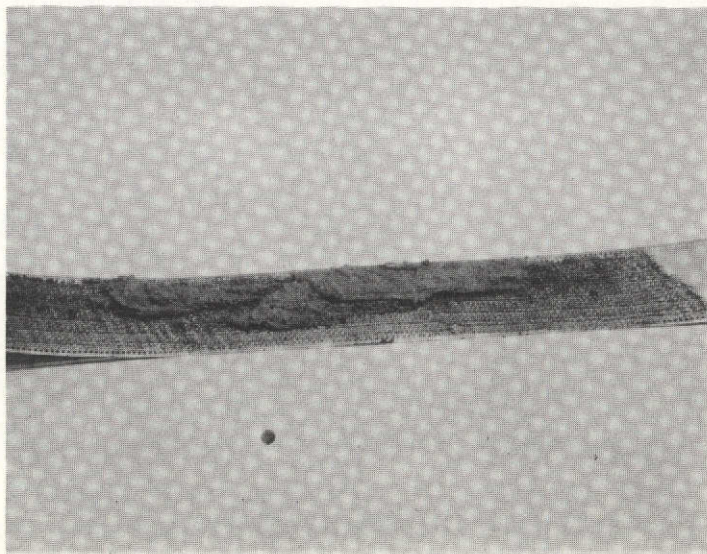


FIGURE 3 - LOCAL ACCUMULATION OF SAMPLE
ON COLLECTION STRIP.

4.2.1 Collection Strip Design

The basic configuration of the collection strip is shown in Figure 4. It consists of a screen, an absorbing backpad, retaining edges, and end attachments.

The screen is made of light weight gauge wire cloth, 16 x 16 mesh, with a wire diameter of .009 inch. The screen material is stainless steel and with the addition of the retaining edges, has sufficient longitudinal stiffness to assure the feeding of the strip to and around the slinger. Vertical rigidity is enhanced by the curvature of the screen when positioned around the slinger and by a support ring around the lower end of the slinger assembly. A relatively good degree of rigidity is required to resist the impact of the sample material breaking away from the slinger times at high speed.

The size of the screen openings is .053 x .053 inch square which is large enough to let most of the liquid material pass through and sufficiently small to prevent the extrusion of the solid samples into the backpad material.

The effective length of the screen is 25 inches with a non-collecting extension of ten inches to connect the strip to the cassette shaft for winding back after collection. The effective width of the screen is 3 inches maximum thus providing a collection surface of 78 square inches which should be capable of sustaining even 400 gms of solids with an average accumulation of .3 inches.

The screen back pad is made of sterile absorbing material such as used for baby diapers and other hygiene type application. It is estimated that a total of 29 gms is adequate to retain a maximum of 500 gms of liquid in zero "g" or 350 gms in a one "g" demonstration type setup. These values are based on the test data reported in Section 5 using commercially available absorbing cotton and may be significantly reduced by using a super-absorber material which is presently being introduced by a manufacturer of feminine hygiene apparel. The pad material is retained against the screen with a thin teflon film (.0015) such as Gortex 28-22D made by W. L. Gore & Associates of Newark, Delaware.

The retaining edges are used to guide the strip from the cassette to the collecting position and back. As shown in Figure 4 the crosssection is relatively small, just large enough to keep the assembly from falling out of the track. Only the top edge is required for positioning and driving and keeping the assembly in place. The lower edge is added to cover the lower edges of the wire screen and to balance the strip assembly in the cassette during the rewinding phase. The material tentatively selected is a polyurethane such as used on timing belts, cast directly on the edge of the wire screen. The very end of the retaining edge, the part that engages to the driving mechanism may be made of softer silicone rubber to facilitate engagement if later tests show that the ease of engagement demonstrated with the lab model using GE RTV 60 cannot be duplicated with cast polyurethane.

The proposed collection strip assembly is attached on one end to the cassette shaft with the ten inch extension previously described. The other end of the strip is fitted with a spring loaded device which "pops" the strip out of the cassette when the sample slide valve is open with a minimum travel equal to the distance to the driving gear assembly. The device consists of a negator spring mounted approximately 1.5 inches from the leading edge and is designed so that the reaction points are against the cassette wall and the cover to minimize any loading on the wire mesh and retaining edges.

FIGURE 4 - PROPOSED SAMPLE CONTAINER

4.2.2 Container Design

The configuration of the cassette type container is also shown in Figure 4.

It consists of a four piece housing, a sliding inlet cover, a drive shaft and bushings.

The housing is made of two end plates, a thin aluminum wall, and an inlet frame. The inlet frame ties all four pieces together and retains the inlet cover with a set of dovetail grooves. The end plates are of the same design except that the bottom one has a bore for the shaft penetration and a counterbore to position and hold the container in place after installation. Both plates are ribbed as shown in the Figure 4 drawing to minimize weight and friction. Friction is reduced by allowing only a small fraction of the surface of the end plates, the edge of the ribs, to come in contact with the moving edges of the collection strip.

The drive shaft is used to pull the collection strip back into the container. It is made of aluminum alloy, except for the steel coupling pin, and its oversized to assure that, in winding, the collection strip does not lock against the stationary hub on the end plates.

Several, thin, small bushings are used near the top and bottom outlet area to minimize lateral binding when the collection strip is being pulled in or out of the cassette container.

All the aluminum parts will be Tufraam coated to impart hardness, corrosion resistance and a slippery teflon like finish. These three properties are essential to the proper operation and performance of the hardware.

It is essential to note that the proposed design is optimized for short run production of demonstration and test units. It is not the best when large quantities are involved. After some detail design changes, the container itself, for instance, may be made faster, cheaper, and lighter by deep drawing in a manner similar to an aluminum beer can. However, this approach involves some relatively expensive manufacturing development and tooling which is not justifiable for a preliminary flight prototype design.

4.2.3 Clearance Requirement

The need to increase the clearance between the slinger and the collection strip has been discussed in Section 4.1. However, in addition to the need to minimize the possibility of physical contact between the slinger and the sample accumulated on the collection strip, there is a second reason which is as important as the first if not more so.

Laboratory tests have shown that a large surface area is required for the return air flow if we are to expect the system to operate effectively for a length of time compatible with the capacity of the container. The relatively narrow path for air flow return for the ABSS shown in Figure 1 must be changed. The entire length from the slinger to the bottom of the container must be used for air return. The revised configuration is shown in Figure 5.

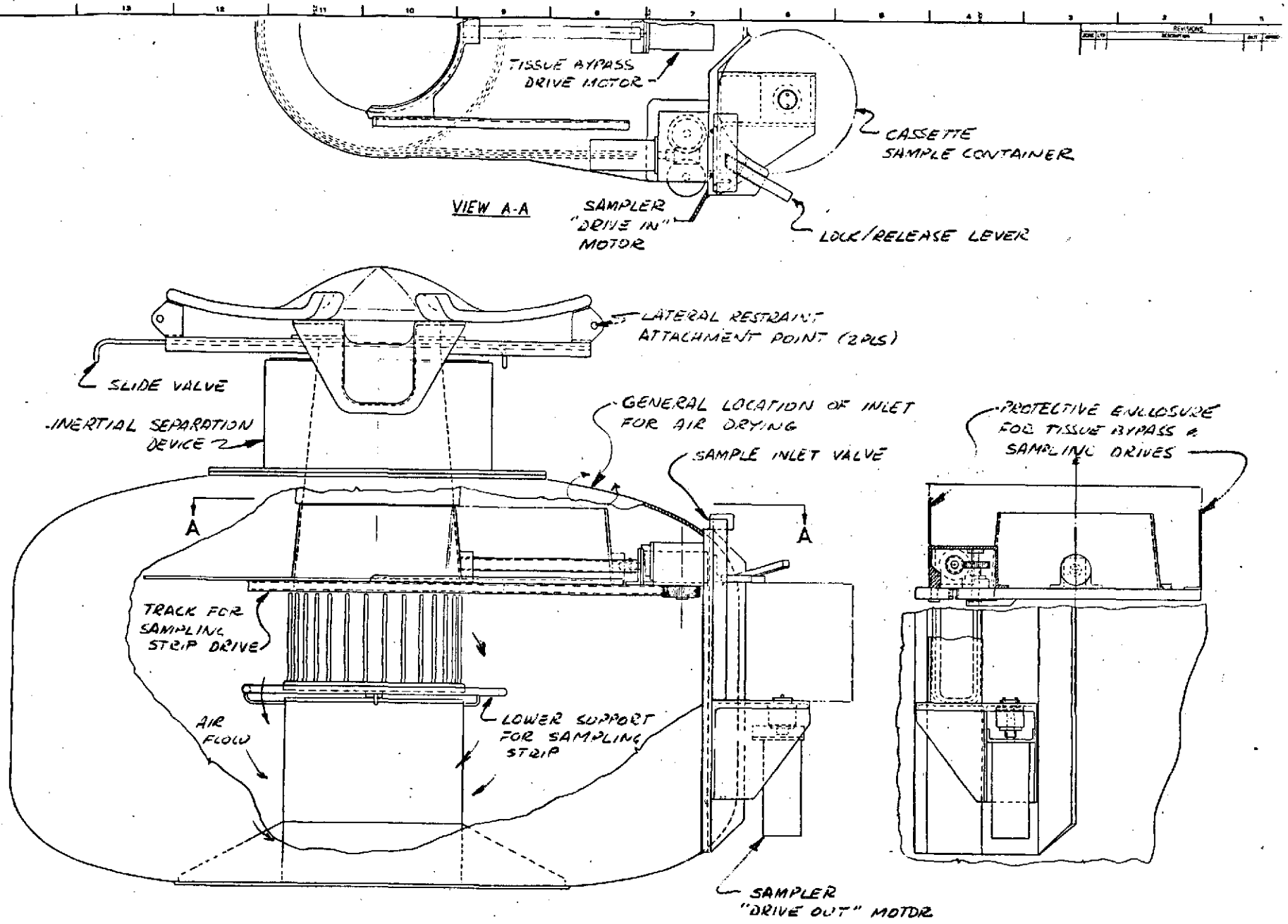


FIGURE 5 - ABSS REVISED CONFIGURATION

ONLY CHANGE WHEN SPECIFIED BY WORKSHEET OR BY THE USER		DATE 10/1/78	BY J.E.
NAME SOLIDS S/S WITH CASSETTE SAMPLING CONCEPT	PART NO. 5X 5619B-841	REVISIONS 1. 10/1/78 J.E.	
MATERIAL ALUMINUM		ABSS	

The diameter of the slinger motor support and filter housing does not exceed the diameter of the slinger. With an increase in diameter of the in place collection strip to 8 inches there should be a one inch nominal clearance around the slinger allowing an unimpeded downward air flow for safe operation. The streamlining of the area below the slinger (compare Figure 5 to Figure 1) results in the elimination of the surface extending past the slinger. This area was easily contaminated and caused loss of sample during the test phase reported in Section 5.

4.2.4 Track Design

The previous ABSS design had two grooved tracks to feed and hold the sampling strip. These have been replaced by a single track which is part of a "ceiling" enclosure for the container which also houses the tissue bypass mechanism and the sample strip drive as shown in Figure 5. The track has a closed groove as opposed to the open grooves of the previous design.



CLOSED GROOVE
TRACK



OPEN GROOVE
TRACK

The closed groove has many definite advantages:

- a) The cavity can be made large or "sloppy" without increasing the chances of clogging with flyby material.
- b) It provides vertical and lateral restraint with a minimum of rigidity requirement on the sampling strip.
- c) It eliminates the lower track connection from the slinger to the sample inlet valve. This connection would be a natural hang up place for toilet tissues unless some additional provisions were implemented to avoid such occurrence.
- d) It saves weight.
- e) It requires less power to operate since the force required to push the strip in and out of the "sloppy" groove is minimized.
- f) It eliminates a complex problem in the mechanical design and assembly of the system.

4.2.5 General Description of the System

The general configuration of the revised ABSS solids subsystem with a cassette type sampler is shown in Figure 5. The location and operation of the sampling inlet valve is the same as the old ABSS. The air drying inlet previously shown below the valve is relocated in the top near the drive mechanism. A wide bracket is mounted outside the sampling inlet valve holding the rewind drive motor. The cassette is engaged to the motor by locating the unit on the bracket and turning clockwise until it falls in place. The cassette is locked in place

with a spring loaded lock/release lever. When the sampling inlet valve is pulled up, the cassette cover moves up with it while the "drive in" motor is energized. The opening of the cassette cover causes the spring loaded leading end of the sampling strip to move forward until it engages with a set of drive gears and is pulled in place around the slinger. After use, the drive out motor is energized thus pulling the strip back into the cassette. Note that at least one of the two drive shafts must have a one directional clutch to avoid matching the changes in linear speed caused by the rewinding in the cassette. Travel control will be done by sensing the presence or position of the collection strip in the storage container with limit switches rather than by counting the number of turns used on the previous ABSS design. Other controls and safety interlocks will be the same. It is also expected that the method of serialization will be simplified by using surface marks identification with magnetic ink or similar methods rather than the perforated tabs which are functional in the urine subsystem (they are used to hold the bags) but plainly cumbersome for the solids subsystem.

5.0 TEST RESULTS

The design recommendations described in Section 4 and pertaining to solids sampling are based on tests conducted in our laboratory using the ABSS solids subsystem and other test hardware available or modified for this purpose.

The testing was relatively limited but adequate to substantiate the findings and can be divided into three phases:

- a) Improvement of ABSS collection strip
- b) New collection strip design
- c) Demonstration of cassette type concept

5.1 Improvement of ABSS Strip

Tests aimed at improving the basic design of the ABSS stainless steel collection strip were conducted using the ABSS solids subsystem and three improved collection strips shown in Figure 6. The strip shown in Figure 6A was a replica of the one tested on the original checkout tests of the ABSS but with better bond between the stainless steel and the open pore foam. The second strip shown in Figure 6B consisted of a stainless steel strip with a double layer of wire screen spot welded to it. The third strip, shown in Figure 6C was the same as the second strip except the screen which had convoluted weaving approximately $\frac{1}{4}$ inch deep thus giving the collection strip better depth than the second type.

The test conditions were as follows:

Slinger speed: 2050 RPM

Power Input: 24 VDC, 29 Watts

Test Material: Dog food, peanut butter mixture same as used on mass measurement development program.

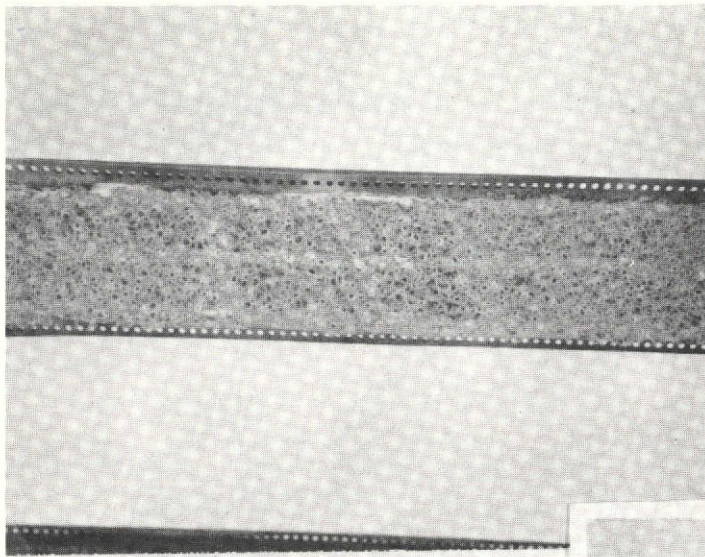


FIG. 6A - STEEL STRIP WITH FOAM

FIG. 6B - STRIP WITH
FLAT WIRE SCREEN

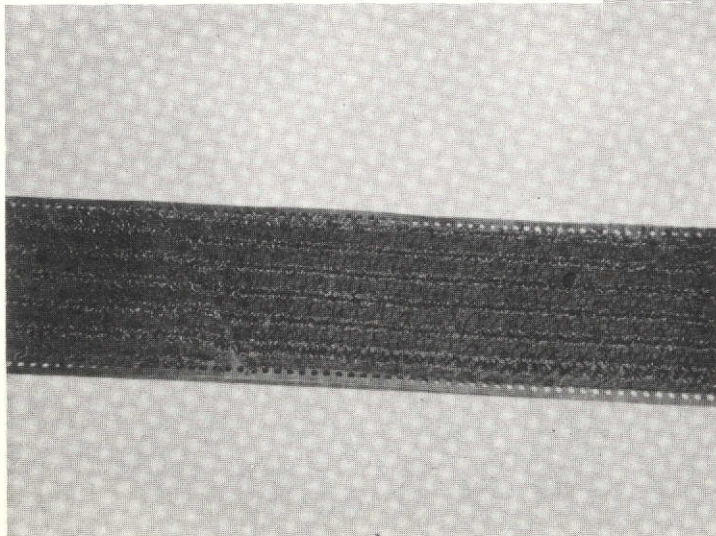
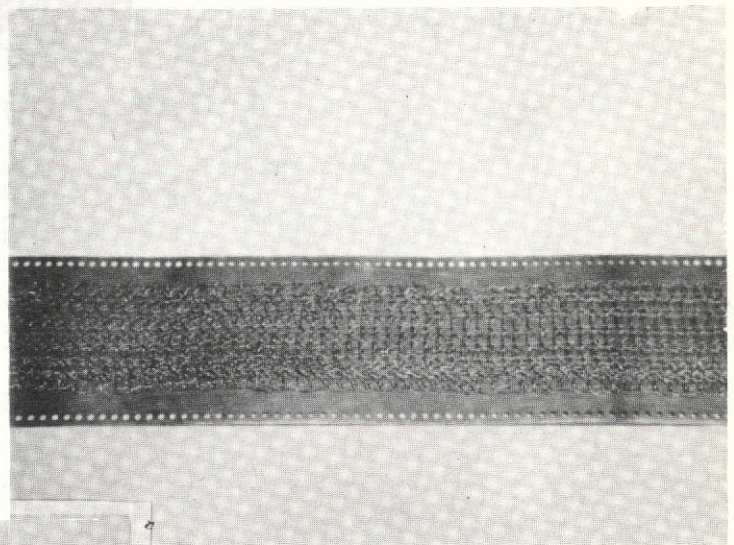
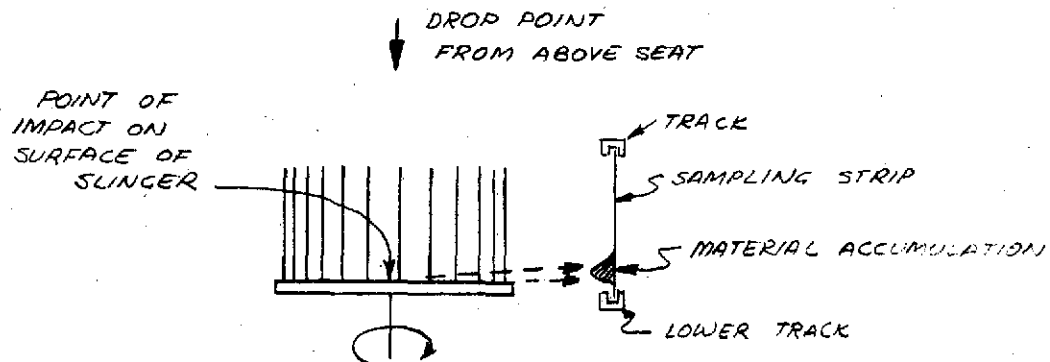


FIG 6C - STRIP WITH CONVOLUTED
WIRE SCREEN

FIGURE 6 - COLLECTION STRIP CONFIGURATION

The first few tests were performed by dropping approximately 100 gms of simulated fecal material on the slinger from the seat level. The strip used was the one shown in Figure 6B. It became obvious soon that this method had to be changed for the reason illustrated by the sketch below.



As the material tended to accumulate near the bottom edge, the probability of contact with the lower track and loss was very high. To avoid this possibility a sample injector was put together which allowed the release of the simulated stool near the tines. This method most closely reproduces the actual Zero "G" conditions. The recently conducted Zero "G" tests showed that the stool never impacts the slinger plate with significant velocity to cause any break up. Break up occurs only upon contact with the slinger tines.

The test results after this initial change in test method are summarized below:

Run #	Sample Input Gms	Sample Collected Gms	% Loss
1	93.5	91	2.68
2	101	98	2.97
3	97	90	7.22
4	99	95	4.04

These results were very good, however, it was suspected that their quality was tied to the fact that the sample size was delivered in two to three segments. The next three runs were made by delivering the entire simulated stool up to 125 gms in weight in one piece. This condition inevitably caused near total loss of sample. The material was sheared off the surface of the collection strip even when using the deep steel weave of configuration #3. It became obvious that, regardless of the improvement in retention capability, whenever the local accumulation due to a large size sample exceeded the clearance between the slinger and the collection strip, all the material above the weave was ripped off and lost.

The next four runs were made to duplicate the first four runs using the deep weave strip with the following results:

Run #	Sample Input Gms	Sample Collected Gms	% Loss
10	71	59.5	16.2
11	84	71	15.5
12	85	56	34.1
13	74	62	16.2

The above tests were run by feeding the collection strip by hand so that the interaction between the slinger and the collection strip could be partially observed through the opening of the slide valve without the box housing the drive sprockets. It became quite clear that the excessive loss was caused by drag between the sample collected on the strip and material accumulated on the lower track. The accumulation would have been sufficient to choke the air flow and cause failure. There was no need of further tests to show that a change was required in the clearance between the slinger and the collection surface and that a redesign of the lower track and its method of attachment was most desirable to minimize the possibility of buildup of sample material. It could also be concluded that the plain stainless steel weave would be adequate for retention as shown by test runs 1 through 4. Increasing the depth of the weave could not improve the performance by much. The loss of sample was caused by factors other than the surface retention as shown by tests 10 through 13. Evaluation of the configuration shown in Figure 6A again had to be quickly abandoned when in attempting to test it, it became clear that separation occurred not so much by the shearing action of the slinger but by absorption of water by the fibers which then led to weakening of the bond to the strip.

5.2 New Collection Strip Design

The design of the new collection strip arose from the need to be able to retain liquid/solid mixtures and the ability to demonstrate in the lab with any degree of verisimilitude that the originally proposed foam lining such as used on the first collection strip, figure 6A, would work adequately in a Zero "G" environment.

At the end of the tests described on the previous section, use of the ABSS solids subsystem was abandoned. The equipment had become soiled and was difficult to clean. Also, most observations had to be based almost solely on deductions rather than the visual observation of cause and effect interactions needed for this type of test. An excellent replacement for the ABSS was provided by the breadboard set up for the mass measurement program. The slinger shown in Figure 7 is the same size as the ABSS's and it could be set to rotate, as it was, at 2050 RPM. A plexiglass enclosure was used as support for the collection strip duplicating the same slinger to positioning track relationship existing in the ABSS. The first few tests were aimed at determining how much water could be retained in a one "G" test with the 1/8" foam of the collection strip shown in Figure 6A. Water was used as an extreme case of diarrhetic discharge although a very small quantity to minimize run off. The results are summarized below.

Run #	W Collection Strip Gms	Water In Gms	Sample Collected Gms
1	61.2	18.5	11.3
2	64.8	48.2	12.4

With a 48.2 gm. water input, a fraction of the 500 gm. capacity requirement, the collection strip had far exceeded its capacity and further testing was stopped. The only apparent hope was to use an absorber such as cotton to replace the foam. Since cotton would not be counted on to retain solids, the basic design of the collection strip was altered to incorporate a front screen which would capture and retain solids samples and a cotton backing which would absorb liquid samples passing through the screen. To prove the concept, a new collection strip was made using a 20 mesh stainless steel screen formed into a cylinder

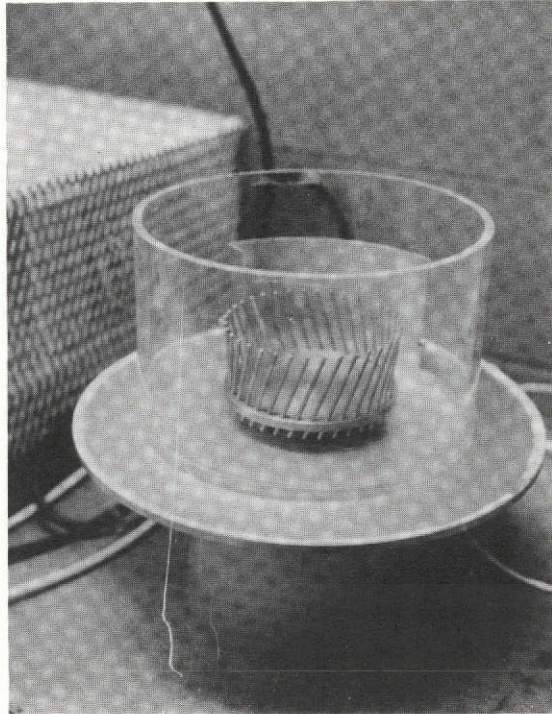


FIGURE 7 - BREADBOARD FOR MASS MEASUREMENT
PROGRAM -

6.75 inches dia. x 3.12 inches high, simulating the size of the collection surface of the ABSS. The screen weighing 68.5 gms. was backed with a thin layer of absorbent cotton and placed around the slinger for test with the following results:

Weight of Collector (screen & cotton)	=	91.8 gms
" " Water Input	=	46.5 gms
" " Sample Collected	=	45.2 gms
Percent Loss	=	2.8%

These results constituted a vast improvement when compared to the better than 74% loss for approximately the same amount of water input used in the second run with the strip with foam.

Additional runs were made using Cotex cotton

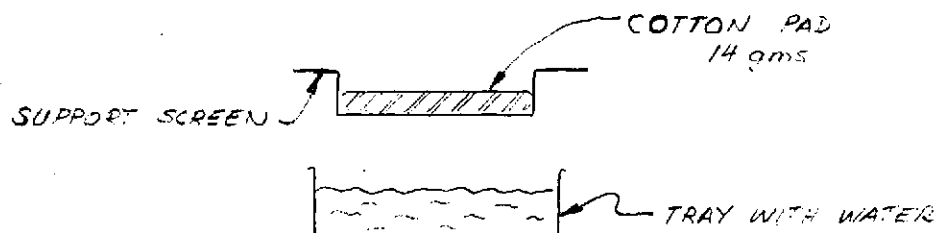
Run #	W of Cotton Gms	W Water Input Gms	W Sample Collected Gms	% Loss
4	22	49.3	47	4.68%
5	27.9	90.8	85.4	5.94%
6	20	94	88.5	5.85%

It should be noted that most of the loss was due to splash back from the water impinging the slinger tines. The amount of water lost from the collector (screen and cotton) was negligible--hardly a few drops accumulated on the plate below the slinger.

The water discharge time was less than 5 seconds. Having established that the screen with cotton backing could be used to collect water most effectively in one "G" conditions, a repeat test was made using simulated solid fecal material, the other extreme of the possible solid sample consistency. The screen retained all the sample with no visible loss. The material did not penetrate the other side of the screen in significant amount to superficially wet the cotton in few places.

The following few tests were aimed at determining how much cotton would be required to absorb the required 500 gm maximum sample size.

The tests were run by immersing a 14 gm cotton pad in a tray full of water, removing the wet pad, and then subtracting the weight of the remaining water from that of the water before immersion. These tests indicated an absorption rate in excess of 10 gm water for 1 gm of cotton. The tests, however, were not too exact due to dripping as the cotton was removed from the tray. The test was rerun using a support screen to hold the cotton pad horizontal to minimize dripping due to hydrostatic pressure in the pad as shown below.



The results were greatly improved. The pads absorbed 244 gms of water indicating that 29 gms of cotton backing should be sufficient to collect the 500 gms maximum sample size. The measured absorption capacity is really not that extraordinary. In addition to the new super absorber material mentioned in Section 4.2.1, other materials are being developed. As an example, Mr. R. Sauer, the Program Technical Monitor, has provided us with information on a product called "super slurper". Developed by the Agriculture Department's Northern Research Laboratory, Peoria, Ill., this material can absorb 600 times its weight in water! Of course, material selection must be made on the basis of factors which, in addition to retention, take into account compatibility with post flight analyses, capability of sample recovery, etc.

5.3 Demonstration of Cassette Concept

The tests described in the previous section proved the feasibility of a two part sample collector, i.e., a screen with an absorber to retain solid or liquid/solid mixture samples in a one "G" as well as zero "G" configuration. A flight type prototype collection strip was designed including a cassette type container for before and after use storage as shown in Figure 4. The cassette type storage container and the single track approach necessitate significant changes to the basic ABSS solids subsystem configuration so that the assembly was redesigned as shown in Figure 5. The critical item in the new design is the automatic engagement of the collection strip from the cassette storage configuration and the feeding of the collection strip around the slinger.

The engagement must be fairly simple and be tolerant of a large degree of misalignment for maximum reliability. The feeding of the strip must be nearly effortless as the basic strip design must remain "soft" to minimize power and weight. A demonstration model was designed and built to show that the system could be made to work and to get a preview of possible problem areas. The model consists of two basic components: the cassette sample container shown in Figure #8, and the track and drive assembly shown in Figure #9. The cassette container is made of plexiglass and is basically of the same functional configuration as the flight type design shown in Figure #4. The track and drive assembly reproduce the configuration shown on Figure #5 with simplification of non critical parts wherever possible. For instance, the only motor drive used is the one required to engage and pull the collection strip. This is essential to the demonstration. The motor to rewind the strip is not essential and, therefore, omitted for the sake of cost and time saving. The parts were fabricated in our shop from hand sketches and verbal instructions. The sketches, SK56198-842 through -848 are attached. One significant deviation between the proposed design shown in Figure #4 and the model shown in Figure #8 is the spring device. The model uses a compression spring to advance the collection strip the required amount to engage with the drive gears. The proposed flight type design of Figure 4 shows a negator spring which would be lighter and take less room.

The collection strip in the demonstration model was made from aluminum screen (same as used for storm windows) with $\frac{1}{4}$ x $\frac{1}{4}$ inch silicone rubber retaining edges.

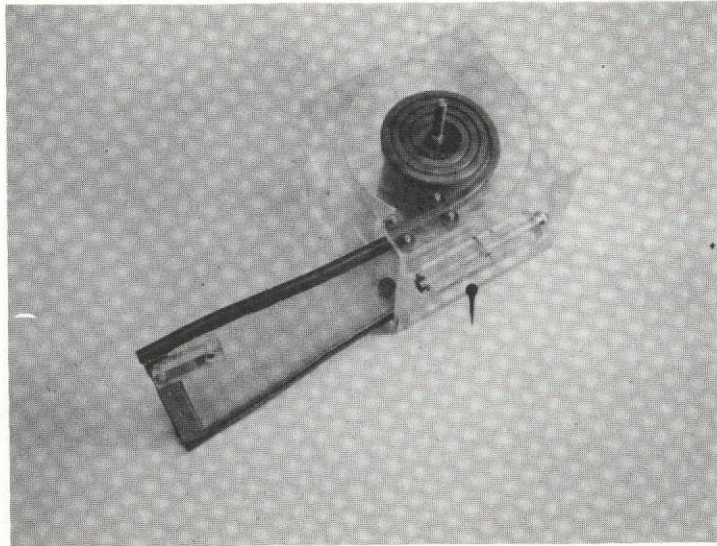


FIGURE 8 DEMONSTRATION MODEL OF
CASSETTE TYPE SAMPLE CONTAINER.

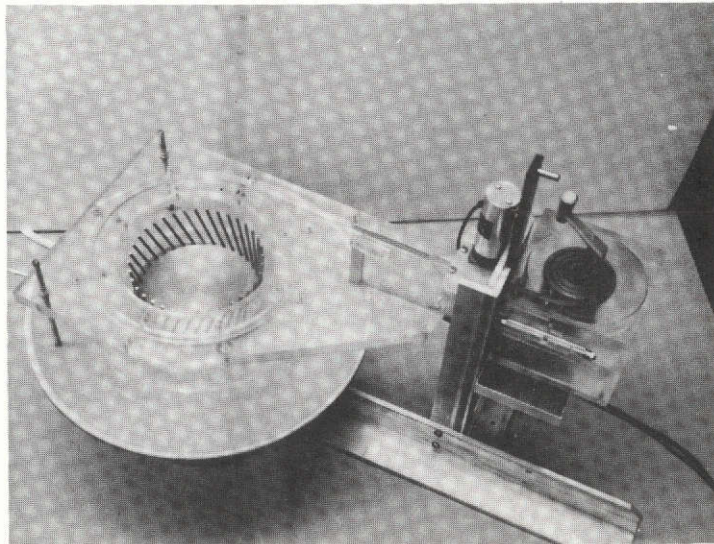
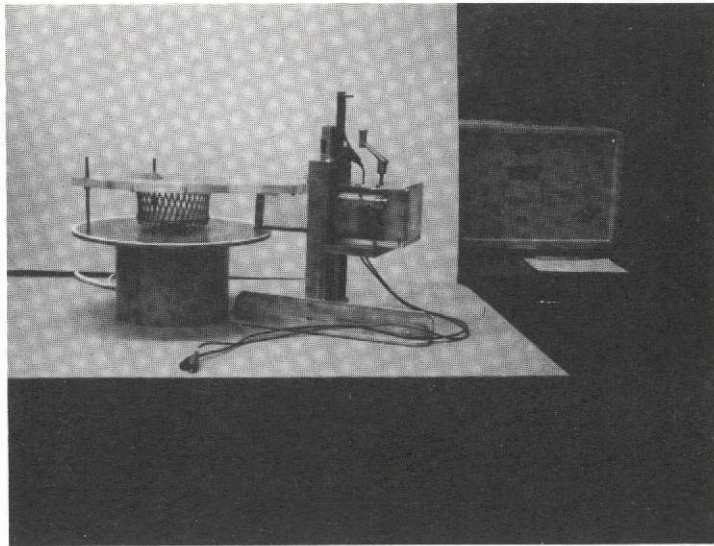


FIGURE 9 - TWO VIEWS OF DEMONSTRATION MODEL ASSY.

The silicone rubber (RTV 60) was cast directly over the edges of the screen. The near end of the screen is stiffened with two aluminum plates, as shown in Figure 8. One of the plates has an extension which is used to cock the spring pin. The spring pin is mounted on the plexiglass box for ease of fabrication. The tests were performed in two stages.

During the first stage the collection strip was fed by hand into the drive gears. The drive gears invariably captured the end of the strip and moved forward into the groove with no apparent trouble. This process was repeated several times driving the strip in and out by reversing polarity on the motor.

During the second phase the strip was assembled to the cassette and installed in place using the simulated slide valve to hold the end of the strip inside the box. When the valve was pulled up, the strip came out, slowly at times, but it did come out to engage the gear and continue to move forward. During this state a problem appeared which was not expected. The winding of the strip in the box causes the silicone rubber retainer to swell against the plexiglass top and bottom surfaces. Silicone rubber tends to "grab" to plexiglass (as most other materials). This makes the winding or unwinding of the strip difficult. This problem is overcome in the flight type design two ways: first, the retainers are made of polyurethane a little harder than silicone rubber and not as sticky; second, the top and bottom surfaces of the cassette have been ribbed so the contact between the strip and the cassette is only a fraction of that existing in the demonstration model.

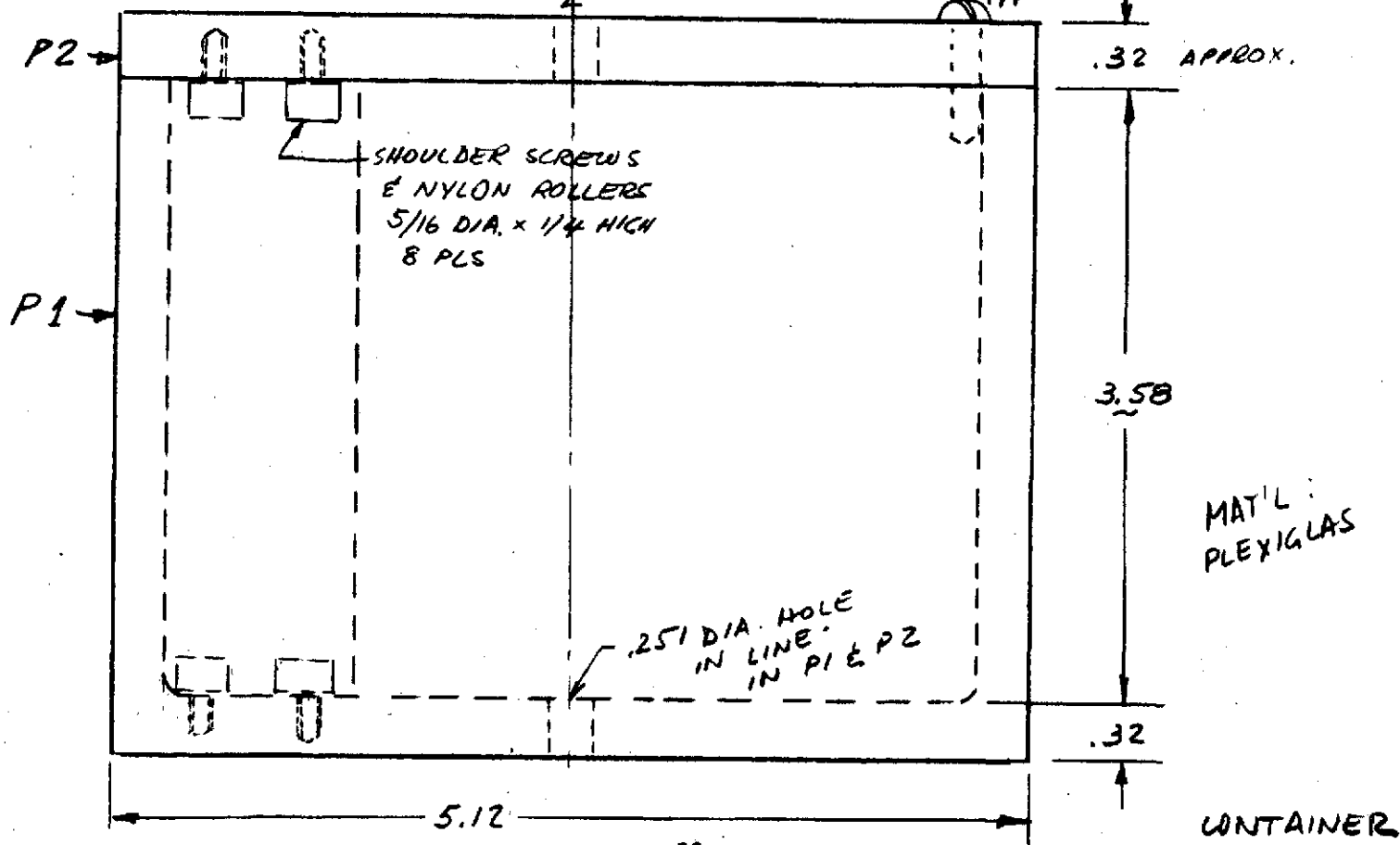
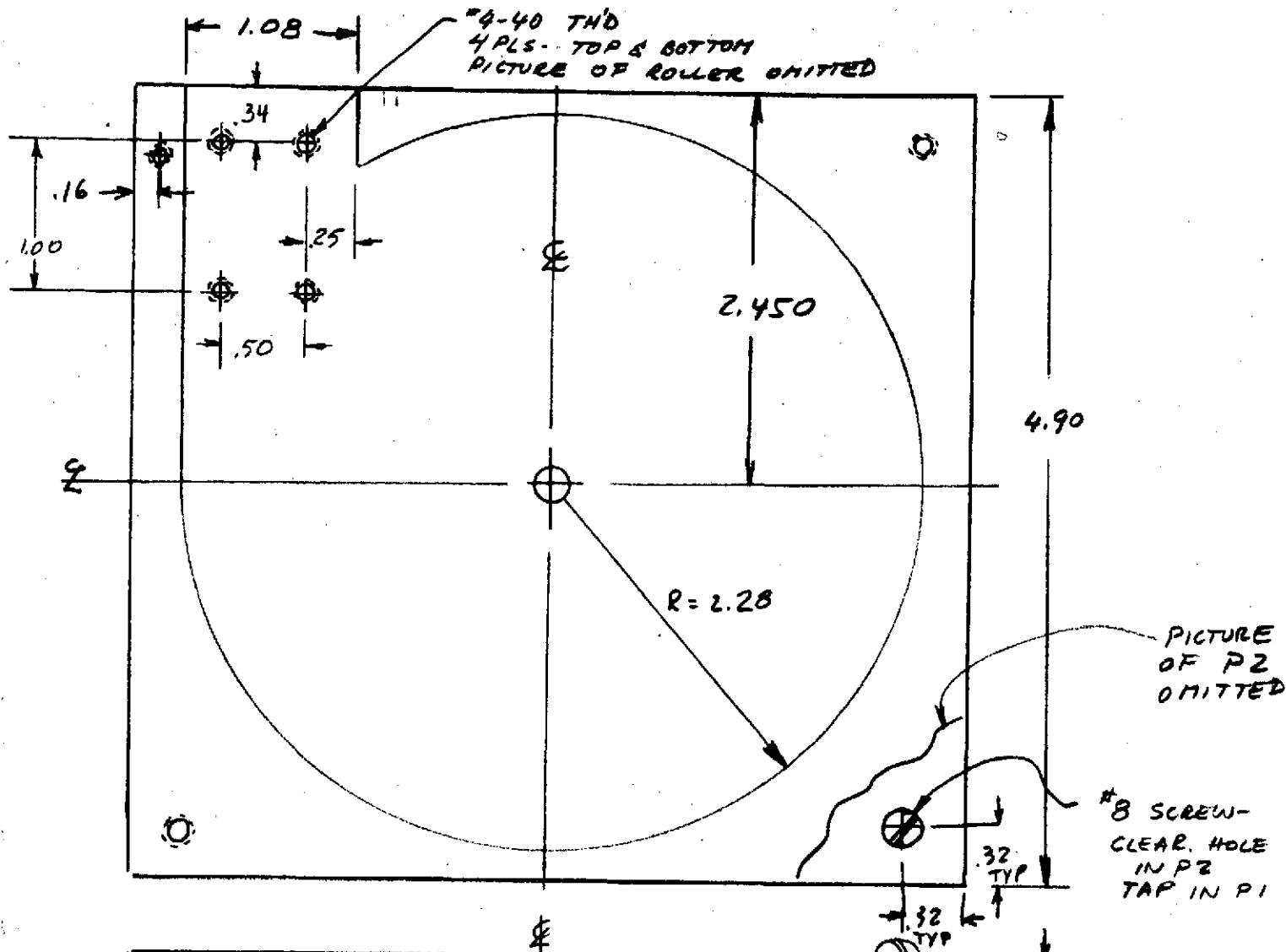
APPENDIX

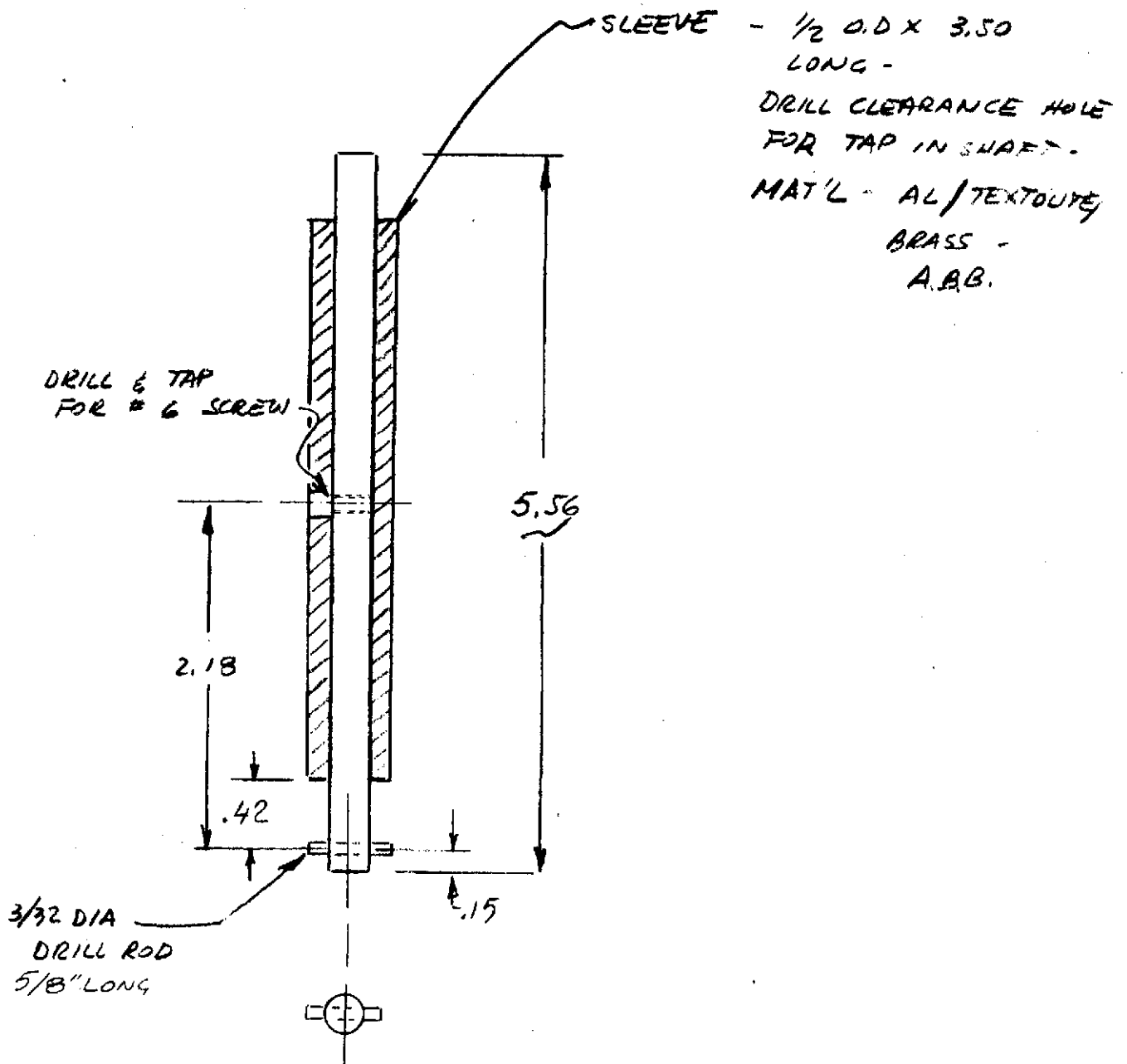
SKETCHES

USED FOR FABRICATION OF

SOLIDS SAMPLING

DEMONSTRATION MODEL ASSEMBLY

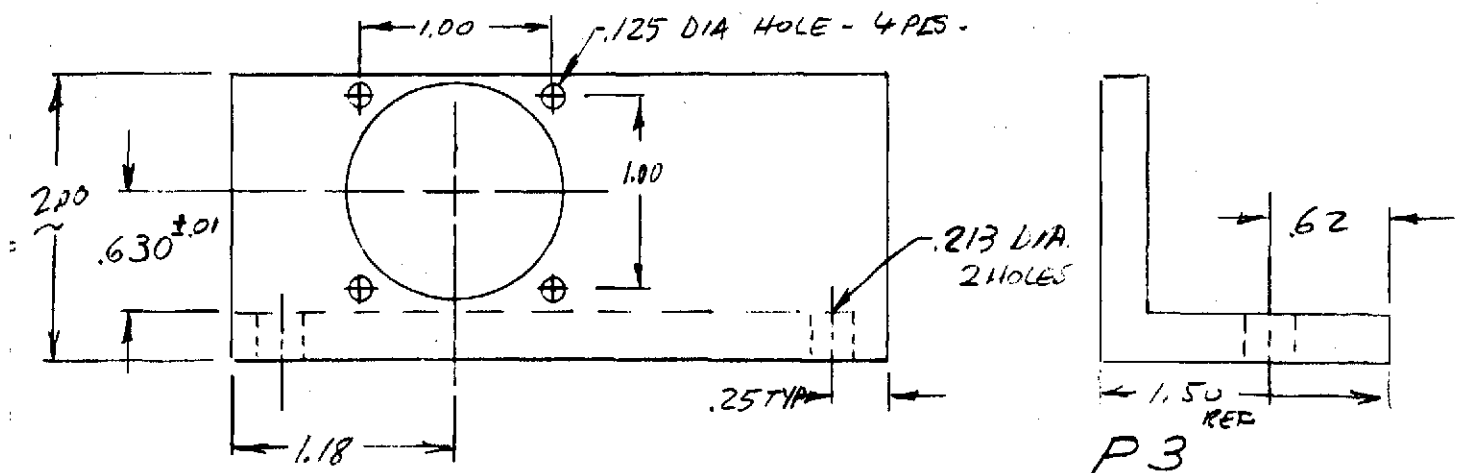
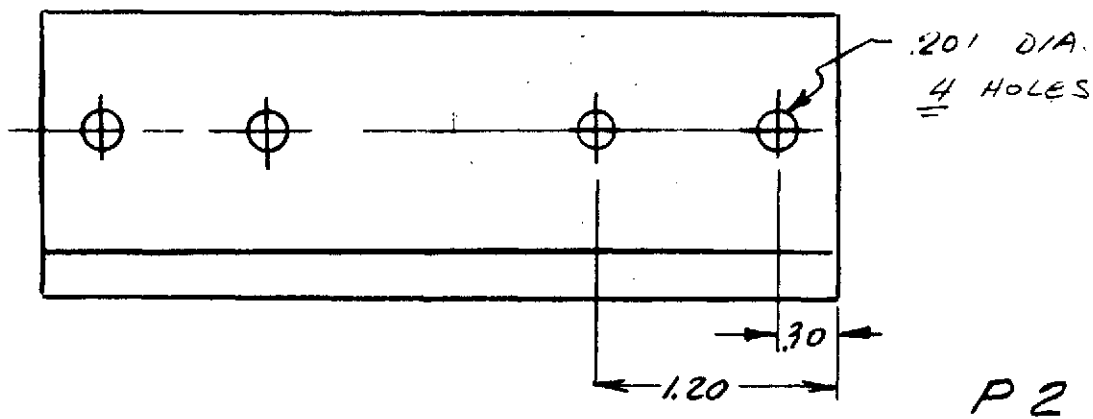
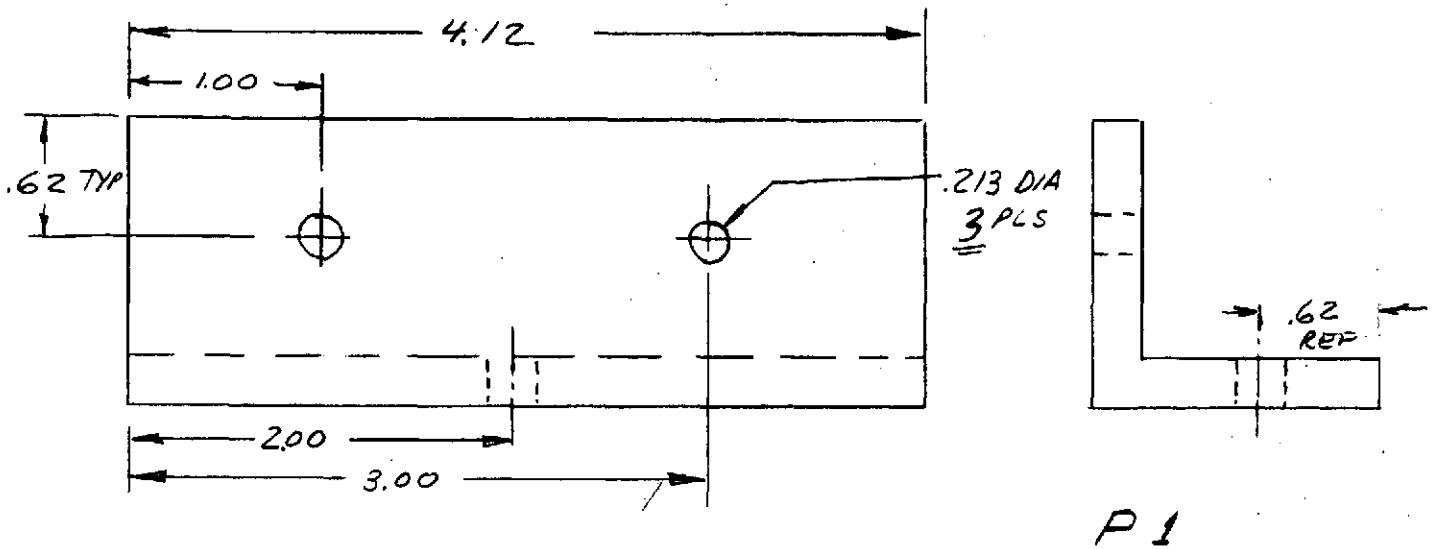




MAT'L - STEEL ROD - $\frac{1}{4}$ DIA.

9/10/44

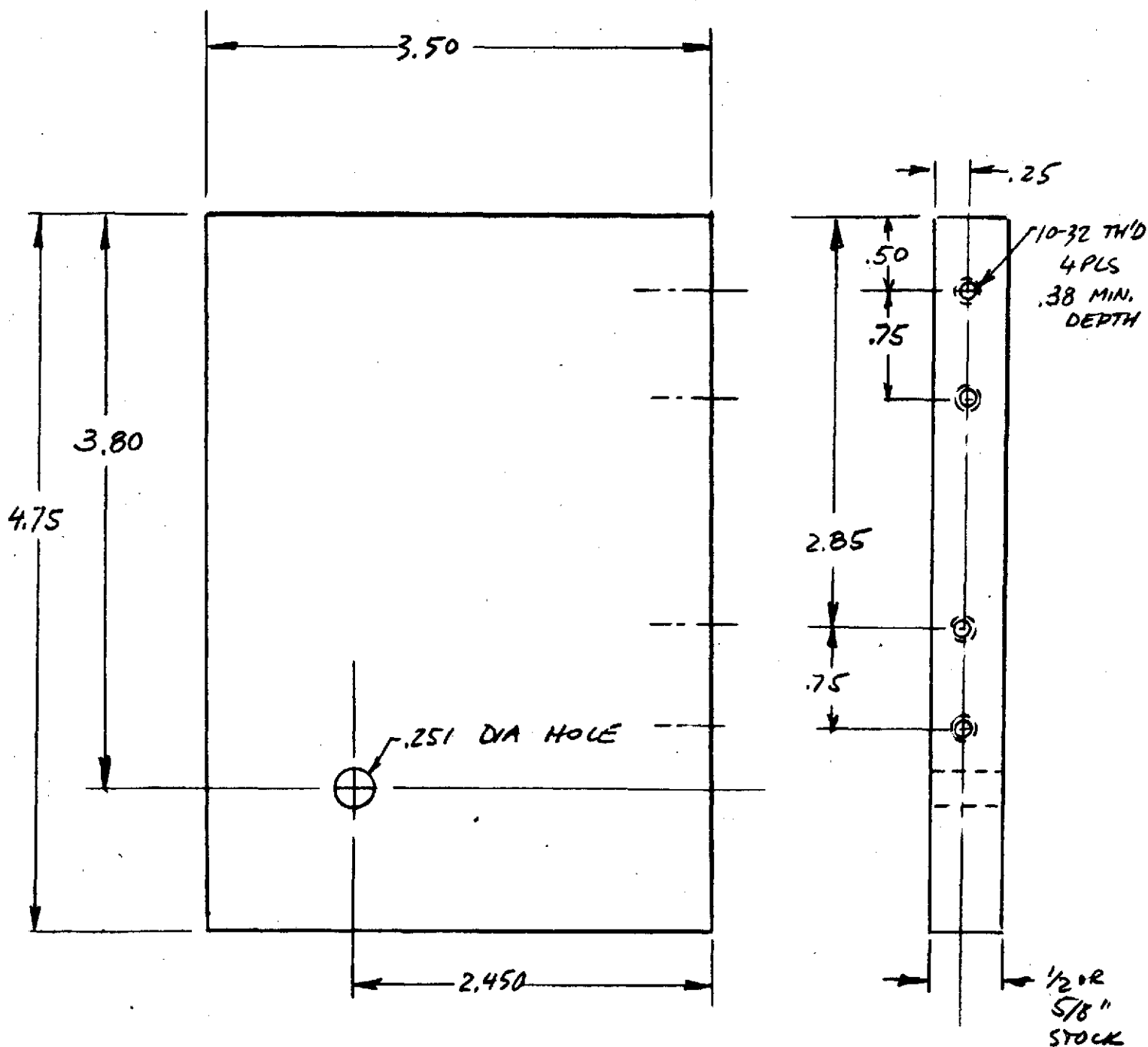
SHAFT
SK56198-B44



MAT- $1\frac{1}{2} \times 1\frac{1}{2} \times \frac{1}{4}$ AL. ALLOY
 $1\frac{1}{2} \times 2 \times \frac{1}{4}$ ANGLE FOR P1 & P2
 $1\frac{1}{2} \times 2 \times \frac{1}{4}$ ANGLE FOR P3
 CHAMFER ALL CORNERS
 .25 x 45° APPROX.

SUPPORT ANGLE

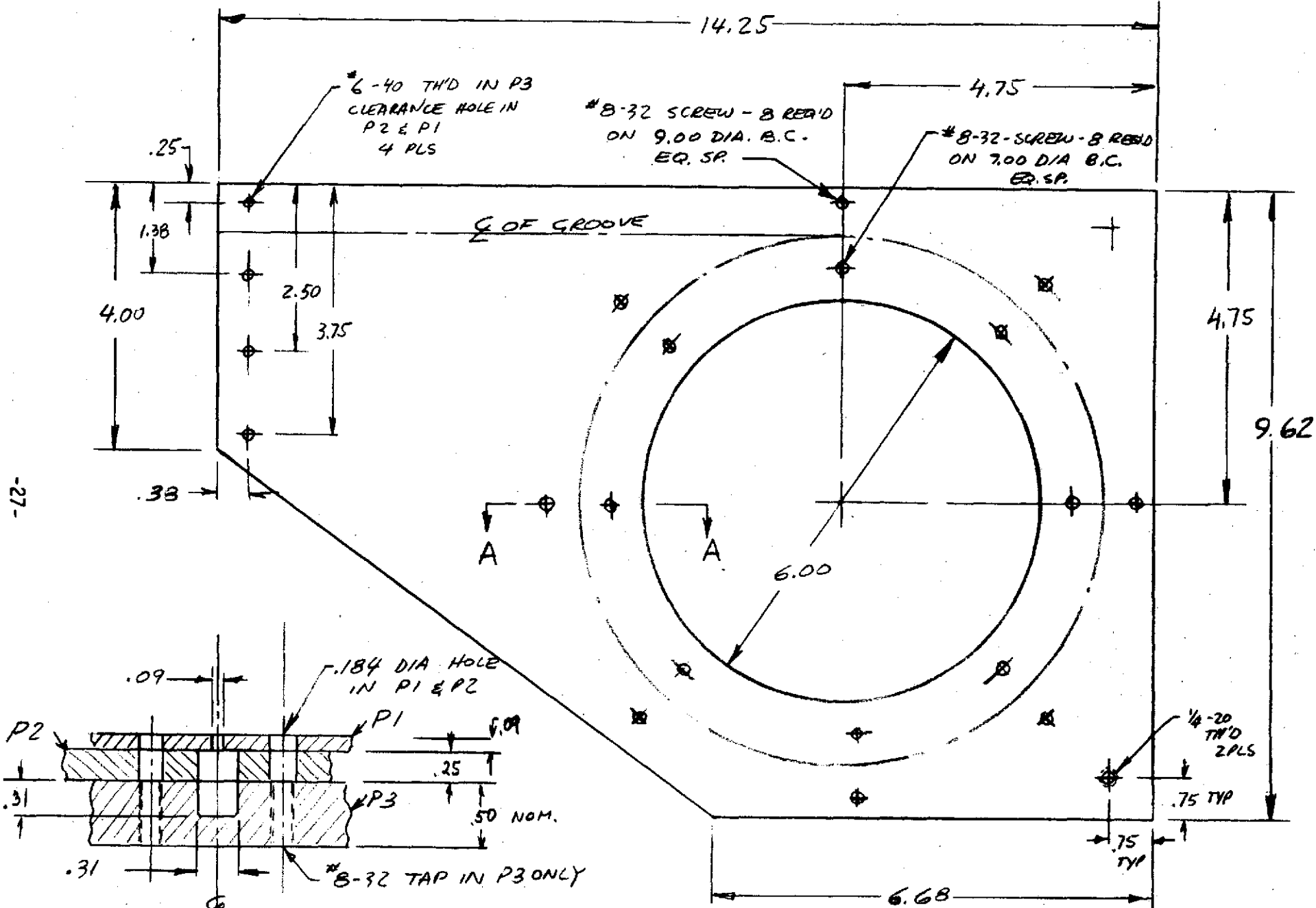
SK56198-845



MAT'L AL. ALLOY

CONTAINER SUPPORT

SK 66198-846



MAT'L PLEXIGLAS

SECT - A-A
FULL SCALE

GUIDE PLATE
SK56198-847

Wm